UNIVERSITÀ DEGLI STUDI
DI GENOVA

Doctoral School on “Clinical and Experimental Neuroscience”

Doctoral Course on Neurosciences

XXXII Cycle

"Impaired presynaptic Ca^{2+} influx in PRRT2-deficient neurons"

Author: Dr. Daniele Ferrante

Supervisor: Prof. Pietro Baldelli and Fabio Benfenati

Cooridinator: Angelo Schenone

To my Father

who taught me a lot,

who was very proud of me even though he never told me

and who will always remain with me in my heart

To my mother

who has always been close to me with her love

I love you

Table of Contents

Summary

PRRT2 is a single causative gene for paroxysmal kinesigenic dyskinesia disease. Several studies have identified an array of heterozygous loss-of-function nonsense/frameshift and missense mutations in the gene encoding this protein that through non-sense mediated RNA decay and/or degradation of truncated/misfolded protein cause a condition of haploinsufficiency.

These mutations are described in a large number of patients affected by paroxysmal disorders such as benign familial infantile seizures, infantile convulsion choreoathetosis, migraine, hemiplegic migraine, paroxysmal kinesigenic dyskinesia/choreoathetosis, benign familial infantile seizures/epilepsy, and episodic ataxia.

PRRT2 is a small gene located on chromosome 16p11.2 already expressed at early postnatal stages, and its expression increases till reaching a plateau at 1 month of life; high levels of PRRT2 mRNA were detected in many tissues of the nervous system, especially in the extrapyramidal system.

We have previously shown that PRRT2 is a key component of regulated exocytosis and its silencing dramatically impairs neurotransmitter release by markedly reducing release probability. Moreover, we demonstrated that PRRT2 interacts with the fast Ca^{2+} sensors synaptotagmin 1/2 and endows the SNARE complex with Ca^{2+} sensitivity. Here, we investigated the altered Ca^{2+} dependence of glutamatergic synaptic transmission as a possible causative role in the pathogenesis of PRRT2-linked paroxysmal diseases by focusing on voltage-gated Ca^{2+}channels (VGCaCh) and presynaptic Ca^{2+} influx.

Thanks to the use of multiple experimental approaches, including electrophysiology, immunocytochemistry, biochemistry and live Ca^{2+} imaging, we investigated the changes of somatic and presynaptic VGCaCh subtypes in PRRT2-

deficient neurons but also the altered Ca^{2+} dependence of the synaptic transmission.

We observed that PRRT2 deletion induces a significant decrease in the amplitude of evoked excitatory synaptic currents (eESPCs) recorded at increasing concentrations of extracellular Ca^{2+}. This effect was associated with a reduction of P/Q- and N-type VGCa currents paralleled by a decrease in the amplitude of N- and P/Q-type sensitive eESPCs.

Using surface biotinylation, we observed that PRRT2 deletion impaired the P/Q-type VGCaChs trafficking to the membrane. Double immunostainings revealed that in presynaptic terminals lacking PRRT2, the P/Q-type VGCaChs diffused in the presynaptic membrane and reduce their clustering at the active zone. In parallel, using SyGCaMP-6s, an ultra-sensitive fluorescent Ca^{2+} indicator selectively expressed at the presynapse, we investigated presynaptic Ca^{2+} influx and observed a significant decrease of the P/Q-dependent presynaptic Ca^{2+} signal in PRRT2-deficient synapses.

Our results strongly suggest that PRRT2 deletion causes mistargeting of P/Q-type VGCaChs far away from the active zone, reducing the availability of VGCaCh strictly associated with the release machinery and thereby the glutamate release probability.

Altogether our data highlights the central role of PRRT2 in the release machinery, indeed, the lack of this protein impaired the N- and P/Q-type channels trafficking from the cytoplasm to the membrane causing of a reduction of intracellular Ca^{2+} in consequence of a reduction of release probability.

1. Introduction

1.1 The Pathology: Paroxysmal Kinesigenic Dyskinesia (PKD)

Paroxysmal kinesigenic dyskinesia (PKD) was first described in 1967 and is now recognized as the most common type of paroxysmal movement disorder (Kertesz, A. 1967). This disease is characterized by recurrent, brief attacks of dyskinesia that are triggered by sudden voluntary movement (Goodenough et al., 1978). The episodes usually present with dystonia, chorea, athetosis, ballism or their combination. The attacks usually last from a few seconds to a few minutes. During the attacks, there is absolutely no loss or alteration of consciousness. However, the prognosis of PKD is favorable and the patients usually show excellent responses to antiepileptic drugs (Kertesz, 1967; Goodenough et al., 1978; Houser et al., 1999; Lotze and Jankovic, 2003; Bruno et al., 2004).

Onset age in PKD varies between 6 months and 33 years, but more frequently between 7 and 15 years. A higher prevalence of the sporadic form was observed in males (4:1, even up to 8:1), but not in familial cases. Typically, an attack is induced by a sudden movement, for example, getting up quickly to answer the doorbell or the telephone. However, even a sudden increase in speed, amplitude, or strength of the movements or even the sudden addition of new actions during ongoing steady movements may induce an attack (Fahn S. 1994; Bhatia KP. 2001; Demirkiran M. et al., 1995). An example of this may be the sudden acceleration from a walk to a run (trying to catch a bus) or a sudden change in direction. Startle, sound and photo stimulation, vestibular stimulation, hyperventilation, or stress may also trigger attacks (Bhatia, 2011). For these reasons PKD attacks are frequent.

Typically, attacks affect limbs on one side, although generalized attacks also can occur. About 30% of the patients experienced speech disturbance (dysarthria or anarthria) that may be the result of face involvement (Houser et al., 1999). In case of multiple attacks, there may be a refractory period of about 20 minutes during which no further attacks can be induced (Lishman et al., 1962). The most

of the attacks are very brief, lasting only seconds (Houser et al., 1999; Bruno et al., 2004). Houser et and colleagues (1999) reported that, attacks lasted less than 2 minutes in 88% of cases and between 30 and 60 seconds in two thirds of patients. Similarly, Bruno et al. (2004) reported that attacks were shorter than 1 minute in 95% of patients. Long PKD-like attacks should thus make the clinician suspicious of a secondary cause, including the possibility of psychogenic paroxysmal disorder.

Most patients have 1–20 attacks per day, whereas some patients may also have more than 20 attacks per day. However, the frequency of PKD episodes usually peaks in puberty with up to 30–100 attacks and then becomes less after age 20 and may even completely remit after age 30 (Bruno et al., 2004).

Because the paroxysmal movements are regarded as an epileptic manifestation, paroxysmal kinesigenic dyskinesia is often misdiagnosed as epilepsy. Among the primary forms, 65%–72% of PKD patients have a family history of a similar disorder with an autosomal dominant inheritance. Identification of the genes underling the pathogenesis has enhanced diagnosis and clarified the mechanisms of disease progression in paroxysmal kinesigenic dyskinesia.

Chen et al. (2011) first reported PRRT2 mutations as the genetic cause of PKD in eight families with PKD, opening the way to the identification of PRRT2 mutation in several clinical syndromes previously associated with PKD such as the so-called infantile convulsions with choreoathetosis (ICCA) syndrome and benign familial infantile seizure syndrome (Ebrahimi-Fakhari D, et al. 2015). Very quickly, a strong interest about this gene suddenly increased, in particular thanks to the next-generation sequencing, combined with classic linkage analysis, that allowed the identification of an array of PRRT2 mutations as the leading cause of the most common type of familial paroxysmal movement disorder, paroxysmal kinesigenic dyskinesia (PKD) (Chen et al. 2011; Wang et al., 2011).

In few years, several studies have identified an array of heterozygous nonsense, frameshift, and missense mutations in the gene encoding proline-rich

transmembrane protein 2 (PRRT2) in a large number of cases affected by different paroxysmal disorders such as benign familial infantile seizures, infantile convulsion choreoathetosis, migraine, hemiplegic migraine, paroxysmal kinesigenic dyskinesia/choreoathetosis, benign familial infantile seizures/epilepsy, and episodic ataxia (Chen et al., 2011; Lee et al., 2012; Valente et al., 2016). Currently, PRRT2 is the major gene accounting for PKD, with a frequency ranging from about 40% to over 90%, depending on case ascertainment (Ebrahimi-Fakhari D, et al. 2015; Erro R., et al. 2017).

2. The PRRT2 Gene

Paroxysmal Kinesigenic dyskinesia Dyskinesia (PKD) is most commonly transmitted in an autosomal dominant mode of inheritance (Bruno et al., 2004). The causative role of PRRT2 mutations in the pathogenesis of PKD and of a variety of additional paroxysmal disorders with a similar pattern of inheritance is now documented by extensive studies and summarized by recent comprehensive reviews (Wood H. 2012; Heron, S.E. and Dibbens, L.M.,2013; Ebrahimi-Fakhari, D. et al., 2015). Interestingly, all PRRT2-associated disorders appear paroxysmal in nature, suggesting the presence of shared pathophysiological mechanisms. In contrast, other common non-paroxysmal movement disorders, such as Parkinson's disease, are not associated with PRRT2 mutations (Kumar et al., 2012). The astonishing pleiotropy of the phenotypic expression of PRRT2 mutations points to an overlap in the pathogenic pathways and to a very important role of this gene in regulating synaptic transmission and network activity. Several linkage studies have identified two regions on chromosome 16 (16p11.2–q12.1 and 16q13–q22.1) that are likely to harbor paroxysmal kinesigenic dyskinesia susceptibility genes in populations of diverse ancestry (Tomita, H. et al., 1999; Swoboda, K.J. et al., 2000; Bennett, L.B., et al., 2000; Valente, E.M.et al., 2000).

PRRT2 is a small gene located on chromosome 16p11.2 and containing four exons, the first of which is noncoding. The main encoded isoform of PRRT2 is a 340 amino acid protein (Chen et al., 2011), highly conserved (~80%) among mammals, with some similarity (~30%) still appreciable in lower vertebrates (e.g., zebrafish). Sequence conservation is particularly prominent (up to 90% in mammals and 60% in zebrafish) in the C-terminal region of the molecule, which includes two hydrophobic helices (M1 and M2) separated by a short polar amino acid sequence and followed by a two-residue C terminus (Lee et al., 2012). The PRRT2 gene contains four exons, with exons 2–4 encoding a multidomain protein of 340 amino acids formed by a long N-terminal domain (1–268) containing a proline-rich region (PRD); two putative transmembrane helices, M1 (269–289) and M2 (318–338), separated by an intracellular loop (CYT, 290–317), and a C-terminal dipeptide (339–340)(Figure 1). Despite the similarity with the proteins of the dispanin family, only M2 is a true transmembrane helix, while M1 is folded into two halves (M1a and M1b) by a hinge formed by two proline residues. As a consequence, M1 does not cross the membrane. Due to its single transmembrane domain, PRRT2 exposes the long N- terminal domain and the short M1–M2 loop to the cytoplasm and maintains a C-terminal anchor, conforming the model of a type II transmembrane protein (Valtorta et al., 2016; Rossi et al., 2016). In a study of the expression profile of PRRT2, high levels of PRRT2 mRNA were detected in many tissues of the nervous system, especially in the extrapyramidal system, which includes the globus pallidus, cerebellum, subthalamic nucleus, cerebellar peduncles and caudate nucleus (Su A.I., et al, 2004; Chen et al., 2011; Lee et al., 2012; Heron et al., 2012; Trabzuni et al., 2011). The PRRT2 gene was already expressed at early postnatal stages, and its expression increased to reach a plateau at 1 month of life, a period of intense synapse formation and rearrangement. The same pattern was reproduced in primary hippocampal and cortical neurons, where PRRT2 expression, already discernible at early stages, was greatly enhanced between 10 and 21 days in vitro (DIVs), a temporal window of intense synaptogenesis (Valente et al 2016).

However, there are no reports of the function of the PRRT2 protein or the relationship between PRRT2 and neurological disorders. The functional role of this protein is totally unknown. A yeast two- hybrid screen highlighted a potential interaction of PRRT2 with synaptosomal-associated protein 25 kDa (SNAP-25), one of the presynaptic soluble N-ethylmaleimide sensitive factor (NSF) attachment protein receptor (SNARE) proteins triggering fusion of synaptic vesicles (SVs) (Stelzl et al., 2005; Lee et al., 2012). Recently, PRRT2 has also been found among proteins associated with a-amino-3-hydroxy-5-methyl-4-isoxazolepro-pionic acid (AMPA)-type glutamate receptors by a high-resolution proteomics study (Schwenk et al., 2014), and its mutation was associated with increased levels of extracellular glutamate (Li et al., 2015).

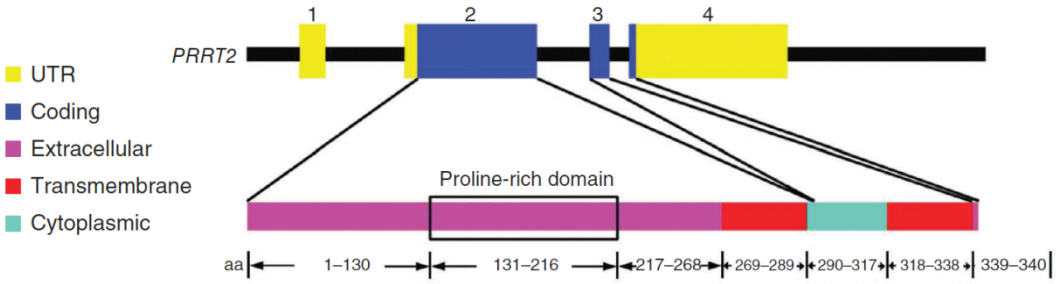

Figure 1. PRRT2 protein domain structure. The PRRT2 gene contains four exons that encode several domains in the PRRT2 protein, including two extracellular domains, two transmembrane domains and one cytoplasmic domain. The proline-rich domain overlaps with the N-terminal extracellular domain (Chen et al., 2011).

2.1 PRRT2 Mutations

Most mutations identified in PRRT2 are phenotypically highly penetrant and cause truncation of the protein because of nonsense or frameshifts mutations that result in mRNA degradation by nonsense-mediated mRNA decay or degradation of the protein (Wu et al., 2014), suggesting a loss- of-function mechanism of action. In spite of the numerous mutations described so far (Figure 2; Heron, S.E. and Dibbens, L.M.,2013; Cloarec, R. et al., 2012; Lee et al., 2012), no specific genotype–phenotype correlations have emerged. A common c.649dupC frameshift mutation segregates in about 80% of the PRRT2 mutant families, resulting in diverse paroxysmal disorders (Ebrahimi-Fakhari et al., 2015). Family members carrying identical PRRT2 mutations often exhibit variable phenotypes, with each of them suffering from a different disease (Brueckner, F. et al. (2014). The phenotype may vary even with different ages of the same individual (in PKD/IC an individual may present with infantile seizures that remit during infancy, and subsequently develop PKD during adolescence). These remarkably pleiotropic effects imply that genetic buffering as well as factors other than the mutations in PRRT2 influence expression of the disease. A vast majority of PRRT2 mutations reported (about 95%) are nonsense or frameshift (Figure 2; Liu et al., 2013). Among these mutations, a common frameshift mutation occurs in an unstable region of nine cytosines (c.641-c.649), causing the introduction of a stop codon seven AAs downstream of insertion (c.649-650insC>p.Arg217Profs*7) (Lee et al., 2012). The c.649dupC frameshift mutation leads to an unstable mRNA or a truncated form of the protein that is degraded, resulting in a loss-of-function pathogenetic mechanism (Lee et al., 2012; Li et al., 2015; Liu et al., 2016).

A variety of other nonsense or frameshift mutations are mostly located in the long N-terminal domain of the protein (figure 2), scattered in the proline-rich domain, and only a few involve the transmembrane domains or the cytoplasmic

loop (Heron et al., 2012). In addition to these truncated mutants, a few missense mutations were also identified (Gardiner et al., 2012).

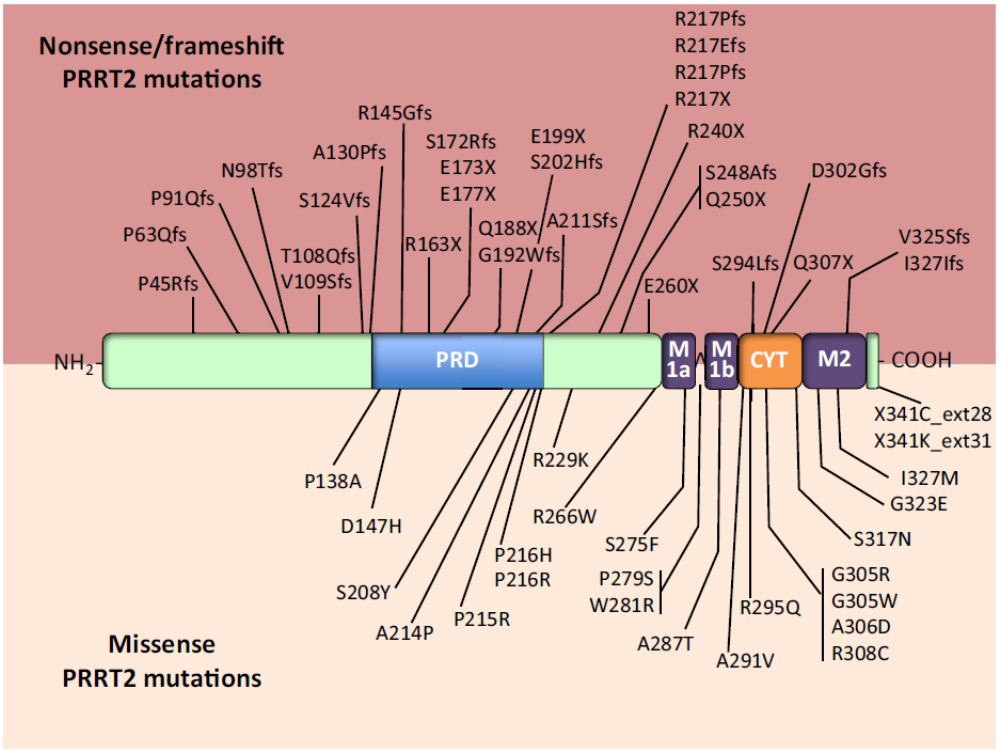

Figure 2. Mapping of PRRT2 Mutations Superimposed to the Domain Structure of Proline-Rich Transmem- brane Protein (PRRT2) Protein. Mutations in PRRT2 have been recently identified as the cause for a heterogeneous group of paroxysmal neurological diseases. The identified nonsense/frameshift and missense mutations are reported on the PRRT2 domain structure in the upper and lower panels, respectively. (Valtorta et al., 2016)

A recent discovery has identified heterozygous mutations in PRRT2, which encodes proline-rich transmembrane protein 2, in most families affected by benign familial infantile seizures (BFIS) (Heron et al., 2012). PRRT2 is also the major causative gene for familial paroxysmal kinesigenic dystonia (PKD) (Chen et al., 2011), a rare disorder characterized by the episodic occurrence of involuntary attacks of choreoathetosis or dystonia. Moreover, these studies illustrated that in a given family both disorders may be variably co-inherited as a single trait (Heron et al., 2012), corroborating the existence of familial infantile convulsions with paroxysmal choreoathetosis (ICCA) (Szepetowski et al., 1997). More recently, other paroxysmal neurological manifestations have been reported in heterozygous patients: paroxysmal non-kinesigenic dyskinesia (PNKD), migraine with or without aura, hemiplaegic migraine, various type of non-infantile

seizures, torticollis and episodic ataxia (EA; Méneret A, et al., 2013) Previous reports of three patients suggested that homozygous PRRT2 mutations may give rise to more severe clinical disease of mental retardation, with or without EA and epilepsy (Najmabadi H, et al., 2011; Labate A, et al., 2012). In addition, a recurrent genomic deletion of about 600 kb at 16p11.2, and encompassing several genes including PRRT2, has been associated with a composite syndromic phenotype displaying dysmorphisms, macrocephaly, speech/language delay, cognitive impairment, and a range of neuropsychiatric conditions including autistic spectrum disorder and intellectual disability, with or without paroxysmal disorders (Figure 3; Shinawi, M. et al., 2010; Weiss, L.A. et al., 2008). The dosage unbalance of multiple genes may have an additive or multiplicative effect on the phenotype and the role of specific genes–including PRRT2–is largely unknown.

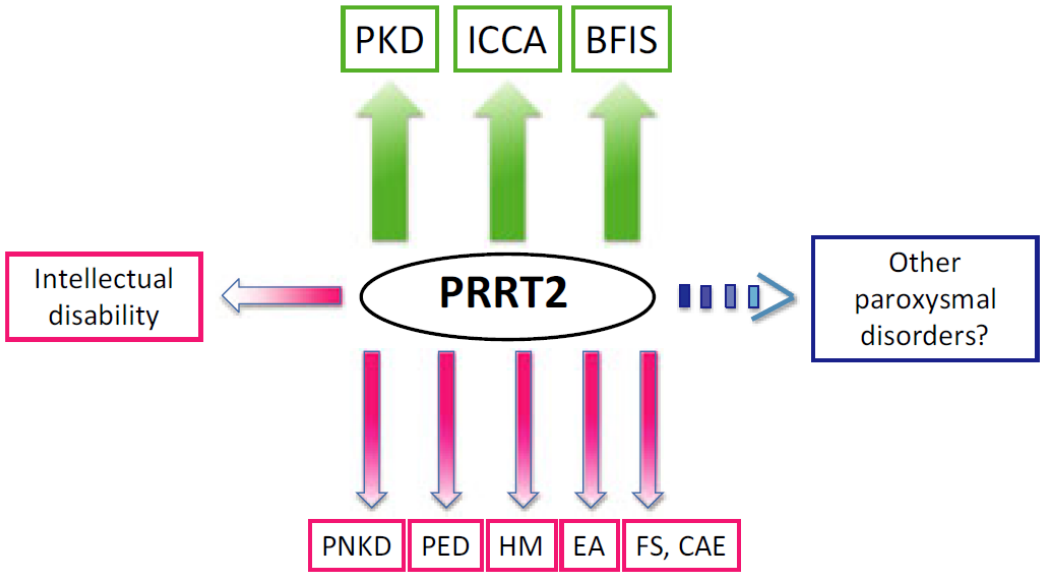

Figura 3. Clinical spectrum of PRRT2 mutations. The large green arrows point to phenotypes predominantly caused by PRRT2 mutations [paroxysmal kinesigenic dyskinesia (PKD), infantile convulsions with choreoathetosis syndrome ICCA), benign familial infantile seizures (BFIS)]. The thin pink arrows point to phenotypes rarely induced by PRRT2 mutations [paroxysmal non-kinesigenic dyskinesia (PNKD), paroxysmal exerciseinduced dyskinesia (PED), hemiplegic migraine (HM), episodic ataxia (EA), febrile seizures (FS), childhood-absence epilepsy (CAE)]. The dashed blue arrow indicates putative but unproven PRRT2 mutation-related phenotypes. (Méneret A, et al., 2013)

2.2 PRRT2 Expression and Localization

The dominant effect of PRRT2 mutations associated with diverse paroxysmal disorders points to an important role of the protein in neuronal activity. PRRT2 expression was prominent throughout the adult brain, with the highest levels in the cerebellum, basal ganglia, and neocortex. In the cerebral cortex and hippocampus, the PRRT2 gene was already expressed at early postnatal stages, and its expression increased to reach a plateau at 1 month of life, a period of intense synapse formation and rearrangement (Valente et al., 2016). In contrast, PRRT2 expression is almost undetectable in primary astroglial cultures, consistent with the neuron-specific expression of PRRT2. To explore the expression pattern of PRRT2 in vivo, in Chen et al. (2011) they measured the levels of PRRT2 mRNA in various body tissues of mice by RT-PCR. At postnatal day 7 (P7), PRRT2 was detected at low levels in the heart, lung, kidney and skin, but was most highly expressed in the brain and spinal cord. From the examination of the temporal expression pattern of PRRT2 in the developing mouse brain they reveal that the levels of PRRT2 mRNA are relatively low before embryonic day 16 (E16) and are markedly increased during early postnatal stages. PRRT2 mRNA levels peaked at P14 and then declined to a relatively low level in adulthood. RT-PCR and in situ hybridization analyses of P14 mouse brain revealed that PRRT2 is expressed throughout the developing brain, with high levels present in the cerebral cortex, hippocampus and cerebellum, and expression is enriched in cortical layers of the cerebral cortex, as well as in granule cells and Purkinje cell layers of the cerebellum. PRRT2 was enriched in the synaptic membrane fraction (LP1), but was also detected in synaptic vesicle (LP2) and postsynaptic density (PSDI) fractions, indicating the presence of PRRT2 at both pre- and post-synaptic membranes (Liu et al., 2016). To verify the subcellular distribution of PRRT2 at the synapse, in Valente et al. (2016) they fractionated purified synaptosomes to isolate synaptic junctions, subsequently separated into active zone (AZ), postsynaptic density (PSD), and a fraction including extrinsic and integral

membrane proteins associated with the presynaptic area (non- synaptic synaptosomal protein [NSSP]) (Phillips et al., 2001). PRRT2 was enriched in the NSSP fraction, like SNAP-25 and synaptophysin. Although the protein appeared to be substantially absent from the PSD, low levels were associated with the AZ fraction.

A yeast two-hybrid screen already revealed a potential interaction of PRRT2 in neural function with synaptosomal-associated protein of 25 kDa (SNAP25) (Stelzl U., et al., 2005), one of the three presynaptic SNARE proteins that govern SV exocytosis (Sudhof, T.C. and Rizo, J., 2011). Consistent with this observation, recombinant PRRT2 was found to distribute in the axons, with the highest concentration at synaptic contacts (Lee, H.Y., et al., 2012). The presynaptic localization of PRRT2 was confirmed by several groups (Heron, S.E., et al., 2013; Valente et al., 2016; Becker, F. et al., 2013; de Vries, B. et al.,2012; Luo, C. et al., 2013). Upon subcellular fractionation of the mouse brain, we found that PRRT2 co-distributed with SNAP25 and with proteins associated with the presynaptic area (Figure 4; Valente et al., 2016). Detectable levels of PRRT2 were also found in association with SVs. These results suggest that during the exo-endocytotic cycle of SVs, PRRT2 cycles between the presynaptic cytoplasm and the SV membrane, as shown for SNAP25.

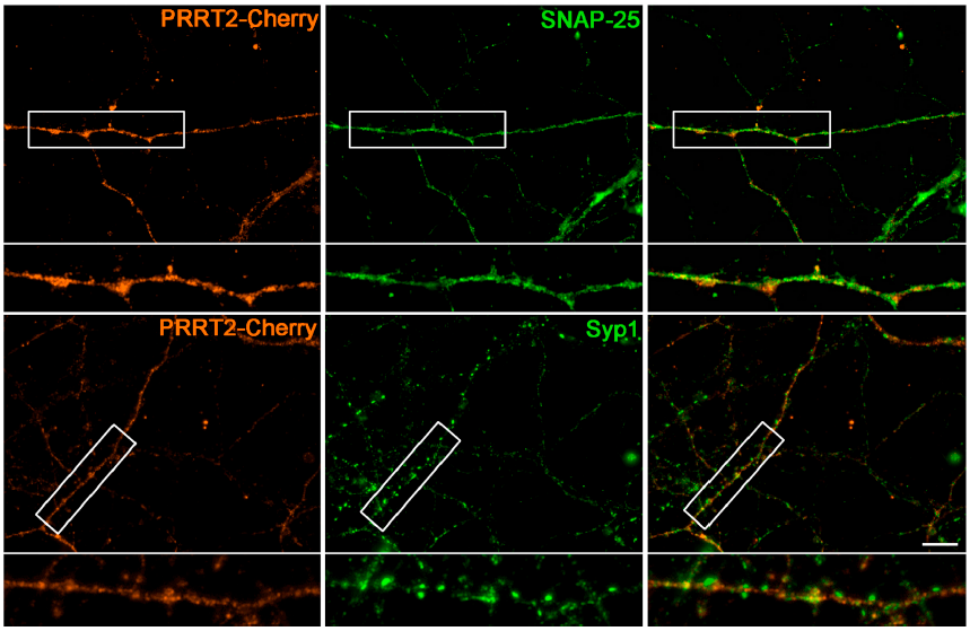

Figure 4. Localization of PRRT2 in mature neurons. Primary hippocampal neurons transduced at 10 DIVs with PRRT2-mCherry (red) were subjected to immunostaining at 15 DIVs with antibodies to PRRT2, SNAP-25, and Syp1. PRRT2 immunoreactivity (red) largely overlapped with the staining of the two presynaptic proteins in axonal and nerve terminal areas. Scale bar, 10 mm. (Valente et al., 2016)

PRRT2 was detected, albeit at very low levels, also in fractions enriched in postsynaptic densities (Valente et al., 2016; Liu, Y.T. et al., 2016). Thus, while its distribution indicates that PRRT2 is primarily a presynaptic protein, it is possible that it plays some role also in the postsynaptic compartment, in line with its putative interaction with the GluA1 subunit (GRIA) of the AMPA-type glutamate receptor complex, suggested on the basis of proteomic (Schwenk, J. et al., 2014; Shanks, N.F. et al., 2012) and co-immunoprecipitation (Li, M. et al., 2015) studies. Indeed, PRRT2 has been found to limit the membrane distribution of GRIA in the postsynaptic membrane (Li, M. et al., 2015), and PRRT2 immunoreactivity has been recently localized at the tip of dendritic spines (Liu, Y.T. et al., 2016).

PRRT2 is transcribed and expressed selectively in neurons (Chen et al. 2011; Valente, Castroflorio et al. 2016). To investigate whether its expression is pan-neuronal or restricted to specific neuronal populations, my colleagues have (Valente et al., 2019) performed double immunostaining of primary hippocampal neurons with antibodies against Ca^{2+}/calmodulin-dependent protein kinase type II (CamKII) and glutamic acid decarboxylase-67 (GAD67) that specifically label glutamatergic and GABAergic neurons, respectively, and a polyclonal antibody raised against an N-terminal domain peptide of mouse PRRT2 (amino acids 1–268; Liu et al. 2016; Figure 5 Upper panels), firstly tested in WT neurons. PRRT2 was widely expressed in both excitatory and inhibitory neurons: not only the percentage of PRRT2-positive cells was approaching 100%, but also the immunoreactivity at the cell body level was quantitatively similar in both neuronal populations. Consistent with its neuron-specific expression, PRRT2 staining was absent from GFAP-positive astrocytes in primary WT cultures (Figure 5 Lower panels).

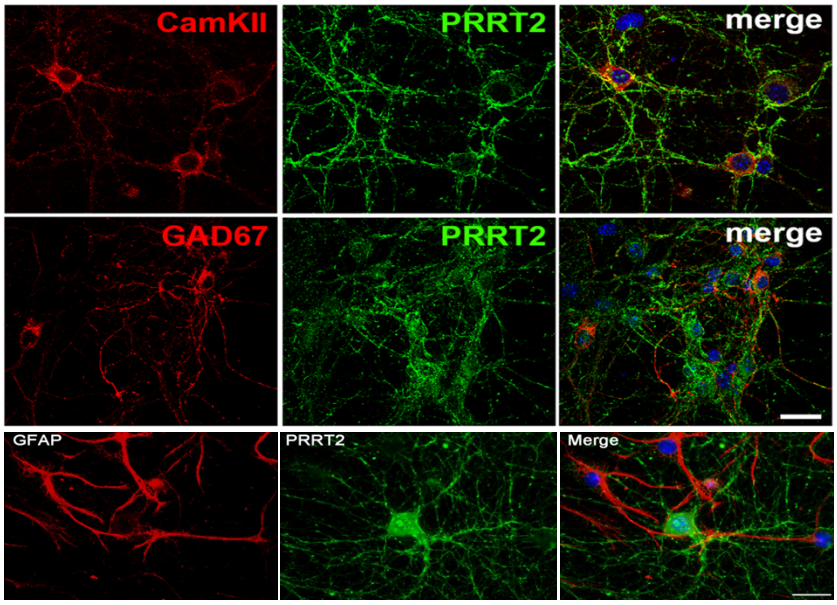

Figure 5. Upper. Immunoreactivity for PRRT2 (green) in CamKII-positive excitatory neurons (upper row, red) and GAD67-positive inhibitory neurons (lower row, red) in hippocampal WT neurons at 17 DIV. Merge panels show the double-labeled neurons. Scale bar, 50 µm. Lower. Representative images of double immunostaining for PRRT2 and GFAP in WT primary hippocampal cultures at 17 DIV. GFAP-positive astrocytes (red) are devoid of specific PRRT2 staining that only decorates adjacent neurons. Scale bar: 20 µm. (Valente et al., 2019)

My research group have also investigated also in detail the PRRT2 distribution at the synaptic level by double immunostaining primary WT neurons for PRRT2 and either the vesicular glutamate transporter-1 (VGLUT1) or the vesicular GABA transporter (VGAT) to label excitatory and inhibitory synapses, respectively (Figure 6). When PRRT2 expression was analyzed at synaptic puncta in which the respective transporter and PRRT2 immunoreactivities were colocalized, PRRT2 was more widely distributed in excitatory synapses (80.6 ± 1.5%) than in inhibitory synapses (47.4 ± 2.8%). Moreover, the analysis of the intensity of PRRT2 immunoreactivity at excitatory and inhibitory synaptic puncta revealed that PRRT2 was more intensely expressed in excitatory than in inhibitory synapses with a higher correlation of its labeling intensity with VGLUT1 than with VGAT immunoreactivity.

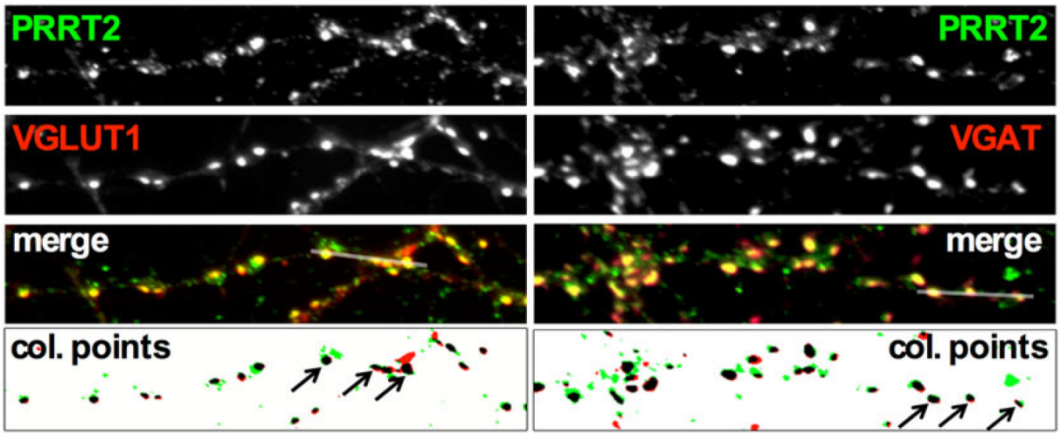

Figure 6. Representative images of synaptic contacts from 17 DIV rat hippocampal neurons labeled with PRRT2 antibodies (green in the merge panel) and either the excitatory presynaptic marker VGLUT1 (red, left panel) or the inhibitory presynaptic marker VGAT (red, right panel). Merge panels identify synaptic puncta in which PRRT2 and the respective transporter colocalize (yellow) and that are reported below in the binary image (Col. points). (Valente et al., 2019)

Silencing of PRRT2 induces extensive defects of synaptic structure and function. The most striking effect of acute silencing is a decreased number of synaptic contacts, observed in primary cultures (where it reaches 50%) as well as in vivo (Valente et al., 2016; Liu, Y.T. et al., 2016). There are also significant changes in the network connectivity. In primary PRRT2-KO hippocampal networks, the population of excitatory neurons was slightly increased and that of GABAergic neurons decreased with respect to WT cultures run in parallel. The PRRT2 deletion acts on the density of synaptic connections. From the analysis of colocalization of synaptic puncta of a couple of specific pre- and postsynaptic markers such as VGLUT1/Homer-1 for glutamatergic synapses and VGAT/Gephyrin for GABAergic synapses, it has been found that the constitutive PRRT2 deletion decreased the density of excitatory synapses, while no significant changes were observed in the density of inhibitory connections (Valente et al., 2019).

The analysis of PRRT2-KO excitatory synapses by conventional transmission electron microscopy revealed a substantial preservation of the nerve terminal ultrastructure. Indeed, the density, diameter, clustering and spatial distribution of SVs in concentric shells from the AZ were unaffected by PRRT2 deletion, except for a significant increase in the number of SVs physically docked at the AZ

that was also previously observed after acute depletion of the protein (Valente, Castroflorio et al. 2016).

Given that PRRT2 is localized at synaptic sites, in Valente et al., (2019) evaluated the expression of a panel of synaptic markers (Snap25, vGLUTs, SYTs, vGAT) using qRT-PCR in primary hippocampal neurons from WT and PRRT2-KO mice at various stages of in vitro development. The mRNA levels of all genes tested showed no significant differences between WT and PRRT2-KO neurons except for PRRT2 at any time point.

3. PRRT2 is a Key Component of the Ca^{2+}-Dependent Neurotransmitter Release Machinery

The presynaptic distribution of PRRT2 indicates a potential role in neurotransmitter release. Such a role could be hindered by mutations of the gene, as documented by the phenotype of the PRRT2-related diseases. To dissect the effects of PRRT2 silencing, were investigated spontaneous release, stochastically occurring at resting [Ca^{2+}] concentrations; evoked synchronous release, temporally bound to the action potential and the ensuing Ca^{2+} inflow at the active zone. To analyze how PRRT2 KD affects the function and strength of excitatory and inhibitory synapses and avoid the confounding effects of non-transduced neurons, in Valente et al. (2016) it was used autaptic hippocampal neurons.

These autaptic neurons was infected with a short hairpin RNAs (shRNA) with a fluorescence tag (turboGFP) that allowed to distinguish the PRRT2 silenced neurons (Sh4) from the Scramble (Scr) one and allowed to proceed to analyze: 1) synaptic density 2) spontaneous and 3) evoked synaptic transmission.

Mature (14 DIVs) neurons was infected with either Sh4 at 7 DIVs and analyzed by counting synapse density. Valente et al. (2016) and colleagues identified Synaptic boutons by counting puncta with a size of <1 mm double-positive for pairs of

pre/postsynaptic proteins such as Bassoon/Homer1 or synaptophysin/PSD95. Strikingly, the density of excitatory synapses along dendrites was decreased by ~50% in neurons silenced for PRRT2 with either shRNA, an effect that was fully rescued by the expression of shRNA-resistant PRRT2. This data confirmed the decrease in synapse density in the absence of major changes in the terminal ultrastructure (Figure 7).

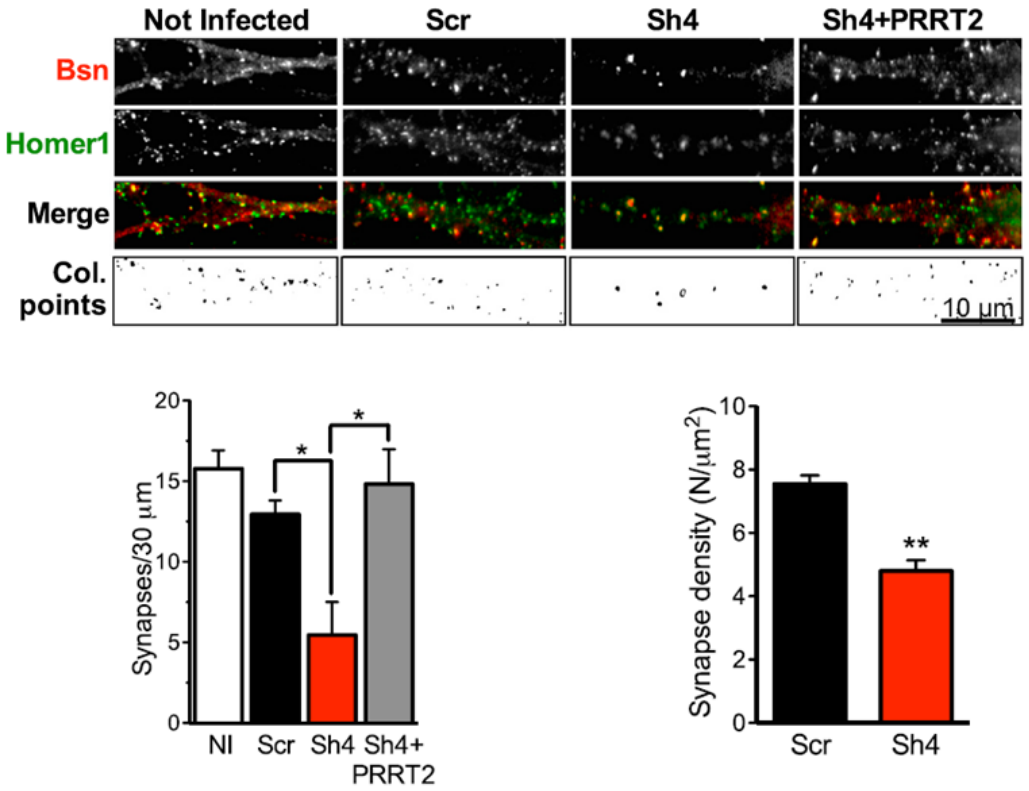

Figure 7. PRRT2 Knockdown Decreases Synapse Density. Upper. Representative images of dendrites of hippocampal neurons infected at 7 DIVs with Scr, Sh4, and Sh4 + Sh4-resistant PRRT2 (Sh4+PRRT2) or left uninfected and analyzed at 14 DIVs. Synaptic boutons were identified by double immunostaining for Bassoon (Bsn, red) and Homer1 (green). The colocalization panels (Col. points) highlight the double-positive puncta (black) corresponding to synapses. Scale bar, 10 mm. Lower left. Quantitative analysis of synaptic puncta counted on 30-mmdendrite tracts starting from the cell body in neurons treated as in upper figure. Data are means ± SEM from three independent experiments, each carried out in duplicate. Five dendrites for each neuron, from at least ten neurons for each sample, were counted. *p < 0.05, one-way ANOVA/Bonferroni's multiple comparison test. NI, not infected. Lower right. Quantitative analysis of the synaptic density from serial ultrathin sections. The volume density of symmetric and asymmetric synapses was calculated from the 2D count of synaptic profiles in sections from Sh4- (red bars) and Scr-treated (black bars) neurons and is expressed as mean (± SEM) number of synapses per square micrometer. (Valente et al., 2016)

Miniature excitatory postsynaptic currents (mEPSCs; Figure 8, upper) were continuously recorded at the soma of voltage-clamped neurons held at –70 mV in the presence of tetrodotoxin (TTX) to block spontaneous APs (Chiappalone et al., 2009). Strikingly, the mEPSC frequency (Figure 8, lower) fell down in PRRT2-silenced cultures, an extent much larger than expected from the decrease in synapse density (Figure 8) observed in PRRT2-silenced autaptic excitatory neurons. A reduction of approximately the same extent was also observed in the mEPSC area and amplitude (Figure 8, lower). Such a change may be attributable to the corresponding reduction in the average SV volume, although concomitant postsynaptic effects cannot be excluded.

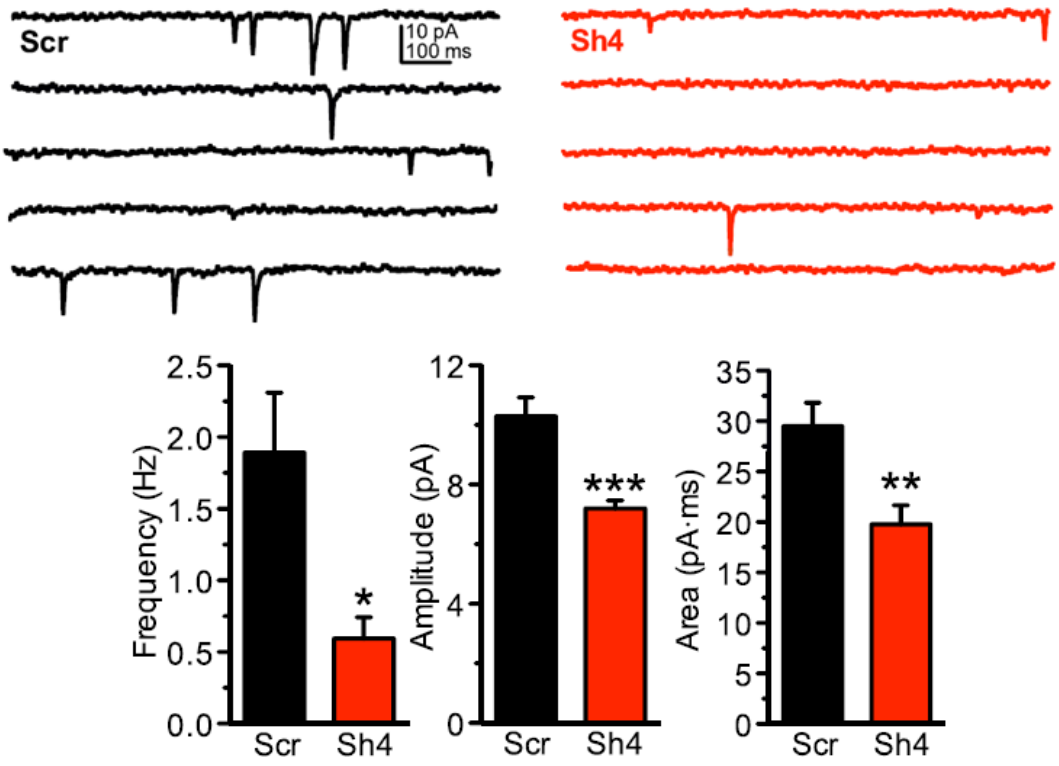

Figure 8 Upper. Representative recording traces of mEPSCs from PRRT2-KD synapses (Sh4, red traces) and control synapses (Scr, black trace). Lower. Analysis of mEPSCs, from left to right, shown are mean ± SEM frequency, amplitude, area of mEPSCs calculated for PRRT2 KD (n = 11, red bars) and control (n = 15, black bars) neurons. All values were obtained from 100–1000 events recorded from each cell in 5-min recordings. (Valente et al., 2016)

For the analysis of evoked transmission, transduced autaptic neurons, identified as excitatory or inhibitory based on the kinetics of postsynaptic currents (PSCs) and sensitivity to specific blockers of AMPA or gamma-aminobutyric acid receptor type A (GABAA) receptors, were stimulated with paired stimuli at an interpulse interval of 50 ms to evaluate the paired-pulse ratio (PPR), an indirect measure of release probability (Fioravante and Regehr, 2011).

In Valente et al. (2016), my research group has shows a dramatic decrease of eEPSC amplitude (Figure 9) in response to single stimuli with a strong increase in paired-pulse facilitation; this effect was reversible with co-infection of the neurons with Sh-resistant PRRT2 that was able to achieve a virtually complete return of current amplitude and PPR to the levels of Scr-infected neurons. A closely similar phenotype was observed in PRRT2-silenced inhibitory neurons, which represent 7%–10% of the total autaptic neuronal population under our culture conditions

The PRRT2 deletion in treated neurons, suggest a presynaptic defect affecting release probability, thereby rendering facilitation more intense in excitatory synapses or depression milder in inhibitory synapses.

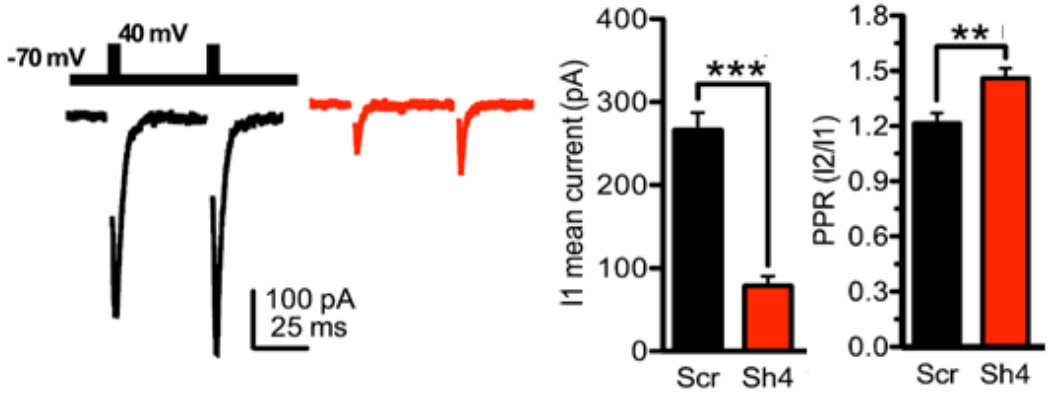

Figure 9. On the left a representative eEPSCs recorded in excitatory autaptic neurons infected with Scr (black trace/ bar, n = 39), PRRT2-Sh4 (red trace/bar, n = 32). eEPSCs were elicited by clamping the cell under study at –70 mV and stimulating it with two voltage steps to +40 mV lasting 0.5 ms at an interstimulus interval of 50 ms. The paired-pulse stimulation was applied every 10 s (inset). On the right decrease of eEPSC amplitude and increase of PPR by PRRT2 KD. (Valente et al., 2016)

In Valente et al. (2016) my colleagues, also performed a cumulative evoked EPSC (eEPSC) amplitude analysis to identify the quantal parameters of release affected by PRRT2 silencing (Figure 10). Stimulating neurons with a train of 2 s at 40 Hz, they shows a significant depression of eEPSCs became apparent during the train in both control and silenced neurons, irrespective of the amplitude of the first current in the train by a slower linear increase, reflecting the equilibrium between the depletion and constant replenishment of the RRP. The reduction of the current amplitude in silenced neurons was contributed by a sharp decrease in the initial Pr together with a significant decrease of the RRPsyn total current, in parallel of an unvaried number of readily releasable SVs (Nsyn) suggesting, a normal priming process generating the RRP in PRRT2 KD neurons. The substantial preservation of the total pool of readily releasable SVs indicates that the same total SV pool is shared by synchronous and asynchronous release and further suggests that SV priming is not affected by PRRT2 silencing. Therefore, the strong impairment in evoked synchronous release is likely to involve changes in the Ca^{2+} dependence of release that can occur at the level of either Ca^{2+} entry or Ca^{2+} sensing.

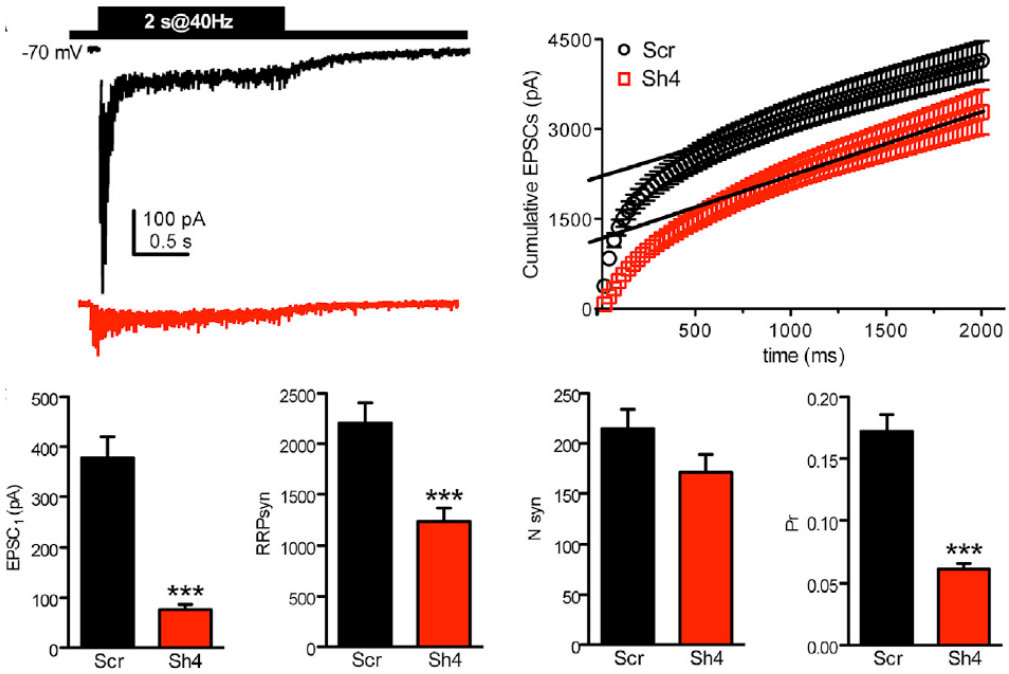

Figura 10. Upper. Representative recordings of eEPSCs evoked by high-frequency stimulation (train of 80 stimuli at 40 Hz, inset) in autaptic hippocampal neurons infected with Scr (black trace) or PRRT2-Sh4 (red trace). Stimulation artifacts were blanked for clarity. Profiles of the mean cumulative amplitude of eEPSCs. Data points in the 1- to 2-s range were fitted by a linear regression and back-extrapolated to time 0 (solid lines) to estimate the RRPsyn. Lower. Results of the quantal analysis. From left to right, shown are the mean ± SEM amplitude of the first eEPSC, RRPsyn size, number of RRPsyn quanta, and initial probability of release (Pr) estimated in neurons infected with Scr (n = 38, black bars) or PRRT2-Sh4 (n = 34, red bars). (Valente et al., 2016)

Given the sharp impairment in spontaneous and evoked release, they investigated the Ca^{2+} sensitivity of release by increasing the extracellular Ca^{2+} concentration. In Scr-treated neurons, the increase in external Ca^{2+} from 2 to 4 mM enhanced the amplitude of eEPSCs while decreasing PPR (Figure 11), consistent with a heightened release probability. Strikingly, PRRT2-silenced neurons were totally insensitive to the increase in extracellular Ca^{2+} as far as evoked release were concerned.

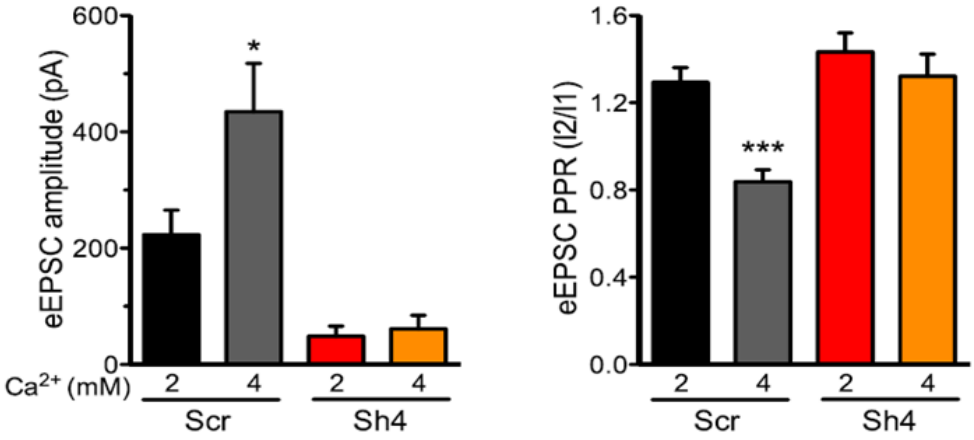

Figura 11. eEPSC amplitude evoked by the first pulse (I1, left) and PPR (I2/I1, right) recorded in neurons transduced with Scr (black/gray bars, n = 7) or PRRT2- Sh4 (red/orange bars, n = 6). The graph bars represent the mean of the EPSC amplitude and PPR recorded in individual cells before (black/red bars) and after (gray/orange bars) the increase of the extracellular Ca^{2+} concentration to 4 mM. (Valente et al., 2016)

Taken together, the data point to a fundamental role of PRRT2 in the machinery for synchronous release, whose strong decrease may depend on an impairment of Ca^{2+} secretion coupling or Ca^{2+} entry.

Thus, the investigation was focused on presynaptic proteins that, when deleted in knockout (KO) mice, cause a strong impairment in evoked release, including the SNARE proteins VAMP2, SNAP-25, syntaxin 1 and the fast Ca^{2+} sensors synaptotagmins (Syt) 1/2. Co-immunoprecipitation experiments from brain

extracts with anti-Syt1 and anti-Syt2 antibodies confirm showed that PRRT2 indeed associates with both Syt1 and Syt2 (Figure 12 upper panels). Both Syts isoforms were decreased in PRRT2 KD neurons. To evaluate whether the phenotype of PRRT2 KD is attributable to the interaction with either or both Syt1/Syt2, Valente and colleagues tried to rescue the impairment in the evoked synchronous release by overexpressing Syt2 in PRRT2 KD autaptic neurons (Figure 12 lower panels). Expression of Syt2 induced a significant but not complete rescue of PRRT2 KD-induced impairment in eEPSC amplitude, although its magnitude was smaller than the complete rescue obtained with Sh-resistant PRRT2.

The lack of a full rescue obtained upon the reintroduction with Syt2 and the insensitivity to the increase in the external calcium (previously shown in Figure 11), suggested us that acute knockdown of PRRT2 could not only play a role in the "Calcium sensing" but also in the "Calcium entry".

In other words, we speculated that the deletion of PRRT2 could negatively affect presynaptic Ca^{2+} influx through presynaptic Ca^{2+} channels and from such hypothesis I have developed my PhD research project.

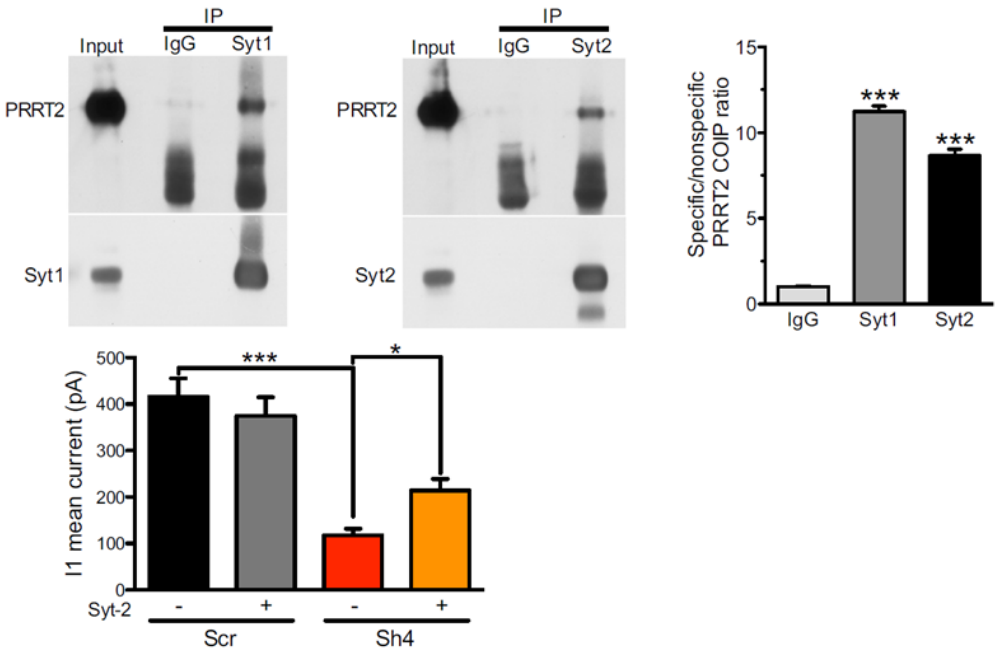

Figura 12. Upper. Co-immunoprecipitation of PRRT2 with Syt1 and Syt2. Detergent extracts of mouse brain were immunoprecipitated (IP) with monoclonal antibodies (mAbs) specific for Syt1 and Syt2 or with the respective control mouse immunoglobulin Gs (IgGs) as indicated. After electrophoretic separation of the immunocomplexes and western blotting, membranes were probed with anti-Syt1/anti-Syt2 antibodies to test the efficiency of the immunoprecipitation as well as with polyclonal anti-PRRT2 antibodies. Left: a representative immunoblot is shown. Right: quantification of the PRRT2 immunoreactive signal in the immunoprecipitated samples, normalized to the binding to the mouse IgG control (means ± SEM, n = 3 independent experiments). Input, 10 mg total extract. Lower. Overexpression of Syt2 partially rescues the impairment in synchronous release of PRRT2 KD neurons. Autaptic hippocampal neurons were infected at 7 DIVs with Scr (n = 31), Sh4/mCherry (Sh4, n = 30), Syt2/GFP (Syt2, n = 28), or Sh4+Syt2 (n = 27) and recorded at 14 DIVs. The histograms show the means ± SEM of the eEPSC amplitude evoked by the first pulse (I1, left) and of the PPR (I2/I1, right). *p < 0.05, **p < 0.01; ***p < 0.001; Kruskal Wallis/Dunn's multiple comparison test (I1); one-way ANOVA/Bonferroni's multiple comparison test (PPR). (Valente et al., 2016)

4. Calcium Channels

Calcium influx into presynaptic nerve terminals via voltage-gated Ca^{2+} channels is an essential step in neurotransmitter release. Voltage-gated Ca^{2+} channels are key routes for Ca^{2+} entry into electrically excitable cells. Increases in free intracellular Ca^{2+} concentrations are linked to a plethora of cellular responses, including the activation of Ca^{2+} dependent enzymes, initiation of gene transcription, and the release of neurotransmitters from presynaptic sites (Reid, C.A. et al. 2003). Multiple types of voltage-gated Ca^{2+} channels are expressed throughout the nervous system and these differ in their cellular and subcellular distributions, biophysical and pharmacological properties, and physiological roles (Snutch, T.P. et al. 2005).

Early electrophysiological recordings from neurons suggested the existence of two major classes of Ca^{2+} channels based upon the membrane potentials at which they first open: low-voltage activated (LVA) and high-voltage activated (HVA). The LVA (or T-type) channels, typically have a small conductance (8-12 pico Siemens (pS)), open in response to small changes from the resting membrane potential and inactivate rapidly kinetics (Carbone et al., 2014). In contrast, the HVA (L-, N-, P/Q- and R-type) currents generally possess larger conductances (15-25 pS), are activated by stronger depolarizations and display variable inactivation kinetics. Nine individual neuronal voltage-gated Ca^{2+} channels have been identified and classified by their biophysical and pharmacological profiles as L-, N-, P-, Q-, R- or T-types. This diversity arises

predominantly from the nature of the principal pore-forming a1 subunit. There are three different families of Ca^{2+} channel a1 subunits: Ca_v1 genes encode L-type channels, Ca_v3 genes encode T-type channels, and Ca_v2 genes encode N-type, P/Q-type and R-type channels, with P-type and Q-type channels arising from alternative splicing of the $Ca_v2.1$ gene (Catterall, W.A. 2000). The a1 subunit comprises four homologous transmembrane domains (I–IV), each of which contains six membrane spanning helices (S1–S6) plus a reentrant p-loop motif that lines the channel pore to enable passage of Ca^{2+}. The four domains are connected through cytoplasmic linkers, and both C and N termini are cytoplasmic (Figure 13). These regions form key interaction sites for regulatory proteins. Members of the Ca_v1 and Ca_v2 families associate with ancillary b subunits (encoded by four different genes), a2–d subunits (four different genes) and possibly g subunits (eight different genes), which aid membrane expression and alter the biophysical characteristics of the a1 subunit (Arikkath, J. and Campbell, K.P. 2003; Klugbauer, N. et al. 2003; Kang, M.G. and Campbell, K.P. 2003). The b subunit is a cytoplasmic protein that binds to the a1 subunit domain I–II linker (Van Petegem, F. et al. 2004). The a2–d subunit is translated as a single protein but cleaved into d (a single transmembrane-spanning helix) and a2 (the extracellular domain), which are linked by a disulfide bonds; however, its interaction site on the Ca^{2+} channel a1 subunit is unknown.

L-type Ca^{2+} channels were initially described in peripheral neurons and cardiac cells, but appear to be present in all excitable as well as many types of non-excitable cells. In certain cells, L-type channels have been shown to be preferentially localized to specific subcellular regions. The L-type channel is the primary route for Ca^{2+} entry into cardiac, skeletal, and smooth muscles. The skeletal muscle L-type channel acts as a voltage sensor for excitation-contraction (E-C) coupling in skeletal muscle, presumably linking membrane depolarization to Ca^{2+} release from intracellular stores. While Ca^{2+} entry through this channel is not required for the initiation of contraction in skeletal muscle, it may provide a source of Ca^{2+} to replenish internal stores.

The predominant Ca^{2+} channel subtypes in synaptic nerve terminals are P/Q-type and N-type channels, where their opening is linked to the rapid release of synaptic vesicles (Reid, C.A. et al. 2003). Although both N-type and P/Q-type channels primarily support neurotransmitter release at hippocampal synapses (Wu, L.G. and Saggau, P. 1994; Scholz, K.P. and Miller, R.J. 1995; Reid, C.A. et al. 1997; Reid, C.A. et al. 1998; Wheeler, D.B. et al. 1996; Qian, J. and Noebels, J.L. 2001), cerebrocortical synapses (Millan, C. et al., 2002; Mintz, I.M. et al. 1995) and calyx-type synapses (Wu, L.G. et al. 1999). R-type channels make a small contribution to evoked transmitter release in some preparations (Iwasaki, S. and Takahashi, T. 1998; Gasparini, S.A. et al. 2001) but play a more important role in synaptic plasticity (Dietrich, D. et al. 2003). L-type and T-type Ca^{2+} channels are not normally involved in excitatory transmitter release.

The a1 pore-forming subunit is a key determinant of the properties of Ca^{2+} channel subtypes (Catterall, W.A. 2000), with P/Q-type channels containing a1A subunits ($Ca_v2.1$), N-type channels containing a1B subunits ($Ca_v2.2$) and R-type channels containing a1E subunits ($Ca_v2.3$) (Ertel, E.A. et al. 2000). Mixed population of N-type and P/Q-type Ca^{2+} channels can coexist at a single release site and contribute jointly to the local Ca^{2+} transient that triggers transmitter release. This view is supported by several findings. Both N-type and P/Q-types of Ca^{2+} channel support the release of glutamate at excitatory synapses in the hippocampus (Luebke et al., 1993; Wu and Saggau, 1994b; Scholz and Miller, 1995) and in the cerebellum (Mintz et al., 1995; Regehr and Mintz, 1994). Several lines of evidence suggest that a mixed population of Ca^{2+} channel subtypes coexists at individual synaptic terminals and cooperate to support neurotransmitter release (Takahashi and Momiyama, 1993; Castillo et al., 1994; Regehr and Mintz, 1994; Wheeler et al., 1994a, 1996; Wu and Saggau, 1994b; Mintz et al., 1995). The mix of subtypes may not be the same at all terminals, and it has been suggested that N-type Ca^{2+} channels are solely responsible for neurotransmitter release at a subset of terminals (Reuter 1995; Wheeler et al. 1996). Both N-type and P/Q-types of Ca^{2+} channels can be modulated

differentially (Wu and Saggau, 1994b; Wu and Saggau, 1995). Thus, a non uniform distribution of Ca^{2+} channel subtypes could permit selective alteration of transmitter release at groups of terminals on a single afferent, which would have important ramifications for synaptic modulation and plasticity.

A mixed population of N-type and P/Q-type Ca^{2+} channels can coexist at a single release site and contribute jointly to the local Ca^{2+} transient that triggers transmitter release. This view is supported by several findings. The most convincing is that the percentage block of synaptic current by a selective N-type antagonist and the block by a selective P/Q-type antagonist sum to +/-100% (Reid, C.A. et al. 1997; Wu, L.G. and Saggau, P. 1994; Wheeler DB et al., 1996). Supra-additivity can be explained only if Ca^{2+} entering through N-type channels can reach the same vesicle release site as Ca^{2+} entering through P/Q-type channels, on the timescale of transmitter release. This evidence (Reid, C.A. et al. 2003) supports a colocalization of both channel subtypes at some presynaptic terminals, but it does not demonstrate that all terminals contain both subtypes.

Both N-type and P/Q-type Ca^{2+} channels contain a specific synaptic protein-interaction site ('synprint') in the intracellular loop that links domains II and III (Rhian M. et al. 2006); this site binds synaptic proteins such as syntaxin 1, synaptosome-associated protein of 25 kDa (SNAP-25), cysteine string protein (CSP), Rim and synaptotagmin 1 (Figure 13).

Besides being a key synaptic targeting motif (Mochida,S. et al. 2003; Szabo, Z. et al. 2006), the synprint region seems to be an important modulatory site that enables synaptic proteins to regulate channel activity per se. In both transient expression systems and neurons, binding of syntaxin 1 and SNAP-25 results in a hyperpolarizing shift in the potential at which half of the P/Q-type and N-type Ca^{2+} channels in a sample are inactivated (the half-inactivation potential), thus reducing channel availability (Verderio, C. et al. 2004; Bergsman, J.B. and Tsien, R.W. 2000; Stanley, E.F. 2003) and presumably the amount of neurotransmitter that is released. N-type and P/Q-type channels undergo different inhibition in

response to activation of G-protein-coupled receptors (GPCRs; Carbone, Carabelli et al., 2001; Zamponi, G.W. 2001; Strock, J. and Diverse-Pierluissi, M.A. 2004). Although both N-type and P/Q-type Ca2+ channels are regulated by second messenger activity and associate with synaptic vesicle release machinery, they differ in their precise regulation and in their abilities to integrate multiple signaling inputs.

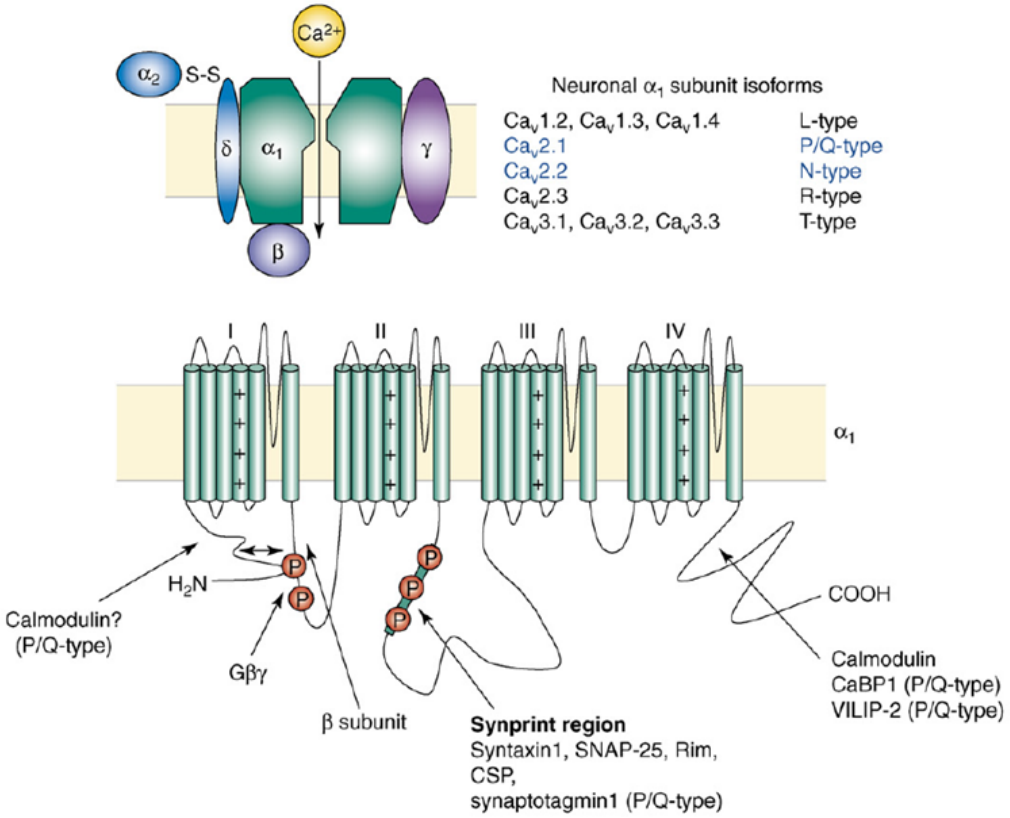

Figura 13. Structural aspects of voltage-gated Ca^{2+} channels. Subunit composition of Ca^{2+}channels and putative transmembrane topology of the α1 subunit. Key protein interaction sites are indicated. Red circles represent key phosphorylation sites and plus symbols denote the voltage-sensitive membrane-spanning helix of each domain. G-protein βγ subunits might interact at a macrosite formed by binding of the N terminus to the domain I–II loop. (Rhian M. et al. 2006)

Pharmacological studies that involve selective calcium channel antagonists (Wheeler DB et al. 1994), and immunocytochemical characterization of calcium channel distribution (Westenbroek RE et al 1992; Westenbroek RE et al. 1998; Timmermann DB et al. 2002), suggest that the N-type and P/Q-type calcium channels are the predominant species involved in synaptic transmission. Because of the high buffering capacity of neurons, it is

thought that free calcium ions diffuse only short distances before being sequestered by calcium binding proteins, which results in a steep drop in intracellular calcium concentration that radiates from the inner mouth of the calcium channel pore in to the cytoplasm (Augustine GJ 2001). Additionally, the putative calcium sensor(s), such as synaptotagmin, are considered to have a relatively low affinity for calcium (Augustine GJ 2001). Hence, to sense calcium entry, the vesicular release machinery must be localized in close proximity to presynaptic calcium channels. Indeed, the presynaptic calcium channels of vertebrate neurons display a highly restricted subcellular distribution in the active zone, and co-localize with the vesicular release machinery (Westenbroek RE et al. 1998). This gives rise to what are expected/observed to be highly ordered presynaptic ultrastructures that can, as in the case of the frog neuro-muscular junction, result in the formation of a protein scaffold that supports rows of docked synaptic vesicles connected to the plasma membrane (Harlow ML et al. 2001). Biochemical evidence has demonstrated that key synaptic proteins involved in the docking of synaptic vesicles to the active zones — syntaxin1, SNAP25 and synaptotagmin 1 — bind to a 225 amino acid stretch in the intracellular domain II-III linker region of thea1subunitof mammalian N-type and P/Q-type calcium channels (termed synaptic protein interaction or 'synprint' site)(Bennett et al., 1992; Leveque C et al., 1994; Sheng Z et al., 1994, 1996, 1997; Rettig Jet al., 1996). This site is considered unique to vertebrate $Ca_v2.2$ (N-type) and $Ca_v2.1$ (P/Q-type) channels, as corresponding regions of other calcium channel subtypes such as L-type (Sheng Z et al., 1994; Rettig Jet al., 1996) or R-type (Pereverzev A et al., 2002) do not appear to associate with syntaxin1 or SNAP25in vitro. The presence of either syntaxin1A, syntaxin1B or SNAP25 results in decreased channel availability because of a hyperpolarizing shift in the voltage-dependence of inactivation of transiently expressed (Bezprozvanny I et al., 1995; Bezprozvanny I et al., 2000; Zhong H et al., 1999; Jarvis SE et al., 200; Jarvis SE et al., 2001) and native N-type and P/Q-type calcium channels

(Bergsman JB et al., 2000). Interestingly, in the presence of both syntaxin1 and SNAP25, channel availability becomes normalized, which would favor calcium entry through channels that are capable of docking to a pre-synaptic vesicle (Zhong H et al., 1999; Jarvis SE et al., 2001).

5. Aims of the project

The goal of my research project was the investigation of the altered Ca^{2+} dependence of the synaptic transmission as a possible causative role in the pathogenesis of PRRT2-Diseases

I focused my research activity on the study of presynaptic calcium influx involved in the impairment of the synaptic transmission caused by acute and chronic deletion of PRRT2.

I have used various technical approaches: electrophysiology, immuncitochemistry, biochemistry and live calcium imaging aimed to analyze changes of somatic and presynaptic voltage gated calcium channel subtypes in PRRT2-deficient neurons.

In particular I have studied:

- The effects of PRRT2 deletion on the glutamate neurotransmission in relation to the increase of extracellular calcium concentration.
- The effects of PRRT2 acute/chronic deletion on the different presynaptic VG-Ca^{2+} channel subtypes that contribute to glutamatergic synaptic transmission.
- The effects of PRRT2 acute/chronic deletion or PRRT2 over-expression on the somatic L-type, N-type and P/Q-type VG-Ca^{2+} currents.
- The effect of PRRT2 chronic deletion on the intracellular and membrane expression of P/Q- and N-type VG-Ca^{2+} channels.
- The effect of PRRT2 deletion on the localization of P/Q-type VG-Ca^{2+} channels at presynaptic boutons.
- The effect of PRRT2 acute deletion or over-expression on the presynaptic calcium signal dependent on P/Q-type VG-Ca^{2+} channels.

I based my investigation on three different experimental *in vitro* models:

1) WT cultured hippocampal neurons infected at 6 div with a lentiviral vector transducing a shRNA inducing an efficient knockdown of PRRT2 expression (Valente et al., 2016) at 6 days after the infection (12 div).
2) WT cultured hippocampal neurons infected at 6 div with a lentiviral vector transducing the native form of PRRT2, able of inducing over-expression of the protein at 12 div (Valente et al., 2016)
3) Cultured hippocampal neurons obtained from PRRT2 knockout (KO) mice, developed by EUCOMM/KOMP that we have extensively previously characterized (Valente et al., 2019; Fruscione et al., 2018; Michetti et al., 2017).

6. Results

6.1 PRRT2 knockdown and knockout reduced the enhancement of eEPSCs induced by increasing extracellular Ca^{2+} concentration

We recorded evoked excitatory synaptic transmission in hippocampal autaptic neurons infected with a Lentiviral Vector encoding a short hairpin RNAs (shRNAs) named SH4, able to massively reduce the expression of the endogenous PRRT2 protein, or with the Scramble (named scrRNAs) control RNA (previously validated in Valente et al., 2016).

The over-expression of PRRT2 was obtained using a lentiviral vector that expresses the native form of the PRRT2 protein (named OVER) or mCherry control RNA. Neurons were infected at 6 DIV and electrophysiological experiments were conducted between 11 and 14 DIVs (figure 14).

Electrophysiological recordings were performed at increasing extracellular Ca^{2+} concentration. We prepared 4 external solutions with a calcium concentration of: 0.5, 1, 2, 4 mM. In these 4 solutions, the concentration of magnesium was progressively decreased from 3.5 to 0 mM, with the goal of maintaining constant the total concentration of bivalent cations ($[Mg^{2+}] + [Ca^{2+}]= 4$ mM). We also used a concentration of 8 mM Ca^{2+} (0 Mg^{2+}) to better appreciate saturation of the dose-response curve.

Voltage-clamp (VC) recordings of eEPSCs were performed using a VC stimulation protocol aimed to maintain the patched-neuron to a holding potential (Vh) of -70 mV. The excitatory glutamatergic transmission was evoked thank to a brief (0.5 ms) depolarizing voltage step at + 40 mV (Fig 14).

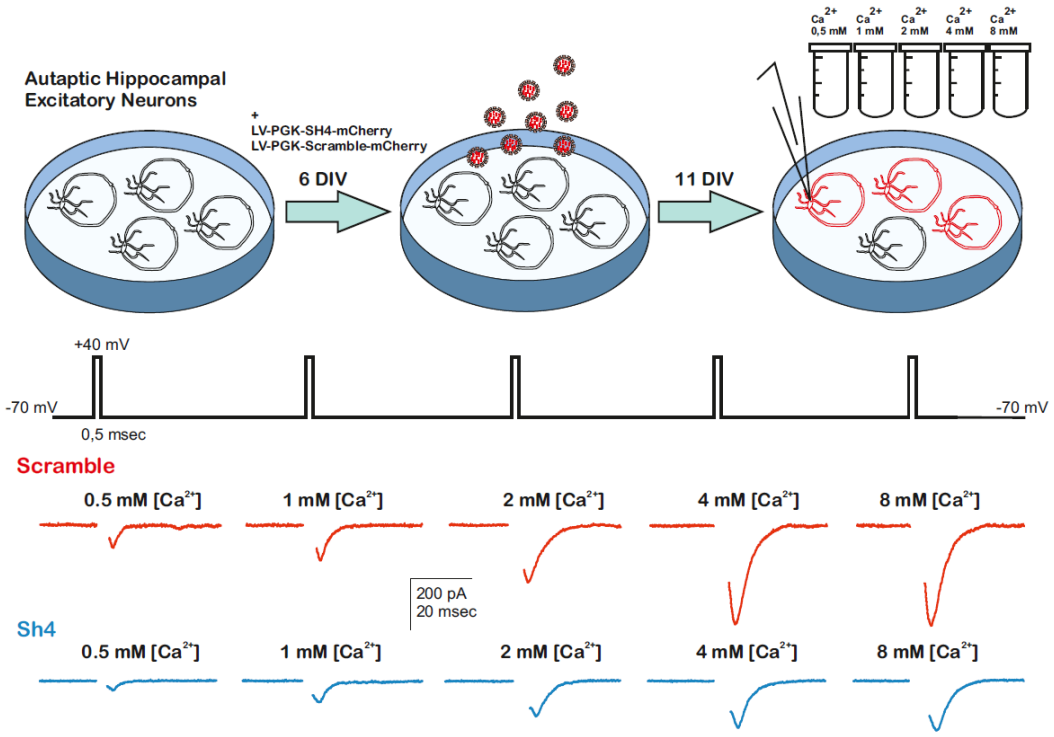

Figure 14. Representative experimental procedure for eEPSC recording. Graphic explanation (upper) of infection of autaptic hippocampal neurons at 6 DIV and recording with a crescent concentration of extracellular calcium and its consequent (lower) increase of synaptic current.

The dose-response curves showing the mean of eEPSCs amplitude at various $[Ca^{2+}]o$ were fitted using a sigmoidal Hill Equation:

$eEPSCs\ (pA) = I_{Max} * [Ca^{2+}]_o^n / ([Ca^{2+}]_o^n + EC50)$ where:

- I_{Max} represents the saturation level of the curve;
- n, named Hill coefficient, represents the slope of the dose-response curve at a $[Ca^{2+}]_o = EC50$;
- EC50 represents the $[Ca^{2+}]_o$ at which it was observed an eEPSC amplitude = $I_{Max}/2$.

Both acute and chronic deletion of PRRT2 did not significantly affect the Hill Coefficient (Figure 15), that show a mean value of ~3.5, in accord with the strong positive cooperativity that has been previously shown for the Calcium dependency of the glutamatergic synaptic transmission (Valente et al., 2016).

Also, the affinity constant (EC50) was not affected by acute and chronic deletion of PRRT2 (Figure 15). On the contrary the lack of PRRT2 induced a strong reduction of the largest eEPSCs evoked at higher calcium concentration. Such effect was particularly evident in knock-down neurons while it was strongly attenuated in knock-out cells (Figure 15).

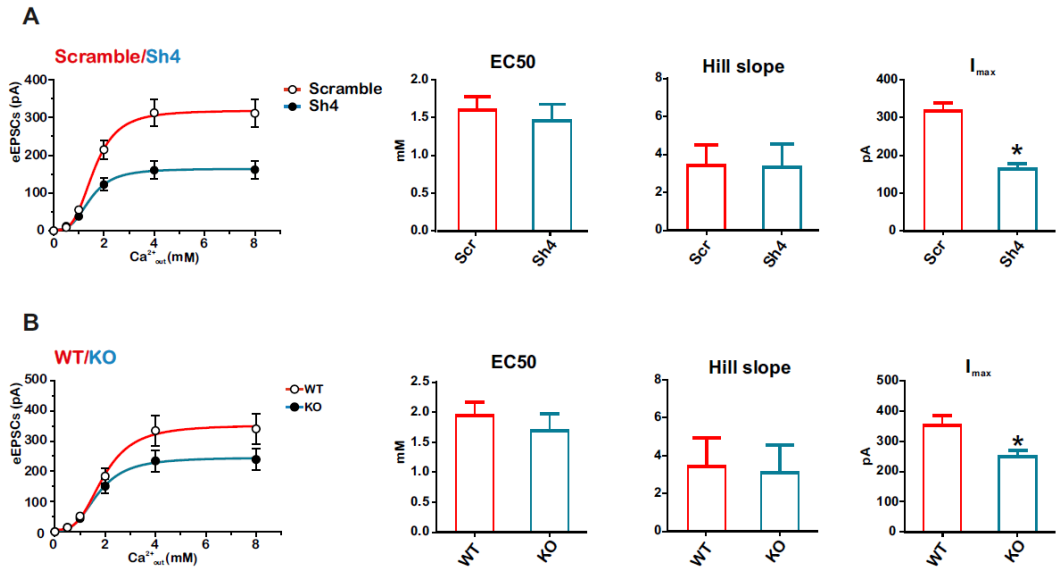

Figure 15. Dose-response curves of the amplitude of the eEPSCs at increasing extracellular calcium concentration. (A) the graph show the mean eEPSCs induced at various extracellular calcium concentration in scr (n=37)/SH4 (n=36) infected neurons *p<0.05 t student (B) the graph show the mean eEPSCs induced at various extracellular calcium concentration in WT (n=53)/KO (n=52) infected neurons *p<0.05 t student

We also studied paired-pulse facilitation induced by the administration of two consecutive voltage stimuli at a time interval of 50 ms (Figure 16). We observed a decreased of synaptic facilitation at higher extracellular calcium concentration (4-8 mM). Notably, the calcium dependent reduction of the facilitation was significantly decreased by PRRT2 deletion (Figure 16).

These results suggest that PRRT2 deletion could reduce presynaptic calcium influx through a negative modulation of VG-calcium channels. To test this hypothesis, we evaluated the contribution of individual VG-calcium channels subtypes on excitatory synaptic transmission.

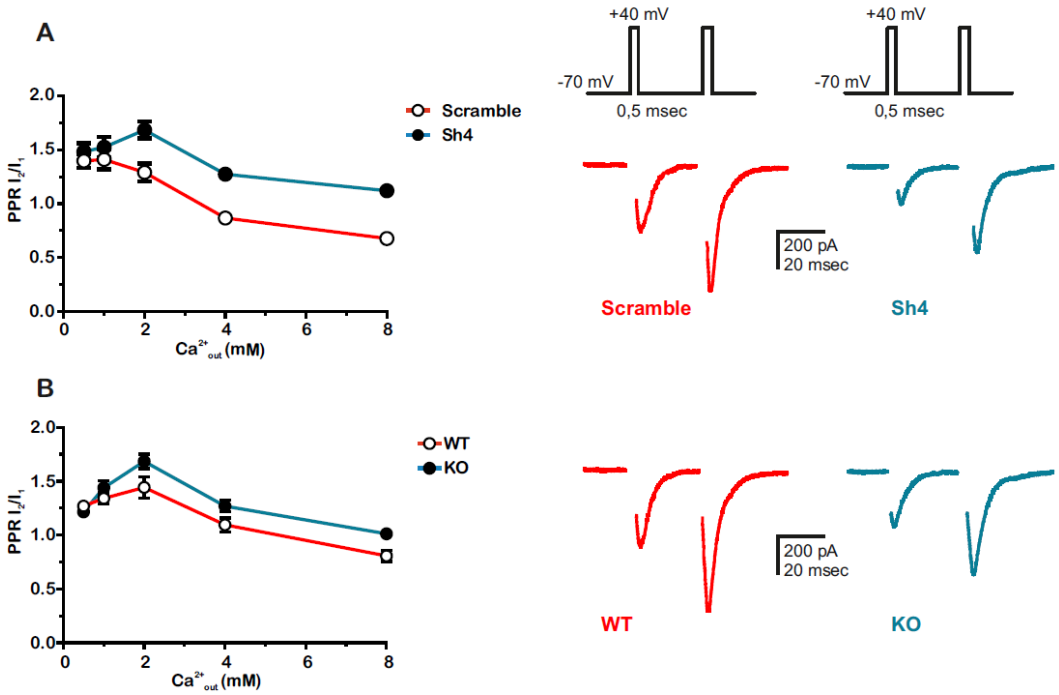

Figure 16. PRRT2 deletion decreased the reduction of synaptic facilitation at higher external calcium concentration. eEPSCs were elicited by clamping the cell under study at –70 mV and stimulating it with two voltage steps to +40 mV lasting 0.5 ms at an interstimulus interval of 50 ms. The paired-pulse stimulation was applied every 10 s. (A) Mean ± S.E.M. of the PPR at increasing calcium concentration in scr (n=37)/SH4 (n=36) and (B) WT (n=53)/KO (n=52) infected neurons *p<0.05 t student

6.2 PRRT2 acute/chronic deletion affects the contribution of presynaptic VG-Ca^{2+} channels to glutamatergic synaptic transmission

To evaluate the contribution of the voltage-gated calcium channels to the glutamatergic synaptic transmission, we initially recorded eEPSCs from autaptic neurons lacking PRRT2. eEPSCs recordings were conducted between 11 and 14 DIV at standard extracellular calcium concentrations (2 mM) and in the presence of 3 different VG-calcium channels selective antagonists. Nifedipine (5 µM) was used to block the eEPSCs due calcium influx through L-Type calcium channels, Agatoxin-IVA (0.2 µM) was used to block the eEPSCs dependent on activation of P/Q-Type calcium channels and Conotoxin-GVIA (3 µM) was used to block the eEPSCs deriving from the N-type calcium channels (figure 17).

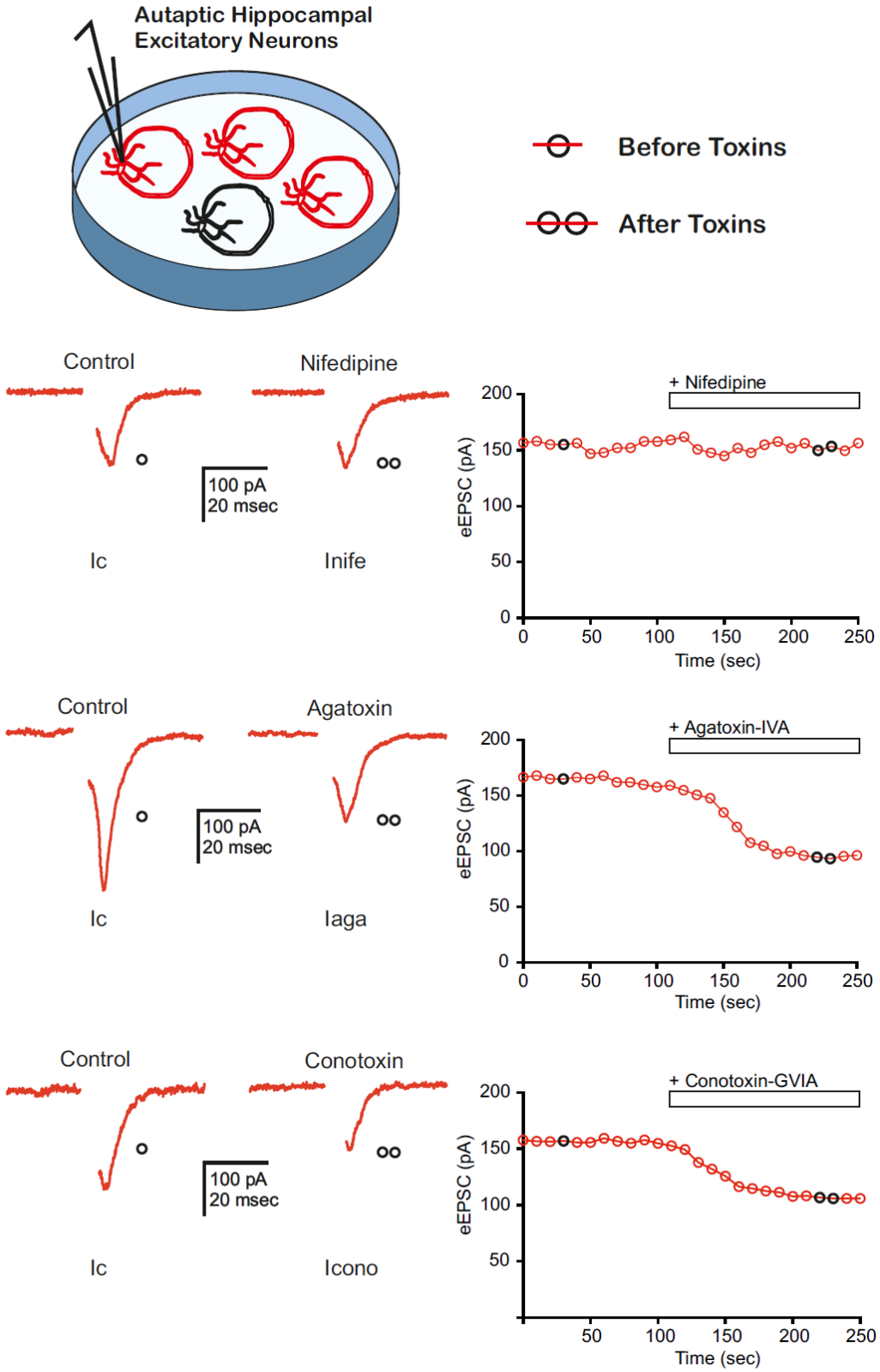

Figure 17. Graphical representation of the effect of toxins overtime on the synaptic current. eEPSCs were elicited by clamping the cell under study at –70 mV and stimulating it with a voltage steps to +40 mV lasting 0.5 ms. The stimulation was applied every 10 s. Toxins were applied after 2/3 minutes of control recording.

Calcium channels antagonists were applied into the recording solution after the stabilization of the eEPSC amplitde (≈ 2/3 minutes) and maintained until the next stabilization of the eEPSC amplitude in presence of the antagonists (Figure 17).

Nifedipine was used to block L-type voltage-gated calcium channels. As expected, (Pfrieger et al., 1992) the block of the L-type channels does not reduce the synaptic current in the control neurons and in PRRT2 KD/KO neurons (Figure 18).

Thus, we studied P/Q-type channels contribution to excitatory synaptic transmission. The percentage block of Agatoxin-IVA (≈40%) on the eEPSCs amplitude was not affected by acute/chronic deletion of PRRT2 while it was significantly reduced the amount of Aga-IVA sensitive eEPSCs, calculated as the difference between the control eEPSCs and the current that remains after the blockage of the P/Q-type channels (Figure 19).

Similar results were obtained in presence of Conotoxin-GVIA, a selective N-type channels blocker. Indeed, the percentage block of Cono-GVIA (≈30%) was not affected by acute/chronic deletion of PRRT2 while it was significantly reduced the amount of Cono-GVIA sensitive eEPSCs (Figure 20).

These results demonstrated that the lack of PRRT2 selectively reduced the glutamate release dependent on N- and P/Q-type calcium channel subtypes, suggesting that presynaptic N- and P/Q-type channels expression or function could be altered by PRRT2 deletion. At the light of these data, the next step was the pharmacological dissection somatic VG-calcium currents.

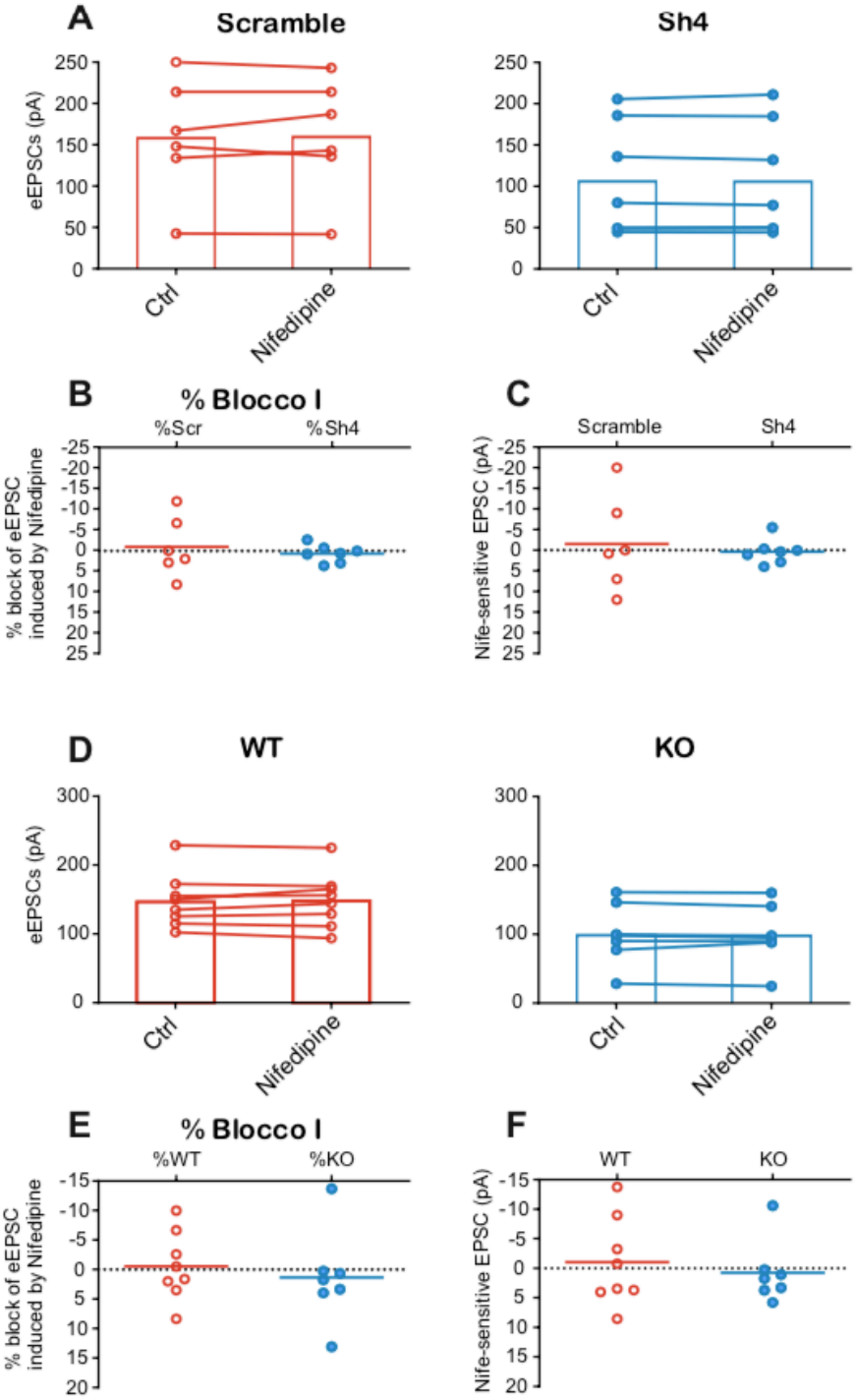

Figure 18. L-Type channels did not contribute to excitatory synaptic transmission in both control and PRRT2 lacking neurons. (A) Bar plots show mean ± S.E.M. eEPSCs in control condition and in presence of Nifedipine (5µM). (B) The graph shows the mean ± S.E.M % block eEPSCs induced by Nifedipine in scr (red, n=6) and SH4 (blu, N=7) p>0.05 unpaired t student (C) The graph shows the mean ± S.E.M of Nife-sensitive EPSC in scr (red, n=6) and SH4 (blu, N=7) p>0.05 unpaired t student. (D) Bar plots show mean ± S.E.M. eEPSCs in control condition and in presence of Nifedipine (5µM). (E) The graph shows the mean ± S.E.M % block eEPSCs induced by Nifedipine in WT (red, n=8) and KO (blu, N=7) p>0.05 unpaired t student (F) The graph shows the mean ± S.E.M of Nife-sensitive EPSC in WT (red, n=8) and KO (blu, N=7) p>0.05 unpaired t student.

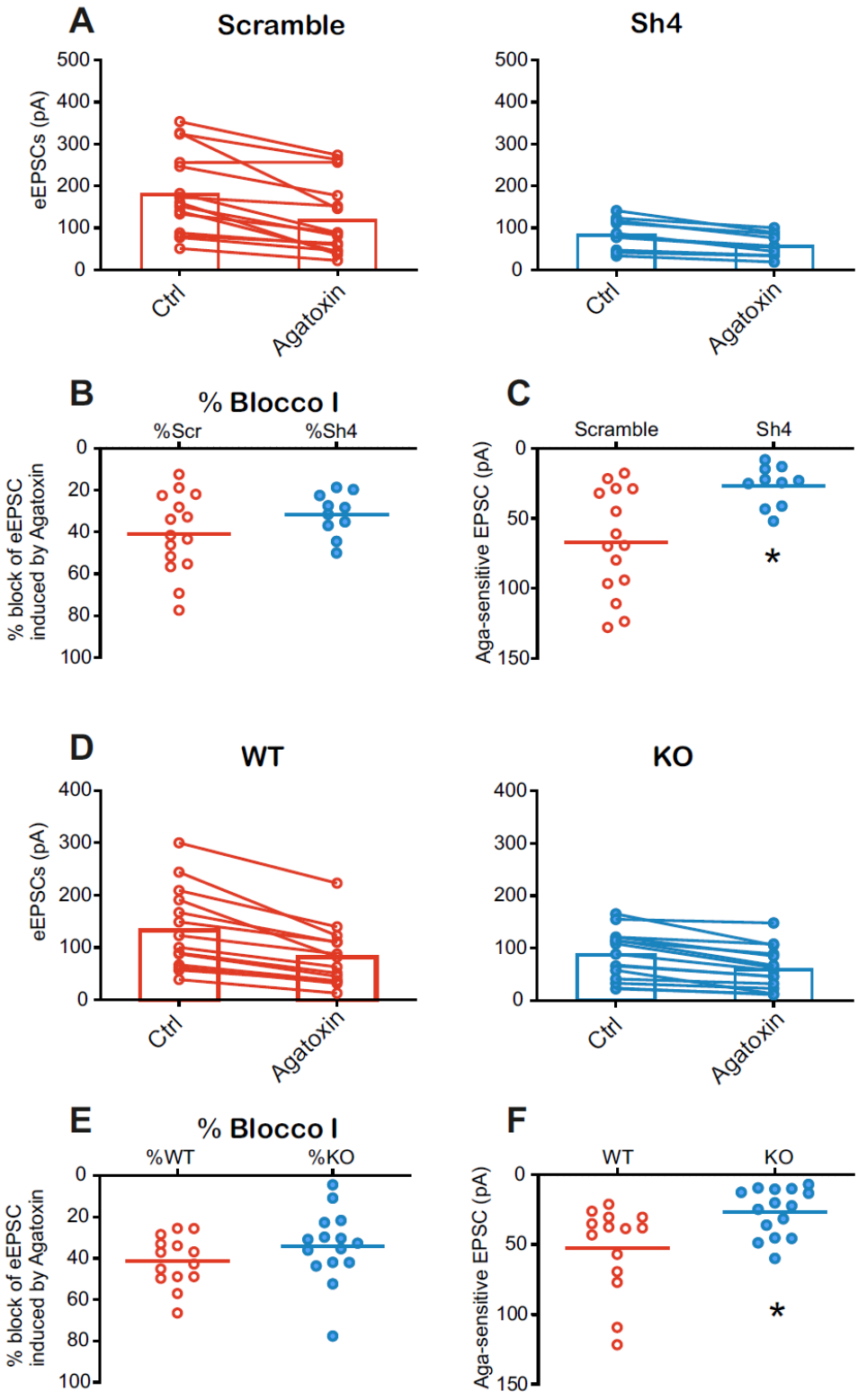

Figure 19. P/Q-Type channels contribution to excitatory synaptic transmission in both control and PRRT2 lacking neurons. (A) Bar plots show mean ± S.E.M. eEPSCs in control condition and in presence of Agatoxin (0,2μM). (B) The graph shows the mean ± S.E.M % block eEPSCs induced by Agatoxin in scr (red, n=15) and SH4 (blu, N=10) p>0.05 unpaired t student (C) The graph shows the mean ± S.E.M of Aga-sensitive EPSC in scr (red, n=15) and SH4 (blu, N=10) p>0.05 unpaired t student. (D) Bar plots show mean ± S.E.M. eEPSCs in control condition and in presence of Agatoxin (0,2μM). (E) The graph shows the mean ± S.E.M % block eEPSCs induced by Agatoxin in WT (red, n=14) and KO (blu, N=15) p>0.05 unpaired t student (F) The graph shows the mean ± S.E.M of Aga-sensitive EPSC in WT (red, n=14) and KO (blu, N=15) p>0.05 unpaired t student.

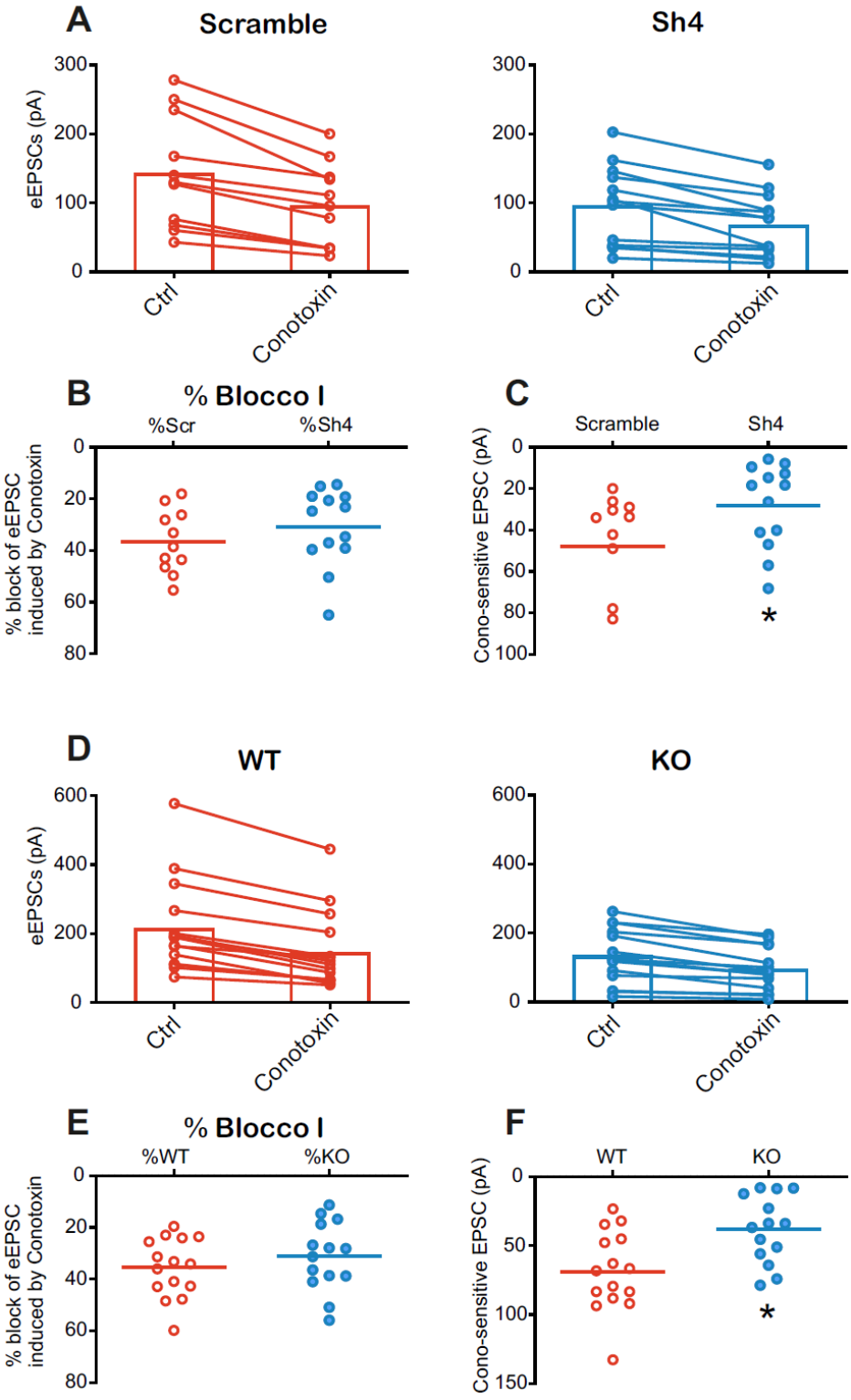

Figure 20. N-Type channels contribution to excitatory synaptic transmission in both control and PRRT2 lacking neurons. (A) Bar plots show mean ± S.E.M. eEPSCs in control condition and in presence of Conotoxin (3µM). (B) The graph shows the mean ± S.E.M % block eEPSCs induced by Conotoxin in scr (red, n=11) and SH4 (blu, N=13) p>0.05 unpaired t student (C) The graph shows the mean ± S.E.M of Cono-sensitive EPSC in scr (red, n=11) and SH4 (blu, N=13) p>0.05 unpaired t student. (D) Bar plots show mean ± S.E.M. eEPSCs in control condition and in presence of Conotoxin (0,2µM). (E) The graph shows the mean ± S.E.M % block eEPSCs induced by Conotoxin in WT (red, n=15) and KO (blu, N=14) p>0.05 unpaired t student (F) The graph shows the mean ± S.E.M of Cono-sensitive EPSC in WT (red, n=15) and KO (blu, N=14) p>0.05 unpaired t student.

6.3 Pharmacological dissection of somatic VG-Ca^{2+} currents

Voltage-gated calcium currents were recorded in low density cultured hippocampal neurons maintained for 10/14 days in vitro (10-14DIV).

The hippocampal neurons were obtained from postnatal (P0-P1) GAD67-GFP transgenic mice (Tamamaki N. et al., 2003).

In these mice, the fluorescent protein reporter, GFP, was specifically expressed in GABAergic neurons, under the control of the endogenous GAD67 promoter. GFP substitutes the introns in the 5' and 3' flanking region in one of the two GAD67 alleles. Thanks to this knock-in, we were able to clearly distinguish GAD67-GFP positive inhibitory interneurons from GAD67-GFP negative excitatory neurons (Figure 21B).

Neurons were infected by the addition of lentiviral vectors into cell medium at 10 DIVs. We have identified excitatory and infected neurons thanks to their negativity to GAD67-GFP and positivity to mCherry, respectively (Figure 21A).

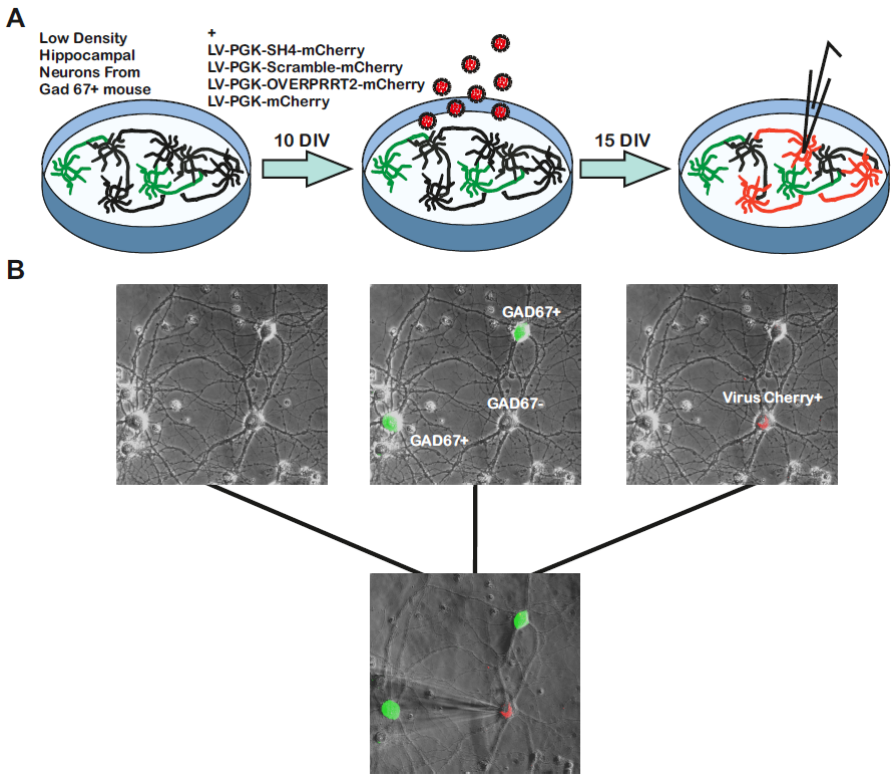

Figure 21. (A) The picture show the infection procedure adopted in cultured hippocampal neurons obtained from GAD67-GFP transgenic mice. (B) Micro photographs representing GAD67-GFP positive and negative neurons infected with scramble or SH4 RNA.

Low-density cultured hippocampal neurons express a cocktail of different LVA and HVA voltage-gated Ca2+ channels. In our cultured hippocampal neurons, we used patch-clamp recordings to investigate HVA calcium currents activated by 100-msec voltage steps from -70 mV to +70 mV in 10-mV increments from a holding potential of -70 mV at 0.2 Hz. This stimulation protocol allowed us to characterize the I/V (current/voltage) relationship and to reveal that the maximum Ca^{2+} current was elicited by 100-msec voltage pulses to -10 mV from the holding potential of -70 mV (Figure 22).

We used the above described test pulse to evaluate the effect of Nifedipine (5 µM), a selective blocker of L-Type Ca^{2+} currents, Agatoxin-IVA (0,2 µM) a selective blocker of P/Q-Type Ca^{2+} currents and Conotoxin-GVIA (3 µM) a selective blocker of N-Type Ca^{2+} currents (Figure 22 red traces).

Nifedipine is very useful because allowed to isolate non-L type Ca^{2+} currents from the somatic L-type currents. Note that DHP-sensitive L-type Ca^{2+} channels are mainly expressed at the level of the cell body, while DHP-insensitive, non-L types Ca^{2+} channels, mainly represented by R-, N- and P/Q-types, play a role at both the cell body and the presynaptic terminal, where they mediate Ca^{2+} influx activating fast synaptic vesicles release. These results revealed that at -10mV about 40% of the total calcium currents was due to L-type Ca^{2+} channels while the remaining 60% of non-L type Ca^{2+} currents was due to R-, N- and P/Q-types channel activation.

PRTT2 deletion did not affected membrane capacitance (Cm) in neurons overexpressign PRRT2 ($Cm_{mCherry}$=58,31 pF: Cm_{OVER}= 55,45 pF) and in neurons were PRRT2 was acutely deleted (Cm_{scr}= 76,09 pF, Cm_{SH4}=71,85pF) or in neurons where PRRT2 was chronically deleted (Cm_{WT}= 45,40 pF; Cm_{KO}= 45,85 pF). For this reason, we plotted absolute value of the calcium current intensity (I_{Ca2+}=pA), but we have also calculated Ca^{2+} current density (D_{Ca2+}=pA/pF) (data not shown)

obtaining similar results in term of changes due to PRRT2 over-expression or deletion.

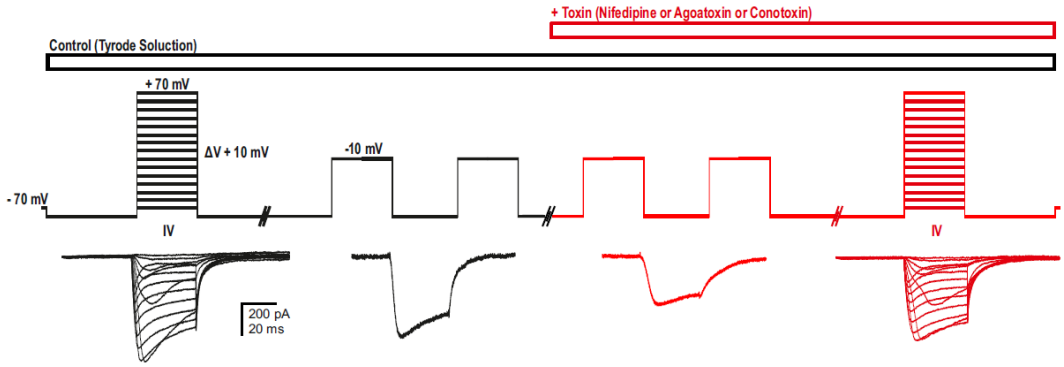

Figure 22. Representative scheme of the recording protocols used to isolate the calcium currents under control conditions (black trace) and in the presence of the three toxins (red trace) with a comparison of current intensity under control conditions (black trace) and post-toxins treatment (red trace).

6.3.1 Isolation of L-Type Ca^{2+} currents in hippocampal neurons overexpressing or lacking PRRT2

Hippocampal neurons have been infected with a shRNA, able to silence PRRT2 expression at 10 DIV and then recorded at 15 DIV to evaluate calcium currents intensity.

Patch-clamp recording revealed that total calcium currents are enhanced by PRRT2 over-expression while it was reduced by the acute deletion of PRRT2 (Figure 23A). These effects were further enhanced in presence of nifedipine suggesting that the lack of PRRT2 mainly affects non-L-type calcium current (Figure 23B), the calcium channel subtypes that drive NTs release at the presynaptic terminals. In accord with these results we also observed that PRRT2 deletion did not affect L-type calcium currents isolated subtracting Nife-insensitive currents from the total calcium currents (Figure 23C).

Thus, we focused our investigation on the N, P/Q-type calcium channels.

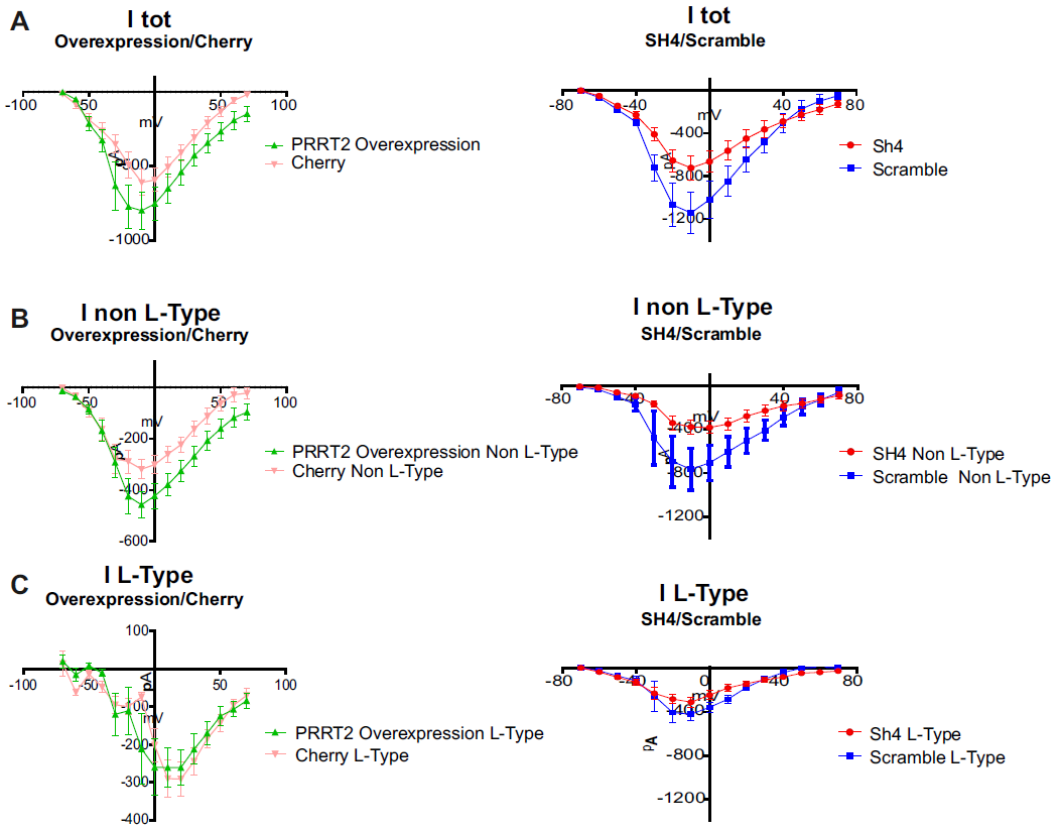

Figure 23. The graph show the current vs voltage relationships of total, non-L and L-type calcium current recorded in cherry(pink; n=8)/OVER(green; n=7) and scr(blu; n=8)/SH4(red; n=10) neurons. Statistical analysis was performed at -10 mV. *P < 0.05, **P < 0.01; Mann-Whitney U test.

6.3.2 Isolation of P/Q- and N-Type Ca^{2+} current in hippocampal neurons overexpressing or lacking PRRT2

Thanks to the experiments conducted in presence of Nifedipine, we identified the non-L-type channels as the main VGCCs subtypes sensitive to PRRT2 deletion. For this reason, we used the same protocol previously described (Figure 22), to evaluate the effect of PRRT2 deletion on the P/Q- and N-type calcium currents.

P/Q-type calcium currents (Figure 24C) have been isolated subtracting Aga-IVA-insensitive calcium currents (Figure 24B) from the total calcium currents (Figure 24A) that have been recorded in presence of Aga-IVA and in control condition, respectively. This analysis revealed that PRRT2 over-expression increased P/Q-type calcium currents, while PRRT2 deletion exerted the opposite effect (Figure 24C).

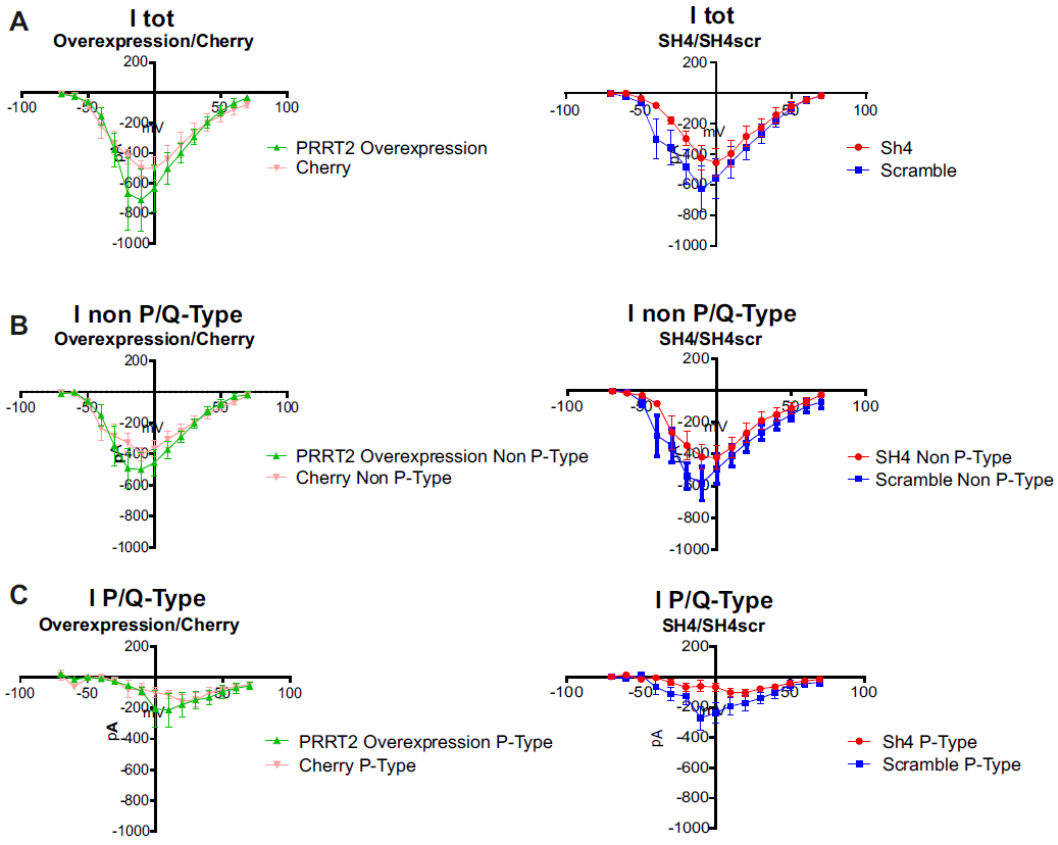

Figure 24. The graph show the current vs voltage relationships of total, non-P/Q and P/Q-type calcium current recorded in cherry(pink; n=9)/OVER(green; n=7) and scr(blu; n=9)/SH4(red; n=10) neurons. Statistical analysis was performed at -10 mV. *P < 0.05, **P < 0.01; Mann-Whitney U test.

We observed a similar behavior, isolating N-type currents, thanks to the application of the Conotoxin-GVIA. Indeed, PRRT2 overexpression and silencing increased and decreased the total Ca^{2+} currents, respectively (Figure 25A). Such effect was lost on non N-type currents (Figure 25B), and in accord with these result the isolation of pure N-type Ca^{2+} currents, obtained subtracting Cono-insensitive current from the total current, were strongly affected by the change in the PRRT2 expression level (Figure 25C).

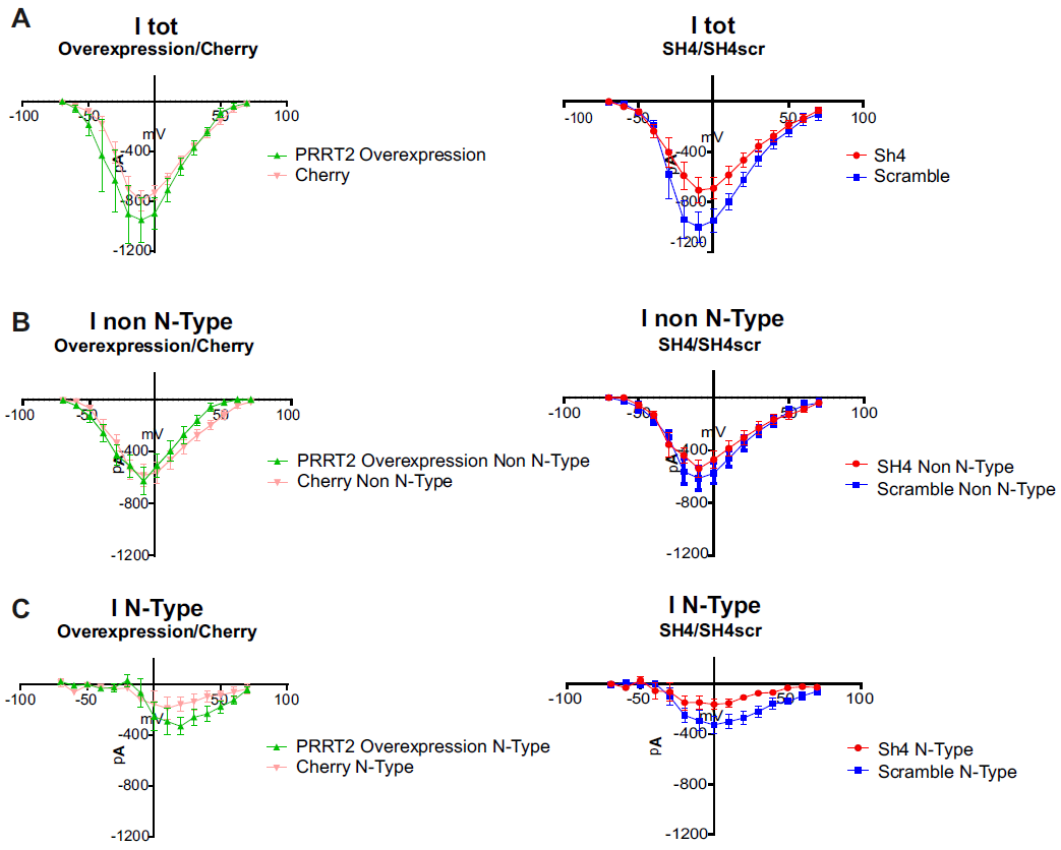

Figure 25. The graph show the current vs voltage relationships of total, non-N and N-type calcium current recorded in cherry(pink; n=10)/OVER(green; n=8) and scr(blu; n=10)/SH4(red; n=12) neurons. Statistical analysis was performed at -10 mV. *P < 0.05, **P < 0.01; Mann-Whitney U test.

To confirm these results, obtained with the acute PRRT2 deletion, we repeated the same experimental procedure comparing WT and PRRT2 KO neurons. The graphs shown in Figure 26, basically demonstrates that the chronic deletion of PRRT2 exerted the same effect observed in presence of the acute deletion (KD) of PRRT2 (Figure 23,24 and 25) with a significant reduction of both N- and P/Q-type currents, while L-type currents were unaffected.

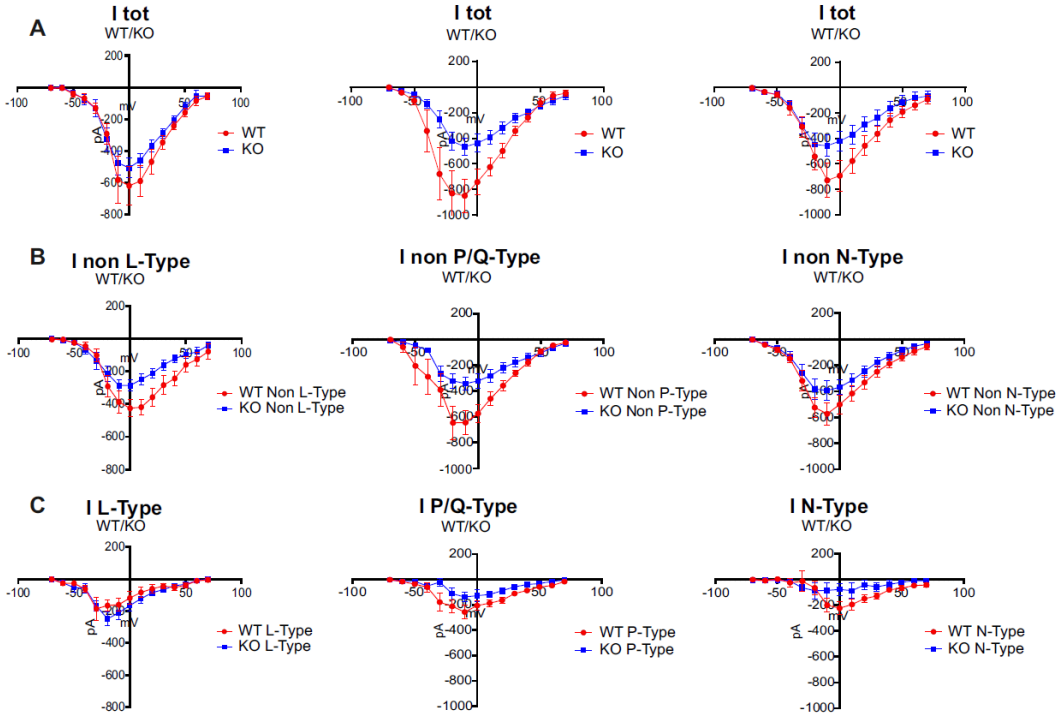

Figure 26. The graph show the current vs voltage relationships of total, non-L-, P/Q-, N and L-, P/Q-, N-type calcium current recorded in WT(red; n≈11)/KO(blu; n≈11) neurons. Statistical analysis was performed at -10 mV. *P < 0.05, **P < 0.01; Mann-Whitney U test.

These results suggested that PRRT2 could play a role in the expression level of N- and P/Q- Ca^{2+} channel subtypes or in their membrane trafficking.

6.4 VG-Ca^{2+} channels expression and membrane trafficking in PRRT2 KO neurons

Thus, we investigated whether the absence of PRRT2 affected P/Q-type VGCCs expression or their trafficking to the membrane by surface biotinylation of neurons.

Biotinylation of intact cells has emerged as an important tool for studying the expression and regulation of channels, receptors and transporters and others membrane proteins from the cytoplasmatic organelles to the plasma-membrane (as previously described in Fruscione et al., 2018).

Our data indicate that PRRT2 KO neurons show a significant decrease of the extracellular levels of P/Q-type VGCCs compared with WT neurons, with a parallel significant increase in the intracellular fraction (Figure 27). These results suggest that the lack of PRRT2 impaired the correct targeting of P/Q-type VGCCs to the plasma-membrane, generating an intracellular accumulation of the P/Q-type channels.

This data also suggests that PRRT2 thanks to a possible direct or indirect interaction with the presynaptic P/Q-type VGCCs channels could play a role in their correct synaptic localization, keeping most of the P/Q-channels intracellularly and therefore impairing their correct contribution to the process of neurotransmitter release.

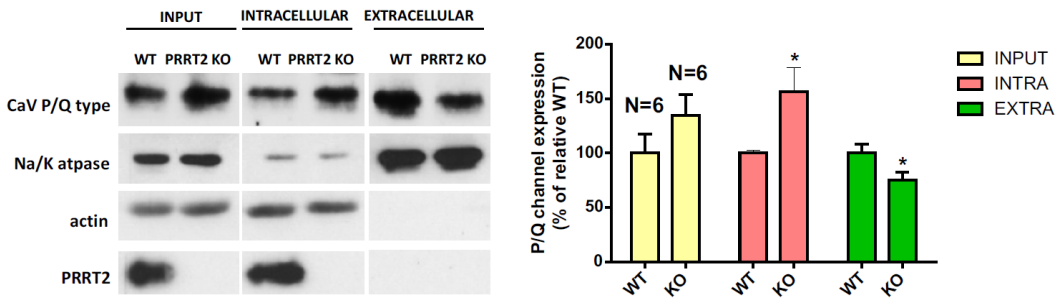

Figure 27. On the left representative immunoblots of cell surface biotinylation performed in primary cortical WT or PRRT2 KO neurons. Total cell lysates (input), biotinylated (cell surface, extracellular) and non-biotinylated (intracellular, intracellular) fractions were analyzed by immunoblotting. Na/K-ATPase and actin were included as markers of the plasma membrane and cytosolic fractions, respectively. On the right the extracellular and intracellular P/Q-type VGCCs expression was normalized on Na/K-ATPase and actin expression (n=5 independent preparations). Data are shown as means ±sem. *p<0.05 Student's t-test.

6.5 PRRT2 alters the localization of P/Q-type VG-Ca^{2+} channels at presynaptic boutons

With the aim of investigating in more detail such interesting biotinylation results, we analyzed synaptic localization of P/Q-type calcium channels, by an immunocytochemical approach combined with confocal imaging analysis.

Cultured WT and PRRT2 KO hippocampal neurons were maintained in vitro for 14 days and then fixed, permeabilizated and double-stained for $Ca_v2.1$, the alfa1 subunit of the P/Q-type VGCCs, and bassoon, a presynaptic protein crucial for the correct function of the release-machinery molecular complex (Figure28A; Thalhammer et al., 2017). We used the colocalization of bassoon and $Ca_v2.1$ for identifying putative synaptic contacts and for investigating a possible mis-localization of the P/Q-type calcium channels to the pre-synapses of PRRT2 lacking neurons.

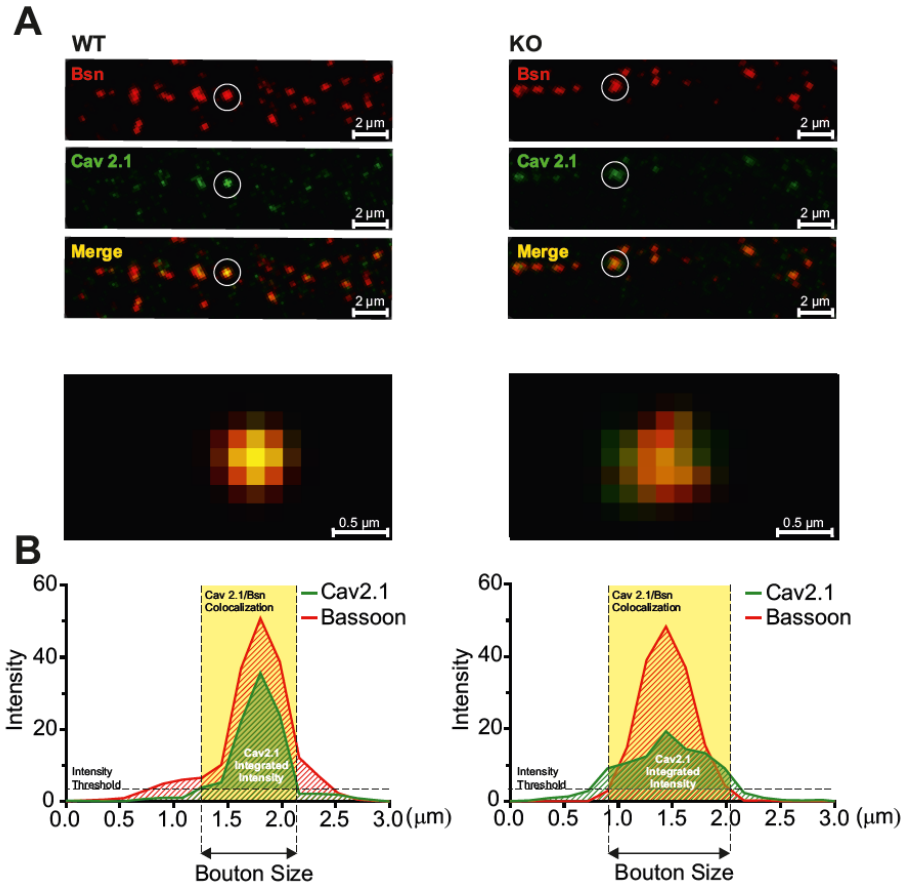

Figure 28. PRRT2 deletion impaired the correct localization of P/Q type VGCCs to the presynaptic boutons. (A) Double-immunostaining for Bassoon (red) and Cav2.1 (green) was used for investigating the localization of P/Q-type calcium channels at the presynaptic boutons in WT (left) and KO neurons (right). (B) Bottom panels show the distribution profile of the immuno-fluorescence intensity for Cav2.1 (green) and bassoon (red) for two (WT-left and KO-right) representative synaptic boutons.

We observed that the chronic deletion of PRRT2 moderately decreases the synaptic density (Figure 29A), in accordance with previous results of our research group (Valente et al. 2019).

By measuring the area of the $Ca_v2.1$ positive puncta, co-localizing with the bassoon positive puncta, we observed an increase in the size of the boutons (Figure 29B) and in agreement with this result we also observed an increase of the Manders' coefficient (Figure 29C).

Moreover, the chronic deletion of PRRT2 reduces the $Ca_v2.1$ integrated fluorescence intensity calculated over the $Ca_v2.1$/Bsn positive puncta (Figure 29D).

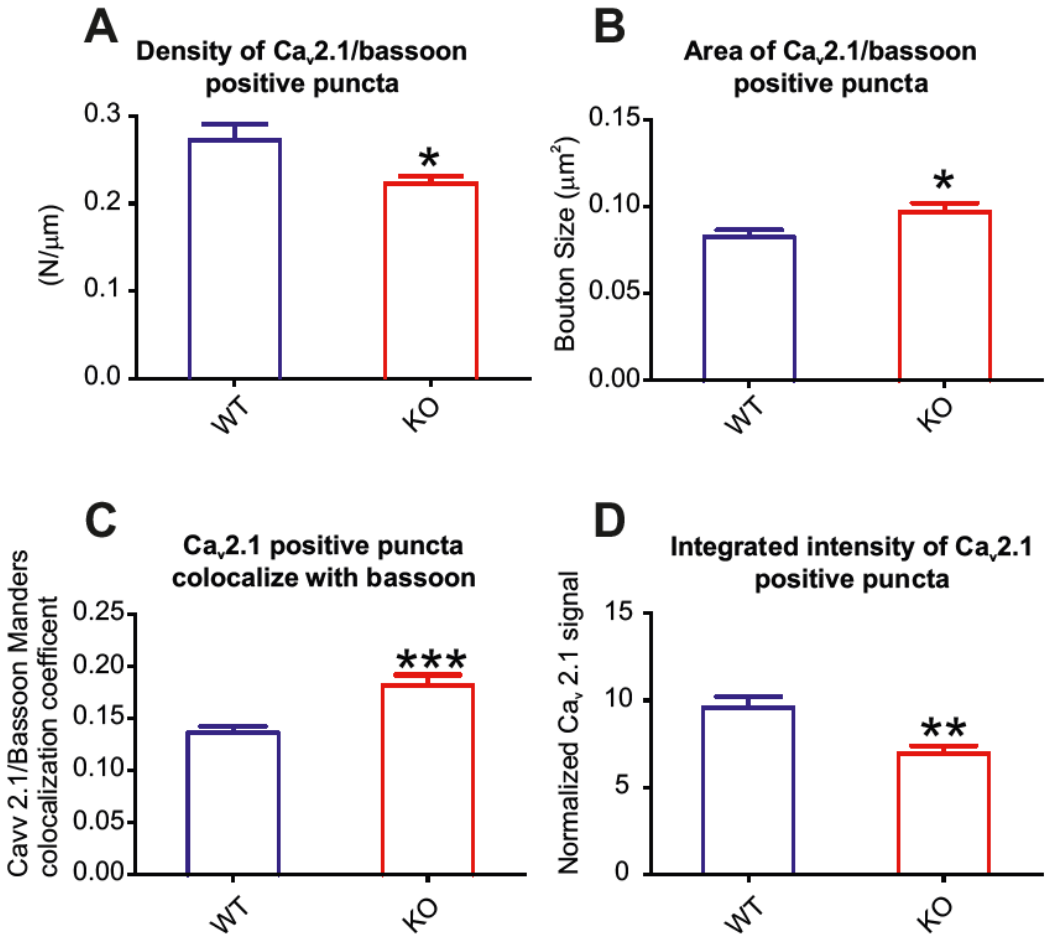

Figure 29. The Lack of PRRT2 moderately decreases the synaptic density and increased the dispersion of Cav2.1 out-side the active zone. (A) The bar graph shows that chronic deletion of PRRT2 moderately decreases the synaptic density; Panel (B) shows a significant increase of the bouton size (estimated measuring the area of the Cav2.1 positive puncta co-localizing with the Bsn positive puncta). In accord with this result panel (C) shows an increase of the Manders' coefficient. Panel (D) shows that the chronic deletion of PRRT2 decreases the integrated intensity of Cav2.1/bsn positive puncta (WT n=32/KO n=33, P<0.05; **, P<0.01 e U test pert tutti I pannelli).

These effects strongly suggest that the lack of PRRT2 induced a mis-localization of P/Q-type channels that diffuse outside the active zone (Figure 30).

In other words, these results suggest that in KO neurons, P/Q-type calcium channels mis-targeted the presynaptic membrane (the active zone) because of an impairment in the trafficking from the intracellular organelle membranes to the plasma membrane (see byotinilation results) and/or an enhanced diffusion and consequent dis-localization of P/Q-type channels outside and far-away the active zone (Figure 30).

For this reason, the area of colocalization between bassoon and $Ca_v2.1$ increased and consequently a similar increase was also observed in the coefficient of Manders' coefficient (P<0.05, P=0.0004) and in the bouton size (P<0.05, P=0.0376), leading to the reduction of the $Ca_v2.1$ integrated fluorescence intensity (P<0.05, P=0.0011), due to the difficulty of the P/Q channels to stay clustered at the active zone (Figure 30).

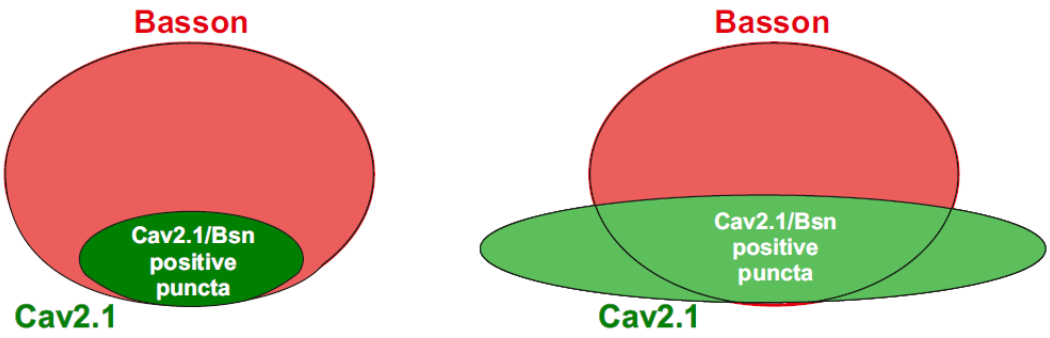

Figure 30. Graphical representation of a possible mechanistic model describing the results obtained in Figure 29. P/Q-type calcium channels diffuse in the area outside the ROI of colocalization and for this reason the integrated intensity colocalizing with bassoon decreased while the colocalization and Manders' coefficient increased.

6.6 PRRT2-dependent modulation of the presynaptic calcium signal

To determine whether the reduction in presynaptic expression of $Ca_v2.1$ was accompanied by changes in the presynaptic Ca^{2+} transients of PRRT2 silenced neurons, we used a highly sensitive calcium indicator SyGCaMP6s, that allows to specifically measure presynaptic Ca^{2+} transients thanks to its targeting to the presynaptic protein, synaptophysin (Thalhammer et al., 2017).

GCaMP is one of the most widely used genetically encoded calcium indicators. GCaMP is developed by fusing a circularly permuted variant of enhanced green fluorescent protein (cpEGFP) with the calcium-binding protein calmodulin (CaM) at the C terminus and a CaM-binding M13 peptide (from myosin light chain) at the N terminus.

Upon Ca^{2+} binding, the CaM moiety of GCaMP interacts with the M13 peptide, and the resulting CaM-M13 complex undergoes a significant structural reorganization, in proximity to the chromophore of cpEGFP (JingJin Ding et al., 2014).

The most recently developed version SyGCaMP6, possesses long-sought ultra-sensitivity to Ca^{2+} dynamics and it is available in three variants, SyGCaMP-6s, -6m and -6f for slow, medium and fast kinetics, respectively.

After various testing in our experimental conditions, we selected the SyGCaMP-6s variant, because, despite its highly non-linear behavior, it was the most sensitive, enabling us to detect presynaptic Ca^{2+} transients in response to a single AP and also after partial blockade of Ca^{2+} entry.

We investigated whether PRRT2 overexpression or KD affected presynaptic Ca^{2+} transients elicited in presynaptic boutons by a train of APs (1-50 APs, 40 Hz) (Figure 31A). While PRRT2 overexpression significantly increased presynaptic Ca^{2+} increase in response to 1-50 APs (Figure 31B), the acute deletion of PRRT2 surprisingly did not exert any significant change (Figure 31C).

The negative result obtained in PRRT2 deficient synapses, could be explained taking in consideration that the SyGCaMP-6s variant is sensitive to Ca^{2+} influx through the presynaptic plasma-membrane not only of the active zone but of the entire presynaptic membrane. Moreover, such Ca^{2+}-probe is also sensitive to calcium-induced calcium release from the cytoplasmic Ca^{2+} stores, present into the presynaptic terminal.

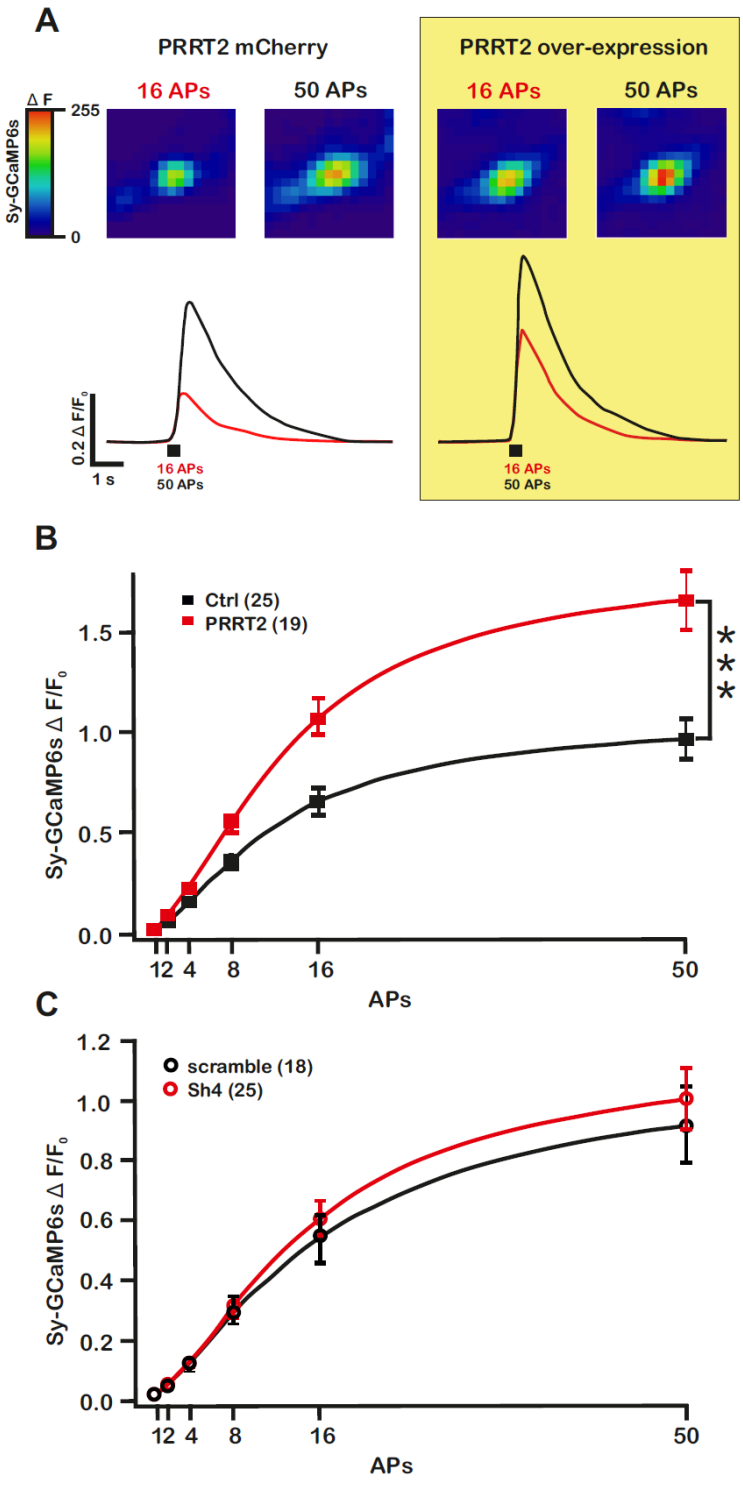

Figure 31. (A) Sy-GCaMP6s recordings from primary cortical neurons expressing Prrt2 (right, yellow background) or control mRFP (left). Representative images of synaptic boutons at peak response to a 8 APs field stimulation (1.5 ms, 60 V @ 40 Hz; maximal projection of 5 images). Exogenous expression of PRRT2 (B,PRRT2 OVER, DIV13-14) and PRRT2 knock-down (C,SH4, DIV15-16) affected Sy-GCaMP6s fluorescence transients of presynaptic boutons elicited by a train of APs (1-50 APs, 40 Hz) in murine hippocampal cultures.

So, with the aim of investigating in more detail the presynaptic Ca^{2+} increase due to the activation of P/Q-type VGCCs, we studied the effect of Aga-IVA on the Ca^{2+} increase induced by 1-50 APs evoked at 0.2 Hz (Figure 32A). We observed that the Aga-IVA-insensitive Ca^{2+} signal that remained after Aga-IVA application was larger in PRRT2 deficient presynaptic boutons (Figure 32B), an effect that is paralleled by a significant decrease of the percentage block induced by the selective P/Q-type antagonist (Figure 32C).

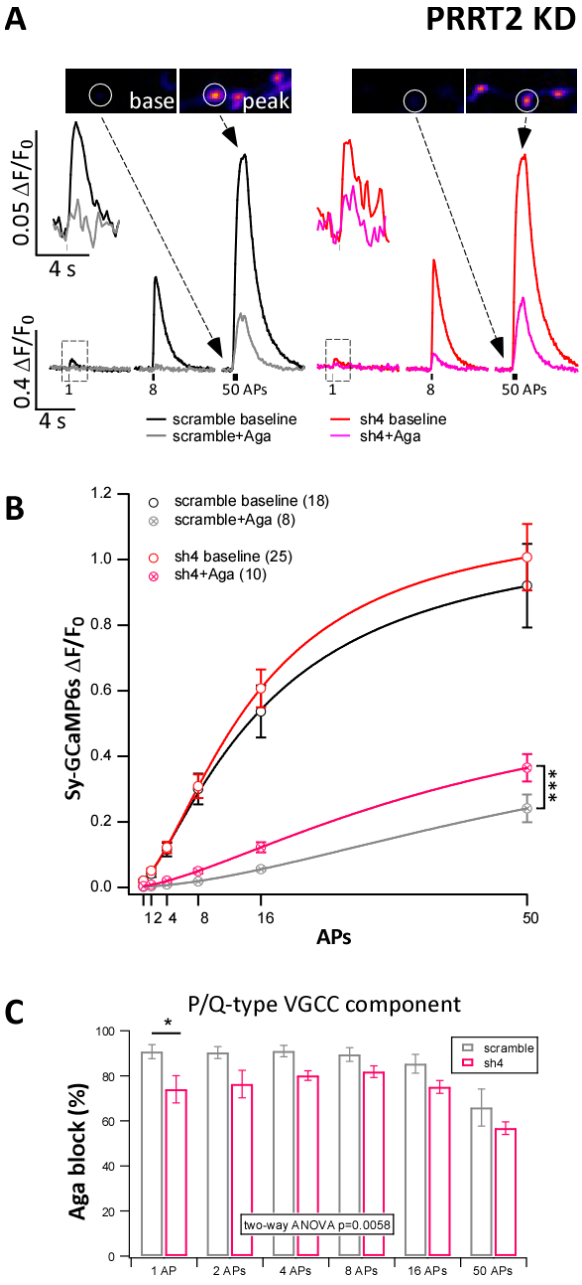

Figure 32. Effect of PRRT2 on presynaptic Calcium transients. (A) Sy-GCaMP6s fluorescence transients elicited by a train of APs (1-50 APs; 40 Hz) in presynaptic boutons of murine hippocampal cultures tansfected with control (scramble) and PRRT2 knock-down (sh4) constructs. Fluorescence transient traces recorded for one field of view are shown before and after application of agatoxin IVA (Aga, 300 nM, 2 min, average of 5-15 boutons). Inset: magnification of response to 1 AP stimulation. Top, partial field of view of images taken before (base) and at peak response (peak) to 50 APs stimulation. Images are derived from a merge of 20 consecutive images recorded at 15 frames/sec. (B) Summary of Sy-GCaMP6s transients recorded before (baseline) and after application of Aga. (C) Blocking effects of on Syn-GCAMP6s transients. Data are shown as mean+/-SEM. Two way ANOVA followed by Bonferroni post-test * $p<0.05$, ***$p<0.001$. Knock-down of PRRT2, while not affecting total size of synaptic Calcium transients ($p=0.5824$), decreases the contribution of P/Q-type channels ($p=0.0058$).

7. Discussion

We have previously shown that PRRT2 is enriched in presynaptic terminals and that its silencing decreases the number of synapses and impairs glutamate release, thanks to a sharp decrease in release probability and Ca^{2+} sensitivity. Moreover, we observed that the lack of PRRT2 strongly attenuates the increase of the eEPSCs amplitude that in WT neurons is normally observed in response to the increase of external calcium concentration from 2 to 4 mM (Valente et al., 2016).

This effect could be due to an altered expression and function of the synaptic calcium sensor, synaptotagmin 1/2, that we have previously demonstrated is a direct or indirect PRRT2-interactor (Valente et al., 2016). These results indicate that PRRT2 is intimately connected with the Ca^{2+}-sensing machinery and that it plays an important role in the final steps of neurotransmitter release. However, PRRT2 modulation of the presynaptic calcium influx could be also implicated.

With the aim of investigating in more detail the altered calcium dependence of glutamate release we have studied eEPSCs amplitude evoked at various extracellular calcium concentration. The analysis of dose/response curve revealed that PRRT2 deletion did not affect the Hill coefficient (n) and affinity constant (EC50), while it significantly decreases the maximal eEPSCs amplitude activated at higher (4-8 mM) external calcium concentration. Although these results demonstrated a clear impairment in the calcium sensitivity of neurotransmitter release, it is not possible to state that such effect depends on an impaired presynaptic calcium influx. Thus, we added a study of the contribution of presynaptic VG-Ca^{2+} channels to glutamatergic synaptic transmission in neurons lacking PRRT2. We observed that the eEPSCs mediated by N- and P/Q-type VGCCs were significantly reduced by PRRT2 deletion, suggesting a deficit of calcium influx through these channels at the presynaptic bouton.

Therefore, we pharmacologically dissected somatic VG-Ca^{2+} currents in cultured hippocampal neurons, observing that PRRT2 over-expression significantly increased N- and P/Q-type calcium currents. On the contrary both acute and chronic deletion of PRRT2 exert the opposite effects. These results strongly suggested a PRRT2 role in the modulation of the functional expression of N- and P/Q-type VGCCs at the plasma membrane.

Thanks to biotinylation assay we have confirmed that PRRT2 deletion impaired P/Q-type VGCCs trafficking to the membrane. Such effect paralleled with P/Q-type VGCCs accumulation into the cytoplasmic fraction, possibly a consequence of the impaired targeting to the membrane.

Thus, we have performed an immunocytochemistry double staining assay with the goal of characterizing the P/Q-type VGCCs targeting to the membrane of the presynaptic boutons. Notably, we revealed that in presynaptic terminals lacking PRRT2, the P/Q-type VGCCs diffuse around the presynaptic terminal reducing its clustering at the active zone.

In parallel, we investigated presynaptic calcium influx, taking advantage from the use of SyGCaMP-6s, an ultra-sensitive fluorescent calcium indicator, selectively expressed at the presynaptic boutons (Thalhammer et al., 2017). We observed that PRRT2 over-expression increased presynaptic calcium influx, while unexpectedly PRRT2 deletion did not exert any significant change. .

However, when we studied the Aga-IVA-induced reduction of the presynaptic calcium signal, a significant decrease of the P/Q-type dependent calcium wave was observed in PRRT2-deficient boutons, demonstrating a selective altered function and possibly, targeting at the active zone, of the P/Q-type VGCCs, known for its crucial role played in the glutamate release process. In summary, our results strongly suggests that the P/Q-type mis-targeting faraway the active zone, or/and cytoplasmic retention, observed thanks to the immunocitochemestry approach (Figure 27), reduced the amount of calcium channels strictly associated to the release machinery complex that in turn

contributed to the glutamate release probability decrease that with have previously observed in PRRT2 knockdown neurons (Valente et al., 2016).

8. Conclusion

Our results could be summarized by the graphical mechanistic model shown in the figure 31. In WT glutamatergic presynaptic terminals, PRRT2 allows the correct trafficking and targeting of N- and P/Q-type channels to the membrane and also contributes to their proximal localization to the release machinery molecular complex and to synaptotagmins.

On the contrary the lack of PRRT2 impaired the N- and P/Q-type channels trafficking from the cytoplasm to the membrane (Figure 33 **(1)**) and in parallel induced the altered-localization of N- and P/Q-type channels that have already targeted the membrane (Figure 33 **(2)**) but are unable to colocalize near to the release machinery molecular complex and the calcium sensors (Syt1/2).

Such altered N- and P/Q-type calcium channels -targeting at the active zone is probably one of the main cause of the impaired neurotransmitter release probability that affects glutamatergic PRRT2 deficient synapses (Valente et al., 2016).

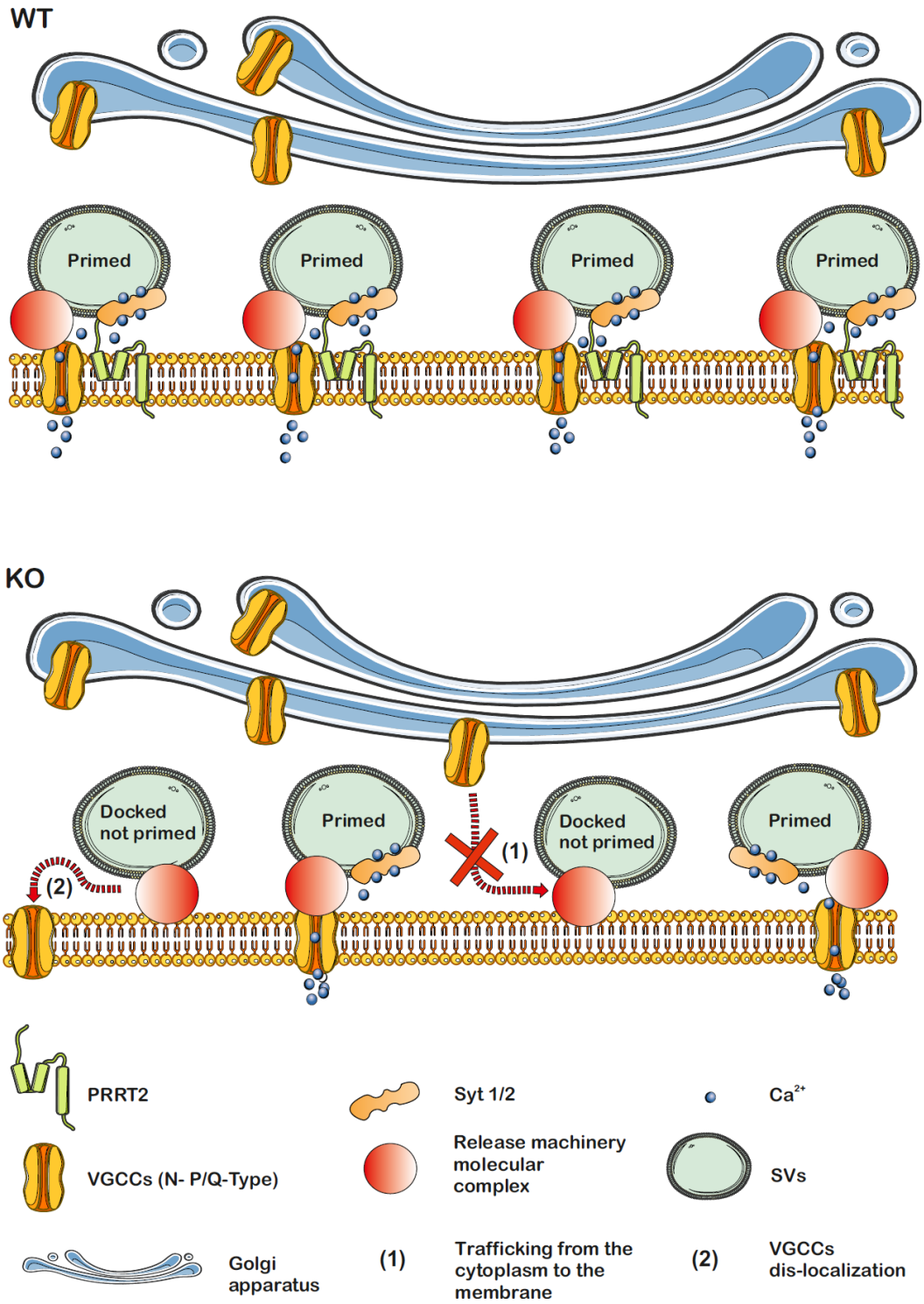

Figure 33. Graphical mechanistic model of our results.

9. Materials and Methods

Animals

GAD67-GFP knock-in mice were generated by inserting the cDNA encoding enhanced GFP into the GAD67 locus in TT2 embryonic stem cells, as described in Tamamaki N, et al. (2003). Heterozygous GAD67-GFP males were mated with wild-type C57BL6/J females, and GFP-positive pups were identified at birth through a Dual Fluorescent Protein Flashlight (DFP-1, NIGHTSEA, Lexington, MA USA) and confirmed by genotyping, performed by PCR with the following primers: TR-1b: GGCACAGCTCTCCCTTCTGTTTGC; TR-3:GCTCTCCTTTCGCGTTCCGACAG; TRGFP-8:CTGCTTGTCGGCCATGATATAGACG. All animals were provided by our institutional animal breeding facility in accordance with the guidelines approved by the local Animal Care Committee of the University of Genova. Experiments used 0–2-day-old pups of either sex. PRRT2-KO mice were generated by EUCOMM/KOMP using a targeting strategy based on the “knockout-first” allele (Skarnes et al. 2011; Michetti, Castroflorio et al. 2017). Mutant animals in a C57BL/6 N background were propagated as heterozygous colonies in the IIT SPF facility. Genotyping was performed by PCR with primers Prrt2_F: AGGTAGACGGGCATTTGAGC, Prrt2_R: CGTGGGGAAGAGGAGACAAC; CAS_R1_Term: TCGTGGTATC GTTATGCGCC, that were used to detect the wild type (WT) (Prrt2_F plus Prrt2_R product, 480 bp) and mutant (Prrt2_F plus Cas_R1_Term product, 200 bp) PRRT2 alleles and to genotype WT, heterozygous, and homozygous mice. The primer Prrt2_F, common to WT and mutant PCR, was designed in the intronic sequence between Prrt2 Exon 1 and Exon 2. The primers Prrt2_R and Cas_R1_Term were designed in the exon 2 of the PRRT2 gene and in the targeting cassette, respectively. Some experiments were done using wild-type C57BL6/J mice. All experiments were carried out in accordance with the guidelines established by the European Communities Council (Directive 2010/63/EU of 4 March 2014) and were approved by the Italian Ministry of Health (authorization 73/2014-PR and 1276/2015-PR).

Cell cultures

Primary hippocampal neurons were prepared from postnatal GAD67-GFP knock-in mice (P0–P1), as previously described (Beaudoin GM et al. 2012, Valente et al., 2016). In brief, hippocampi were dissociated by enzymatic digestion in 0.25% trypsin for 6 min at 37 °C and then triturated with a fire-polished Pasteur pipette (Banker G and Goslin K, 1998). No antimitotic drugs were added to prevent glia proliferation. The following solutions were used for cell culture preparations: HANKS solution, prepared from HBSS (GIBCO 14170-088; red) supplemented with 10 mM HEPES, 30 mM D-glucose, 5 µg/ml Gentamycin, pH 7.4 with KOH; dissection solution, prepared from HANKS solution supplemented with 10% bovine serum albumin and 6mM MgSO4*7H2O. Some Primary hippocampal neurons were prepared from C57BL6/N and PRRT2 KO mice. Animals were sacrificed by CO2 inhalation, and 17/18-day embryos (E17-18) were removed immediately by cesarean section. In brief, hippocampi or cerebral cortices were dissociated by enzymatic digestion in 0.125% Trypsin for 20 min at 37°C and then triturated with a firepolished Pasteur pipette. No antimitotic drugs were added to prevent glia proliferation. Primary hippocampal neurons were plated at low density of 80 cells/mm^2 on 3.5-cm-diameter Petri dishes (Falcon® 35 mm, 353001) treated previously for 24 h with poly-L-lysine (0.1 mg/ml; Sigma-Aldrich) in borate buffer (0.1 M). Autaptic neurons were prepared as described previously (Bekkers and Stevens, 1991; Chiappalone et al., 2009) with slight modifications. Dissociated neurons were plated at very low density (40 cells/mm^2) on microdots (40-300 µm in diameter) obtained by spraying a mixture of poly-L-lysine (0.1 mg/ml) in borate buffer (0.1 M) on petri dishes, previously pretreated with 0.15% agarose. Cells were grown in a culture medium consisting of Neurobasal A (Gibco™) supplemented with 2% B-27 (Invitrogen, Italy), 1 mM Glutamax, and 5 µg/ml Gentamycin and maintained at 37 °C in a humidified incubator with 5% CO2.

Transduction of Primary Neurons with PRRT2 shRNA and/or Sh-OVEREXPRESSED PRRT2

shRNAs (Scr: GCCGACACTCGTCAGTTTAAA, Sh4: CATGTGGCCTGTCAACATTGT and OVER; CATGTGGCCAGTGAATATCGT) were inserted into the pLKO.1-CMV-mCherry plasmid expressing either mCherry for the identification of the transfected cells. The PRRT2 Sh-

OVEREXPRESSED isoforms were subcloned into lentiviral vectors 743.pCCLsin.PPT.hPGK.GFP.Wpre (a gift from Dr. L. Naldini). Lentiviral vectors encoding Sh4, or the Scr control RNAs were used to knock down the endogenous PPRT2 protein in hippocampal neurons. Neurons were infected by the addition of lentiviral vectors into cell medium at 6 DIVs. After 24 hr, the medium was removed and replaced with fresh and conditioned medium (1:1). A multiplicity of infection (MOI) of 5 of the lentivirus was used.

Electrophysiological recordings

Patch-clamp recordings were performed using a Multiclamp 700B amplifier (Axon Instruments, Molecular Devices, Sunnyvale, CA, USA) using an IX71 inverted phase/fluorescence (Olympus, Japan). The age of the patched neurons ranged between 16 and 18 div for Ca^{2+} current and between 11 and 14 div for eEPSCs. Patch electrodes, fabricated from thick borosilicate glasses were pulled and fire-polished to a final resistance of 3–5 MΩ. The standard external solution for the Ca^{2+} current for the whole-cell experiments was (in mM): 5 BaCl2, 140 NaCl, 1 MgCl2, 10 HEPES (pH7.4); The standard internal solution for the Ca^{2+} current was (in mM): 90 CsCl, 20 TEACl, 10 EGTA, 10 Glucose, 1 MgCl2, 4 ATP and 15 phosphocreatine to prevent current run-down (pH 7.4). Voltage-clamp recordings were performed at a holding potential of -70mV. To isolate the calcium current were use nifedipine (5uM), a selective blocker of L-Type Ca^{2+} channels, ω-Agatoxin IVA (Peptide institute, Code: 4256-s) a selective blocker of P/Q-Type Ca^{2+} channels and ω-Conotoxin GVIA (Peptide institute, Code: 4161-v) a selective blocker of N-Type Ca^{2+} channels. Voltage- clamp recordings of voltage-gated Ca^{2+} currents were acquired at 50 kHz and low-pass filtered at 2 kHz. Data acquisition was performed using pCLAMP program (Molecular Devices, LLC) and using PatchMaster programs (HEKA Elektronic, Lambrecht, Germany).

Voltage-clamp recordings of voltage gated Ca^{2+} currents were performed on Hippocampal neurons using external solution for the Ca^{2+} current supplemented with D-AP5 (50 µM), CNQX (10 µM), BIC (30 µM) and Tetradotoxin (1mM). Whole-cell family Ca^{2+} currents were evoked by 10 mV steps from -70 to 70 mV. Linear capacity and leakage currents were eliminated by P/N leak subtraction procedure with a subpulse of

– 100 mV. Blockade of L-type calcium channels was allowed by the use of a selective blocker for these channels, Nifedipine (5µM).

Voltage-clamp recordings for eEPSC currents were performed on Hippocampal neurons using Standard external solution containing (in mM): 140 NaCl, 4 KCl, 10 glucose, 10 HEPES (pH 7.3 with NaOH) supplemented with D-(-)-2-amino-5 phosphonopentanoic acid (D-AP5; 50 µM; Tocris, Bristol, UK); This solution was added with 5 type of concentrations of CaCl2 and MgCl2, in particular(in mM): Solution 1, 0.5 CaCl2, 3.5 MgCl2; Solution 2, 1 CaCl2, 3 MgCl2; Solution 3, 2 CaCl2, 2 MgCl2; Solution 4, 4 CaCl2, 0 MgCl2; Solution 5, 8 CaCl2, 0 MgCl2. The standard internal solution was (in mM): 126 KGluconate, 4 NaCl, 1 MgSO4, 0.02 CaCl2, 0.1 BAPTA, 15 Glucose, 5 HEPES, 3 ATP, 0.1 GTP (pH 7.2 with KOH). All experiments were performed at room temperature (22-24 °C). Neurons were voltage-clamped at -70 mV. Unclamped action potentials (APs) were evoked by a brief depolarization of the cell body to +40 mV for 0.5 ms @ 0.1 Hz. Data acquisition was performed using PatchMaster programs (HEKA Elektronic, Lambrecht, Germany).

*Analisys.*The Ca^{2+} current density (J) was obtained by dividing the peak inward current by the cell capacitance (pA/pF). All the electrophysiological data were analyzed using the Clampfit software (Molecular Devices, LLC), OriginPro 8 (OriginLab Corp.) and the Prism software (GraphPad Software, Inc.). To analyze paired-pulse ratio (PPR), two brief depolarizing pulses were applied to autaptic neurons at 50 ms time intervals. For each couple of eEPSCs, PPR was calculated as the ratio I2/I1, where I1 and I2 are the amplitudes of the eEPSCs evoked by the conditioning and test stimuli, respectively.

Statistical Analysis

Data are shown as means ± SEM or as box plots, with median (line), second and third interquartile ranges (box), and whiskers representing the min and the max values. The F-test was used to compare variance between two sample groups. To compare two normally distributed sample groups, the unpaired Student's two-tailed t test was used. To compare two sample groups that were not normally distributed, the Mann-

Whitney's U test was used. Statistical analysis was carried out using OriginPro-8 (OriginLab Corp., Northampton, MA, USA) and Prism (GraphPad Software, Inc.) software.

Surface biotinylation

Cortical neurons from WT or PRRT2 KO mice at 13 DIV were incubated with 1 mg/ml of EZ-Link™ Sulfo-NHS-SS-Biotin (Thermo Fisher, Waltham, MA USA) in cold phosphate-buffered saline (PBS) for 35 min at 4 °C, constantly moving. Free biotin was quenched, twice, with 100 mM Tris pH 8 and once with cold PBS to remove biotin excess. Cells were then lysed in lysis buffer (150 mM NaCl, 50 mM Tris, 1 mM EDTA and 1 % Triton X-100) supplemented with protease inhibitor cocktail (Cell Signaling, Danvers, MA, USA). Total cell lysates were centrifuged at 10,000 x g at 4 °C for 10 min. The supernatant fraction (0.5 mg protein) was incubated with 150 µl of NeutrAvidin-conjugated agarose beads for 3 h at 4 °C, and the remaining supernatant was kept as input. After extensive washes of the beads, samples were eluted. Sodium dodecyl sulfate polyacrylamide gel electrophoresis (SDS-PAGE) was performed according to Laemmli (1970) and samples were subjected to SDS polyacrylamide gel electrophoresis on 8% polyacrylamide gels and blotted onto nitrocellulose membranes (Whatman, Sigma-Aldrich, St. Louis, MO). Membranes were blocked for 1 h in 5% non-fat dry milk/Tris-buffered saline (10 mM Tris, 150 mM NaCl, pH 8.0) plus 0.1 % Triton X-100 and incubated overnight at 4 °C or for 2 h at room temperature with the following primary antibodies: anti P/Q-type calcium channel (1:500, Cat. No. 152203, Synaptic Systems), anti actin (1:1000 Sigma-Aldrich, St. Louis, MO, USA), anti Na+/K+ ATPase (1:2000, Thermo Scientific, Waltham, MA, USA) and anti PRRT2 (1:1000, Sigma-Aldrich, St. Louis, MO, USA HPA 014447).

Immunocytochemistry

Primary hippocampal neurons (from WT or KO mice, 60 cells/mm^2), were fixed at 15 div with 4% paraformaldehyde/4% sucrose for 12 min at room temperature and then washed with phosphate buffered saline (PBS). Cells were then permeabilized with methanol (-20°C; 10 min on ice) followed by 0.2% Triton X-100 for 10 min (Liao et al., 1999) and blocking with 5% FBS/0.1% BSA for 30 min in PBS, before their incubation for 2h with primary antibodies in PBS/5% FBS/0.1% BSA, then washed with PBS and final

incubation for 2h with secondary antibodies. For immunofluorescence analysis, neurons were immunostained with antibodies rabbit anti-P/Q-type calcium channel (cav1:500, Cat. No. 152203, Synaptic Systems) and guinea pig anti-bassoon (1:500 Cat. No. 141004, Synaptic Systems). Secondary antibodies were Alexa 488 goat anti-rabbit and Alexa647 goat anti-guinea pig IgGs (1:1000 in all cases; Cat. No. A11001, and A21450, respectively, Invitrogen). Images of cultured neurons were acquired with a Leica SP8 confocal microscope using a 63× objective and 1024×1024 pixels (1pixel=0.24 µm).

Confocal images were analyzed using ImageJ. Each single stack was filtered at the maximal fluorescence intensities of stacks were Z-projected. Analysis of fluorescence intensity was performed on axonal ROIs (2-3 per image) of ≈60 µm in lengths and somatic ROIs (1-2 per image) of ≈300 µm^2 in manually selected blind to the experimental condition.

The intensity of each ROIs has been calculated as the average intensity divide to the integrated intensity of each synapses that circumscribes the Cav2.1 and Bassoon positive synaptic signal. The synaptic densities were obtained by counting the total number of positive puncta divided by the Area (on Somas in µm^2) or lenght (on dendrites in µm) of the colocalizated segment. Colocalization between bassoon and Cav2.1 was estimated for the thresholded ROIs with the Coloc2 plugin using the Manders' coefficients (MA=Σi Ai,coloc/Σi Ai, where Σi Ai is the sum of intensities of all pixels above threshold for channel A and Σi Ai,coloc is calculated as Σi Ai but only for pixels where also the second channel B is above threshold). The number of samples (n) represents the number of coverslips from at least three neuronal preparations conducted in parallel. From each coverslip, at least 10–15 images were collected.

Presynaptic Ca^{2+} imaging with SyGCaMP6s

Imaging was performed in murine primary cultures at room temperature in aCSF containing (in mM): 140 NaCl, 2.5 KCl,2.2 CaCl2, 1.5 MgCl2, 10 D-glucose, 0.01 CNQX, 0.05 D-APV and 10 HEPES-NaOH (pH 7.38; osmolarity adjusted to 310 mOsm). Cultures were cotransfected with SyGCaMP6s, the auxiliary subunit β4 and the respective control and PRRT2 KD constructs in a 1:1:1 DNA ratio 5-6 days prior to experiments, and measured at 15-16 DIV. prior to experiments, and measured at 16-18 DIV. Boutons were imaged using a cooled charge-coupled device (CCD) camera (ORCA-R2, Hamamatsu)

mounted on an inverted microscope (DMI6000B, Leica) with a 40x, 1.25 NA oil immersion objective. A 200W metal halide lamp (Lumen200Pro, Prior Scientific) and a filter set comprising a BP 470/40 nm excitation filter, a 500 nm dichroic mirror and a BP 525/50 emission filter (Leica) were used for illumination. Images were captured at 15.3 Hz with 50

ms integration times at a depth of 8 bits. APs were evoked by field stimulation (60 V, 1 ms pulses; Isolated Pulse Stimulator, A-M systems) using a custom-made chamber with two parallel platinum wires 6 mm apart. Trains of APs were delivered at a frequency of 40 Hz every 18 s. Images were analyzed in ImageJ (http://rsb.info.nih.gov/ij) with the plugin Time Series Analyzer V2.0 (http://rsb.info.nih.gov/ij/plugins/time-series.html) and with customized routines in Igor Pro 6.03. Regions of interest (ROIs) with a diameter of 3.2 µm were positioned on all boutons responding to 20 APs for SyGCaMP6s with a signal above two SD of the background noise. The intensity of a twin ROI positioned within 10 µm from the first was used to subtract the local background noise. Signals were quantified as ΔF/F0, where ΔF=F-F0, with F0 measured over 1 s period prior to stimulation.

10. List of abbreviations

PKD = Paroxysmal kinesigenic dyskinesia

PRRT2 = Proline-rich transmembrane protein 2

ICCA = Infantile convulsions with choreoathetosis

DIV = Days in vitro

SNAP-25 = Synaptosomal-associated protein 25

NSF = N-ethylmaleimide sensitive factor

SNARE = Soluble N-ethylmaleimide-sensitive fusion protein attachment protein receptors

SVs = Synaptic vesicles

AMPA = α-amino-3-hydroxy-5-methyl-4-isoxazolepro-pionic acid

IC = Infantile convulsions

BFIS = Benign familial infantile seizures

PNKD = Paroxysmal non-kinesigenic dyskinesia

EA = Episodic ataxia

PED = Paroxysmal exercise induced dyskinesia

HM = Hemiplegic migraine

FS = Febrile seizures

CAE = Childhood-absence epilepsy

PSD = Postsynaptic density

NSSP = Non- synaptic synaptosomal protein

GRIA = GluA1 subunit

AZ = Active Zone

PSCs = Postsynaptic currents

mEPSCs = Miniature excitatory postsynaptic currents

eEPSCs = Evoked excitatory postsynaptic current

PPR = Paired-pulse ratio

RRP = Readily releasable pool

$GABA_A$ = Gamma-aminobutyric acid receptor type A

GPCRs = G-protein-coupled receptors

Syt = Synaptotagmins

GPCRs = G-protein-coupled receptors

VGCCs = Voltage-gated calcium channels

CamKII = Ca^{2+}/calmodulin-dependent protein kinase type II

GAD67 = Glutamic acid decarboxylase-67

GFAP = Glial fibrillary acidic protein

VGLUT1 = Vesicular glutamate transporter-1

VGAT = Vesicular GABA transporter

shRNA = Short hairpin RNAs

11. References

1. Andrew I. Su, Tim Wiltshire, Serge Batalov, Hilmar Lapp, Keith A. Ching, David Block, Jie Zhang, Richard Soden, Mimi Hayakawa, Gabriel Kreiman, Michael P. Cooke, John R. Walker, John B. Hogenesch (2004) A gene atlas of the mouse and human protein-encoding transcriptomes. Proc. Natl. Acad. Sci. USA 101, 6062–6067.
2. Arikkath, J. and Campbell, K.P. (2003) Auxiliary subunits: essential components of the voltage-gated calcium channel complex. Curr. Opin. Neurobiol. 13, 298–307
3. Augustine GJ (2001) How does calcium trigger neurotransmitter release? Curr Opin Neurobiol,11:320-326.
4. Banker G and Goslin K (1998) Culturing nerve cells, 2nd edn. MIT Press, Cambridge MA, pp. 339–370.
5. Beaudoin GM 3rd, Lee SH, Singh D, Yuan Y, Ng YG, Reichardt LF, Arikkath J (2012) Culturing pyramidal neurons from the early postnatal mouse hippocampus and cortex.Nat Protoc 7:1741–1754.
6. Bekkers, J. M., & Stevens, C. F. (1991). Excitatory and inhibitory autaptic currents in isolated hippocampal neurons maintained in cell culture. Proceedings of the National Academy of Sciences of the United States of America, 88(17), 7834–7838. doi:10.1073/pnas.88.17.7834
7. Bennett LB, Roach ES, Bowcock AM. (2000) A locus for paroxysmal kinesigenic dyskinesia maps to human chromosome 16. Neurology; 54: 125–30.
8. Bennett MK, Calakos N, Scheller RH, (1992) Syntaxin: a synaptic protein implicated in docking of synaptic vesicles at presynaptic active zones. Science, 257:255-259.
9. Bergsman, J.B. and Tsien, R.W. (2000) Syntaxin modulation of calcium channels in cortical synaptosomes as revealed by botulinum toxin C1. J. Neurosci. 20, 4368–4378

10. Bezprozvanny I, Scheller RH, Tsien RW (1995) Functional impact of syntaxin on gating of N-type and Q-type calcium channels. Nature, 378:363-366.
11. Bezprozvanny I, Zhong P, Scheller RH, Tsien RW (2000) Molecular determinants of the functional interactions between syntaxin and N-type Ca^{2+} channel gating. Proc Natl Acad Sci USA, 97:13943-13948.
12. Bhatia K (2011). Paroxysmal dyskinesias. Mov Disord. May; 26(6): 1157-65.
13. Bhatia KP. (2001) Familial (idiopathic) paroxysmal dyskinesias: an update. Semin Neurol; 21:69–74.
14. Blakeley J, Jankovic J. (2002) Secondary causes of paroxysmal dyskinesia. Adv Neurol; 89:401– 420.
15. Boukje de Vries, Petra M.C. Callenbach, Jessica T. Kamphorst, Claudia M. Weller, Stephany C. Koelewijn, Robert ten Houten, Irenaeus F.M. de Coo, Oebo F. Brouwer, Arn M.J.M. van den Maagdenberg (2012) PRRT2 mutation causes benign familial infantile convulsions. Neurology 79, 2154–2155
16. Bruno MK, Hallett M, Gwinn-Hardy K, Sorensen B, Considine E, Tucker S, Tucker S, Lynch DR, Mathews KD, Swoboda KJ, Harris J, Soong BW, Ashizawa T, Jankovic J, Renner D, Fu YH, Ptacek LJ. (2004) Clinical evaluation of idiopathic paroxysmal kinesigenic dyskinesia: new diagnostic criteria. Neurology; 63: 2280–7.
17. Carbone E, Calorio C, Vandael DH. (2014) T-type channel-mediated neurotransmitter release Pflugers Arch.;466(4):677-87.
18. Carbone E1, Carabelli V, Cesetti T, Baldelli P, Hernández-Guijo JM, Giusta L. (2001) G-protein- and cAMP-dependent L-channel gating modulation: a manyfold system to control calcium entry in neurosecretory cells. Pflugers Arch.;442(6):801-13.
19. Catterall WA, Perez-Reyes E, Snutch TP, Striessnig J (2005). International Union of Pharmacology. XLVIII. Nomenclature and structure-function

relationships of voltage-gated calcium channels. Pharmacol Rev. Dec; 57(4): 411-25.

20. Catterall, W.A. (2000) Structure and regulation of voltage-gated Ca2+ channels. Annu. Rev. Cell Dev. Biol. 16, 521–555
21. Chen J, Zhou L, Pan SY (2014). A brief review of recent advances in stem cell biology. Neural Regen Res. Apr 1; 9(7): 684-7.
22. Chen, W.J. Lin Y, Xiong ZQ, Wei W, Ni W, Tan GH, Guo SL, He J, Chen YF, Zhang QJ, Li HF, Lin Y, Murong SX, Xu J, Wang N, Wu ZY. (2011) Exome sequencing identifies truncating mutations in PRRT2 that cause paroxysmal kinesigenic dyskinesia. Nat. Genet. 43, 1252–1255
23. Chiappalone, M., Casagrande, S., Tedesco, M., Valtorta, F., Baldelli, P., Martinoia, S., and Benfenati, F. (2009). Opposite changes in glutamatergic and GABAergic transmission underlie the diffuse hyperexcitability of synapsin I-deficient cortical networks. Cereb. Cortex 19, 1422–1439.
24. Christopher A.Reid, John M.Bekkers, John D.Clements (2003) Presynaptic Ca2+ channels: a functional patchwork Volume 26, Issue 12, December 2003, Pages 683-687
25. Cuenca-Leon E, Cormand B, Thomson T, Macaya A. (2002) Paroxysmal kinesigenic dyskinesia and generalized seizures: clinical and genetic analysis in a Spanish pedigree. Neuropediatrics; 33: 288–93.
26. Demirkiran M, Jankovic J. (1995) Paroxysmal dyskinesias: clinical features and classification. Ann Neurol; 38:571–579.
27. Dietrich, D. Kirschstein T, Kukley M, Pereverzev A, von der Brelie C, Schneider T, Beck H. (2003) Functional specialization of presynaptic Cav2.3 Ca2+ channels. Neuron 39, 483–496
28. E. M. Valente, S. D. Spacey, G. M. Wali, K. P. Bhatia, P. H. Dixon, N. W. Wood, M. B. Davis (2000) A second paroxysmal kinesigenic choreoathetosis locus (EKD2) mapping on 16q13-q22.1 indicates a family of genes which give rise to paroxysmal disorders on human chromosome 16. Brain 123, 2040–2045.

29. Ebrahimi-Fakhari D, Saffari A, Westenberger A, Klein C. (2015) The evolving spectrum of PRRT2- associated paroxysmal diseases. Brain;138(Pt 12):3476–95.
30. Erro R, Bhatia KP, Espay AJ, Striano P (2017) The epileptic and nonepileptic spectrum of paroxysmal dyskinesias: channelopathies, synaptopathies, and transportopathies. Mov Disord; 32:310–8.
31. Ertel, E.A. Campbell KP, Harpold MM, Hofmann F, Mori Y, Perez-Reyes E, Schwartz A, Snutch TP, Tanabe T, Birnbaumer L, Tsien RW, Catterall WA. (2000) Nomenclature of voltage-gated calcium channels. Neuron 25, 533–535
32. Fahn S. (1994) The paroxysmal dyskinesias. In: Marsden CD, Fahn S, eds. Movement Disorders. Oxford, UK: Butterworth Heinmann Ltd.;310–345.
33. Felicitas Becker, Julian Schubert, Pasquale Striano, Anna-Kaisa Anttonen, Elina Liukkonen, Eija Gaily, Christian Gerloff, Stephan Müller, Nicole Heußinger, Christoph Kellinghaus, Angela Robbiano, Anne Polvi, Simone Zittel, Tim J. von Oertzen, Kevin Rostasy, Ludger Schöls, Tom Warner, Alexander Münchau, Anna-Elina Lehesjoki, Federico Zara, Holger Lerche,Yvonne G. Weber (2013) PRRT2-related disorders: further PKD and ICCA cases and review of the literature. J. Neurol. 260, 1234–1244
34. Fioravante, D., and Regehr, W.G. (2011). Short-term forms of presynaptic plasticity. Curr. Opin. Neurobiol. 21, 269–274.
35. Frieder Brueckner, Bernhard Kohl, Burkhard Puest, Silke Gassner, Judith Osseforth, Matthias Lindenau, Stefan Stodieck, Saskia Biskup, Ebba Lohmann (2014) Unusual variability of PRRT2 linked phenotypes within a family. Eur. J. Paediatr. Neurol. 18, 540–542
36. Fruscione F, Valente P, Sterlini B, Romei A, Baldassari S, Fadda M, Prestigio C, Giansante G, Sartorelli J, Rossi P, Rubio A, Gambardella A, Nieus T, Broccoli V, Fassio A, Baldelli P, Corradi A, Zara F, Benfenati F.

(2018) PRRT2 controls neuronal excitability by negatively modulating Na+ channel 1.2/1.6 activity. Brain. Apr 1;141(4):1000-1016.

37. Gardiner AR, Bhatia KP, Stamelou M, Dale RC, Kurian MA, Schneider SA, Wali GM, Counihan T, Schapira AH, Spacey SD, Valente EM, Silveira-Moriyama L, Teive HA, Raskin S, Sander JW, Lees A, Warner T, Kullmann DM, Wood NW, Hanna M, Houlden H (2012). PRRT2 gene mutations: from paroxysmal dyskinesia to episodic ataxia and hemiplegic migraine. Neurology. Nov 20; 79(21): 2115-21.
38. Gasparini S, Kasyanov AM, Pietrobon D, Voronin LL, Cherubini E. (2001) Presynaptic R-type calcium channels contribute to fast excitatory synaptic transmission in the rat hippocampus. J. Neurosci. 21, 8715–8721
39. Goodenough, D.J., Fariello, R.G., Annis, B.L. & Chun, R.W. (1978) Familial and acquired paroxysmal dyskinesias. A proposed classification with delineation of clinical features. Arch. Neurol. 35, 827–831.
40. Harlow ML, Ress D, Stoschek A, Marshall RM, McMahan UJ (2001) The architecture of active zone material at the frog's neuromuscular junction.Nature,409:479-484
41. Heron SE, Grinton BE, Kivity S, Afawi Z, Zuberi SM, Hughes JN, Pridmore C, Hodgson BL, Iona X, Sadleir LG, Pelekanos J, Herlenius E, Goldberg-Stern H, Bassan H, Haan E, Korczyn AD, Gardner AE, Corbett MA, Gécz J, Thomas PQ, Mulley JC, Berkovic SF, Scheffer IE, Dibbens LM. (2012). PRRT2 mutations cause benign familial infantile epilepsy and infantile convulsions with choreoathetosis syndrome. Am. J. Hum. Genet. 90, 152–160.
42. Heron, S.E. and Dibbens, L.M. (2013) Role of PRRT2 in common paroxysmal neurological disorders: a gene with remarkable pleiotropy. J. Med. Genet. 50, 133–139
43. Houser MK, Soland VL, Bhatia KP, Quinn NP, Marsden CD. (1999) Paroxysmal kinesigenic choreoathetosis: a report of 26 patients. J Neurol; 246: 120–6.

44. I. M. Mintz, B. L. Sabatini, and W. G. Regehr (1995) Calcium control of transmitter release at a cerebellar synapse Volume 15, Issue 3, September, Pages 675-688
45. Iwasaki, S. and Takahashi, T. (1998) Developmental changes in calcium channel types mediating synaptic transmission in rat auditory brainstem. J. Physiol. 509, 419–423
46. Jarvis SE, Magga J, Beedle AM, Braun JEA, Zamponi GW (2000) G protein modulation of N-type calcium channels is facilitated by physical interactions between syntaxin 1A and Gbc. J Biol Chem, 275:6388-6394.
47. Jarvis SE, Zamponi GW (2001) Distinct molecular determinants govern syntaxin 1A-mediated inactivation and G-protein inhibition of N-type calcium channels. J Neurosci, 21:2939-2948.
48. JingJin Ding, Andrew F. Luo, LiYan Hu, DaCheng Wang, Feng Shao (2014) Structural basis of the ultrasensitive calcium indicator GCaMP6, Volume 57, Issue 3, pp 269–274
49. K.J. Swoboda, B.-W. Soong, C. McKenna, E.R. P. Brunt, M. Litt, J.F. Bale, T. Ashizawa, L.B. Bennett, A.M. Bowcock, E.S. Roach, D. Gerson, T. Matsuura, P.T. Heydemann, M.P. Nespeca, J. Jankovic, M. Leppert, L.J. Ptáček (2000) Paroxysmal kinesigenic dyskinesia and infantile convulsions: clinical and linkage studies. Neurology; 55: 224–30.
50. Kang, M.G. and Campbell, K.P. (2003) g Subunit of voltage-activated calcium channels. J. Biol. Chem. 278, 21315–21318
51. Kato, N, Sadamatsu M, Kikuchi T, Niikawa N, Fukuyama Y. (2006) Paroxysmal kinesigenic choreoathetosis: from first discovery in 1892 to genetic linkage with benign familial infantile convulsions. Epilepsy Res. 70 (Suppl 1), S174–S184
52. Kertesz, A. (1967) Paroxysmal kinesigenic choreoathetosis. An entity within the paroxysmal choreoathetosis syndrome. Description of 10 cases, including 1 autopsied. Neurology 17, 680–690.

53. Kikuchi T, Nomura M, Tomita H, Harada N, Kanai K, Konishi T, Yasuda A, Matsuura M, Kato N, Yoshiura K, Niikawa N. (2007) Paroxysmal kinesigenic choreoathetosis (PKC): confirmation of linkage to 16p11-q21, but unsuccessful detection of mutations among 157 genes at the PKC-critical region in seven PKC families. J Hum Genet; 52: 334–41.
54. Klugbauer, N. Marais E, Hofmann F. (2003) Calcium channel a2–d subunits: differential expression, function, and drug binding. J. Bioenerg. Biomembr. 35,639–647
55. Kumar, K.R. Lohmann K, Klein C. (2012) Genetics of Parkinson disease and other movement disorders. Curr. Opin. Neurol. 25, 466–474
56. Labate A, Tarantino P, Viri M, Mumoli L, Gagliardi M, Romeo A, Zara F, Annesi G, Gambardella A. (2012) Homozygous c.649dupC mutation in PRRT2 worsens the BFIS/PKD phenotype with mental retardation, episodic ataxia, and absences. Epilepsia;53:e196–9.
57. Laemmli UK (1970) Cleavage of structural proteins during the assembly of the head of bacteriophage T4. Nature 227:680-685.
58. Lee, H. Y., Huang, Y., Bruneau, N., Roll, P., Roberson, E. D., Hermann, M., Quinn E, Maas J, Edwards R, Ashizawa T, Baykan B, Bhatia K, Bressman S, Bruno MK, Brunt ER, Caraballo R, Echenne B, Fejerman N, Frucht S, Gurnett CA, Hirsch E, Houlden H, Jankovic J, Lee WL, Lynch DR, Mohammed S, Müller U, Nespeca MP, Renner D, Rochette J, Rudolf G, Saiki S, Soong BW, Swoboda KJ, Tucker S, Wood N, Hanna M, Bowcock AM, Szepetowski P, Fu YH, Ptáček, L. J. (2012). Mutations in the gene PRRT2 cause paroxysmal kinesigenic dyskinesia with infantile convulsions. *Cell reports*, *1*(1), 2–12. doi:10.1016/j.celrep.2011.11.001
59. Leveque C, el Far O, Martin-Moutot N, Sato K, Kato R, Takahashi M, Seagar MJ (1994) Purification of the N-type calcium channel associated with syntaxin and synaptotagmin. A complex implicated in synaptic vesicle exocytosis. J Biol Chem, 269:6306-6312.

60. Li HF, Ni W, Xiong ZQ, Xu J, Wu ZY (2013). PRRT2 c.649dupC mutation derived from de novo in paroxysmal kinesigenic dyskinesia. CNS Neurosci Ther; 19: 61-5.
61. Li J, Zhu X, Wang X, Sun W. Feng B, Du T, Sun B, Niu f, Wei H, Wu X, Dong L, Li L, Cai X, Wang Y and Liu Y (2012). Targeted genomic sequencing identifies PRRT2 mutations as a cause of paroxysmal kinesigenic choreoathetosis. J Med Genet. Feb; 49(2): 76–78.
62. Li, M., Niu, F., Zhu, X., Wu, X., Shen, N., Peng, X., and Liu, Y. (2015). PRRT2 Mutant Leads to Dysfunction of Glutamate Signaling. Int. J. Mol. Sci. 16, 9134–9151.
63. Lishman WA, Symonds CP, Whitty CW, Willison RG. (1962) Seizures induced by movement. Brain;85:93.
64. Liu XR, Wu M, He N, Meng H, Wen L, Wang JL, Zhang MP, Li WB, Mao X, Qin JM, Li BM, Tang B, Deng YH, Shi YW, Su T, Yi YH, Tang BS, Liao WP (2013). Novel PRRT2 mutations in paroxysmal dyskinesia patients with variant inheritance and phenotypes. Genes Brain Behav. Mar; 12(2): 234-40.
65. Liu YT, Nian FS, Chou WJ, Tai CY, Kwan SY, Chen C, Kuo PW, Lin PH, Chen CY, Huang CW, Lee YC, Soong BW, Tsai JW (2016). PRRT2 mutations lead to neuronal dysfunction and neurodevelopmental defects. Oncotarget. Jun 28; 7(26): 39184- 39196.
66. Lotze T, Jankovic J. (2003) Paroxysmal kinesigenic dyskinesias. Semin Pediatr Neurol; 10: 68–79.
67. Lu¨ Q, Atkisson MS, Jarvis SE, Feng ZP, Zamponi GW, Dunlap K (2001) Syntaxin 1A supports voltage-dependent inhibition of a1B Ca^{2+} channels by Gbc in chick sensory neurons. J Neurosci, 21:2949-2957.
68. Luebke, Jennifer & Dunlap, Kathleen & Turner, Tim. (1993). Multiple calcium channel types control synaptic transmission in the hippocampus. Neuron. 11. 895-902. 10.1016/0896-6273(93)90119-C.

69. Luo, C, Chen Y, Song W, Chen Q, Gong Q, Shang HF. (2013) Altered intrinsic brain activity in patients with paroxysmal kinesigenic dyskinesia by PRRT2 mutation: altered brain activity by PRRT2 mutation. Neurol. Sci. 34, 1925–1931
70. M. A. Kamp, A. Krieger, M. Henry, J. Hescheler, M. Weiergra¨ber and T. Schneider (2005) Presynaptic 'Cav2.3-containing' E-type Ca2+ channels share dual roles during neurotransmitter release European Journal of Neuroscience, Vol. 21, pp. 1617–1625
71. Méneret A, Gaudebout C, Riant F, Vidailhet M, Depienne C, Roze E (2013). PRRT2 mutations and paroxysmal disorders. Eur J Neurol. Jun; 20(6): 872-8.
72. Michetti, C., Castroflorio, E., Marchionni, I., Forte, N., Sterlini, B., Binda, F., Fruscione F, Baldelli P, Valtorta F, Zara F, Corradi A, Benfenati, F. (2017). The PRRT2 knockout mouse recapitulates the neurological diseases associated with PRRT2 mutations. Neurobiology of disease, 99, 66–83. doi:10.1016/j.nbd.2016.12.018
73. Millan, C, Luján R, Shigemoto R, Sánchez-Prieto J. (2002) Subtype-specific expression of group III metabotropic glutamate receptors and Ca2þ channels in single nerve terminals. J. Biol. Chem. 277, 47796–47803
74. Mintz, I.M. B.L.Sabatini, W.G.Regehr (1995) Calcium control of transmitter release at a cerebellar synapse. Neuron 15, 675–688
75. Mochida S, Westenbroek RE, Yokoyama CT, Zhong H, Myers SJ, Scheuer T, Itoh K, Catterall WA. (2003) Requirement for the synaptic protein interaction site for reconstitution of synaptic transmission by P/Q-type calcium channels. *Proc Natl Acad Sci U S A*. Mar 4;100(5):2819-24. doi: 10.1073/pnas.262787699.
76. Nachbauer W, Nocker M, Karner E, Stankovic I, Unterberger I, Eigentler A, Najmabadi H, Hu H, Garshasbi M, Zemojtel T, Abedini SS, Chen W, Hosseini M,Behjati F, Haas S, Jamali P, Zecha A, Mohseni M, Püttmann L, Vahid LN, Jensen C, Moheb LA, Bienek M, Larti F, Mueller I, Weissmann R,

Darvish H, Wrogemann K, Hadavi V, Lipkowitz B, Esmaeeli-Nieh S, Wieczorek D, Kariminejad R, Firouzabadi SG, Cohen M, Fattahi Z, Rost I, Mojahedi F, Hertzberg C, Dehghan A, Rajab A, Banavandi MJ, Hoffer J, Falah M, Musante L, Kalscheuer V, Ullmann R, Kuss AW,Tzschach A, Kahrizi K, Ropers HH (2011). Deep sequencing reveals 50 novel genes for recessive cognitive disorders. Nature. Sep 21; 478(7367): 57-63.

77. Pereverzev A, Leroy J, Krieger A, Malecot CO, Hescheler J, Pfitzer G, Klockner U, Schneider T (2002) Alternate splicing in the cytosolic II-III loop and the carboxy terminus of human E-type voltage- gated Ca $^{2+}$ channels: electrophysiological characterization of isoforms. Mol Cell Neurosci, 21:352-365.
78. Pfrieger, F. W., Veselovsky, N. S., Gottmann, K., & Lux, H. D. (1992). Pharmacological characterization of calcium currents and synaptic transmission between thalamic neurons in vitro. The Journal of neuroscience : the official journal of the Society for Neuroscience, 12(11), 4347–4357.
79. Phillips, G.R., Huang, J.K., Wang, Y., Tanaka, H., Shapiro, L., Zhang, W., Shan, W.S., Arndt, K., Frank, M., Gordon, R.E., et al. (2001). The presynaptic particle web: ultrastructure, composition, dissolution, and reconstitution. Neuron 32, 63–77.
80. Pierluigi Valente, Alessandra Romei, Manuela Fadda, Bruno Sterlini, Davide Lonardoni, Nicola Forte, Floriana Fruscione, Enrico Castroflorio, Caterina Michetti, Giorgia Giansante, Flavia Valtorta, Jin-Wu Tsai, Federico Zara, Thierry Nieus, Anna Corradi, Anna Fassio, Pietro Baldelli, Fabio Benfenati, (2019) Constitutive Inactivation of the PRRT2 Gene Alters Short-Term Synaptic Plasticity and Promotes Network Hyperexcitability in Hippocampal Neurons, Cerebral Cortex, Volume 29, Issue 5, Pages 2010–2033, https://doi.org/10.1093/cercor/bhy079

81. Pietrobon D (2010). Insights into migraine mechanisms and CaV2.1 calcium channel function from mouse models of familial hemiplegic migraine. J Physiol. Jun 1; 588(Pt 11): 1871-8.
82. Qian, J. and Noebels, J.L. (2001) Presynaptic Ca2+ channels and neurotransmitter release at the terminal of a mouse cortical neuron. J. Neurosci. 21, 3721–3728
83. Rajakulendran S, Graves TD, Labrum RW, Kotzadimitriou D, Eunson L, Davis MB, Davies R, Wood NW, Kullmann DM, Hanna MG, Schorge S (2010). Genetic and functional characterisation of the P/Q calcium channel in episodic ataxia with epilepsy. J Physiol.Jun 1; 588(Pt 11): 1905-13.
84. Reid, C.A. John D. Clements, John M. Bekkers (1997) Nonuniform distribution of Ca2þ channel subtypes on presynaptic terminals of excitatory synapses in hippocampal cultures. J. Neurosci. 15, 2738–2745
85. Reid, C.A. John D. Clements, John M. Bekkers (1998) N- and P/Q-type Ca2þ channels mediate transmitter release with a similar cooperativity at rat hippocampal autapses. J. Neurosci. 18, 2849–2855
86. Reid, C.A. John D. Clements, John M. Bekkers (2003) Presynaptic Ca2+ channels: a functional patchwork. Trends Neurosci. 26, 683–687
87. Rettig J, Sheng ZH, Kim DK, Hodson CD, Snutch TP, Catterall WA: (1996) Isoform-specific interaction of the alpha1A subunits of brain Ca^{2+} channels with the presynaptic proteins syntaxin and SNAP-25. Proc Natl Acad Sci USA, 93:7363-7368.
88. Rhian M. Evans and Gerald W. Zamponi (2006) Presynaptic Ca2+ channels – integration centers for neuronal signaling pathways TRENDS in Neurosciences Vol.29 No.11
89. Robin Cloarec, Nadine Bruneau, Gabrielle Rudolf, AnnickMassacrier, Man al Salmi, Marc Bataillard, Clotilde Boulay, RobertoCaraballo, Natalio Fejer man, Pierre Genton, Edouard Hirsch, Alasdair Hunter, Gaetan Lesca, Jacq ues Motte, Agathe Roubertie, Damien Sanlaville, Sau-

Wei Wong, YingHui Fu, JacquesRochette, Louis
J. Ptáček, Pierre Szepetowski (2012) PRRT2 links infantile convulsions and paroxysmal dyskinesia with migraine. Neurology 79, 2097–2103

90. Rossi P, Sterlini B, Castroflorio E, Marte A, Onofri F, Valtorta F, Maragliano L, Corradi A, Benfenati F. (2016) A Novel Topology of Proline-rich Transmembrane Protein 2 (PRRT2): HINTS FOR AN INTRACELLULAR FUNCTION AT THE SYNAPSE. *J Biol Chem*. Mar 18;291(12):6111-23.
91. Scholz, K.P. and Miller, R.J. (1995) Developmental changes in presynaptic calcium channels coupled to glutamate release in cultured rat hippocampal neurons. J. Neurosci. 15, 4612–4617
92. Schwenk, J., Baehrens, D., Haupt, A., Bildl, W., Boudkkazi, S., Roeper, J., Fa- kler, B., and Schulte, U. (2014). Regional diversity and developmental dy- namics of the AMPA-receptor proteome in the mammalian brain. Neuron 84, 41–54.
93. Sheng Z, Rettig T, Takahashi M, Catterall WA (1994) Identification of a syntaxin-binding site on N-type calcium channels. Neuron, 13:1303-1313.
94. Sheng Z-H, Rettig J, Cook T, Catterall WA (1996) Calcium-dependent interaction of N-type calcium channels with the synaptic core complex. Nature, 379:451-454.
95. Sheng ZH, Yokoyama CT, Catterall WA (1997) Interaction of the synprint site of N-type Ca^{2+} channels with the C2B domain of synaptotagmin I. Proc Natl Acad Sci USA, 94:5405-5410.
96. Shinawi M, Liu P, Kang SH, Shen J, Belmont JW, Scott DA, Probst FJ, Craigen WJ, Graham BH, Pursley A, Clark G, Lee J, Proud M, Stocco A, Rodriguez DL, Kozel BA, Sparagana S, Roeder ER, McGrew SG, Kurczynski TW, Allison LJ, Amato S, Savage S, Patel A, Stankiewicz P, Beaudet AL, Cheung SW, Lupski JR. (2010) Recurrent reciprocal 16p11.2 rearrangements associated with global developmental delay, behavioural problems, dysmorphism, epilepsy, and abnormal head size. *J Med Genet*.;47(5):332-41.

97. Skarnes WC, Rosen B, West AP, Koutsourakis M, Bushell W, Iyer V, Mujica AO, Thomas M, Harrow J, Cox T, Jackson D, Severin J, Biggs P, Fu J, Nefedov M, de Jong PJ, Stewart AF, Bradley A. (2011) A conditional knockout resource for the genome-wide study of mouse gene function. *Nature*. Jun 15;474(7351):337-42.
98. Snutch, T.P. Jean Peloquin, Eleanor Mathews, and John E. McRory (2005) Molecular properties of voltage-gated calcium channels. In Voltage-Gated Calcium Channels (Molecular Biology Intelligence Unit) (Zamponi, G.W., ed.), pp. 61–94, Landes Bioscience
99. Spacey SD, Valente EM, Wali GM, Warner TT, Jarman PR, Schapira AH, Dixon PH, Davis MB, Bhatia KP, Wood NW (2002) Genetic and clinical heterogeneity in paroxysmal kinesigenic dyskinesia: evidence for a third EKD gene. Mov Disord; 17: 717–25.
100. Stanley, E.F. (2003) Syntaxin I modulation of presynaptic calcium channel inactivation revealed by botulinum toxin C1. Eur. J. Neurosci. 17, 1303–1305
101. Stelzl, U., Worm, U., Lalowski, M., Haenig, C., Brembeck, F.H., Goehler, H., Stroedicke, M., Zenkner, M., Schoenherr, A., Koeppen, S., Timm J, Mintzlaff S, Abraham C, Bock N, Kietzmann S, Goedde A, Toksöz E, Droege A, Krobitsch S, Korn B, Birchmeier W, Lehrach H, Wanker EE. (2005). A human protein-protein interaction network: a resource for annotating the prote- ome. Cell 122, 957–968.
102. Strock, J. and Diverse-Pierluissi, M.A. (2004) $^{Ca2+}$ channels as integrators of G protein-mediated signaling in neurons. Mol. Pharmacol. 66, 1071–1076
103. Sudhof, T.C. (2013). Neurotransmitter release: the last millisecond in the life of a synaptic vesicle. Neuron 80, 675–690.
104. Sudhof, T.C. and Rizo, J. (2011) Synaptic vesicle exocytosis. Cold Spring Harb. Perspect. Biol. 3, a005637

105. Szabo, Z, Obermair GJ, Cooper CB, Zamponi GW, Flucher BE. (2006) Role of the synprint site in presynaptic targeting of the calcium channel Cav2.2 subunit in hippocampal neurons. Eur. J. Neurosci. 24, 709–718
106. Szepetowski P, Rochette J, Berquin P, Piussan C, Lathrop GM, Monaco AP. (1997) Familial infantile convulsions and paroxysmal choreoathetosis: a new neurological syndrome linked to the pericentromeric region of human chromosome 16. Am J Hum Genet 61:889–898.
107. Takahashi, T., Momiyama, (1993) A. Different types of calcium channels mediate central synaptic transmission. *Nature* **366,** 156–158 doi:10.1038/366156a0
108. Tamamaki N, Yanagawa Y, Tomioka R, Miyazaki J, Obata K, Kaneko T (2003). Green fluorescent protein expression and colocalization with calretinin, parvalbumin, and somatostatin in the GAD67-GFP knock-in mouse. J Comp Neurol. 467(1):60-79.
109. Thalhammer A, Contestabile A, Ermolyuk YS, Ng T, Volynski KE, Soong TW, Goda Y, Cingolani LA (2017) Alternative Splicing of P/Q-Type Ca2+ Channels Shapes Presynaptic Plasticity. Cell Rep. Jul 11;20(2):333-343.
110. Timmermann DB, Westenbroek RE, Schousboe A, Catterall WA (2002) Distribution of high-voltage-activated calcium channels inculturedc-aminobutyric acidergic neurons from mousecerebellar cortex.J Neurosci Res,67:48-61.
111. Todorov B, Kros L, Shyti R, Plak P, Haasdijk ED, Raike RS, Frants RR, Hess EJ, Hoebeek FE, De Zeeuw CI, van den Maagdenberg AM (2012). Purkinje cell-specific ablation of Cav2.1 channels is sufficient to cause cerebellar ataxia in mice. Cerebellum. Mar; 11(1): 246-58.
112. Tomita Ha, Nagamitsu S, Wakui K, Fukushima Y, Yamada K, Sadamatsu M, Masui A, Konishi T, Matsuishi T, Aihara M, Shimizu K, Hashimoto K, Mineta M, Matsushima M, Tsujita T, Saito M, Tanaka H, Tsuji S, Takagi T, Nakamura Y, Nanko S, Kato N, Nakane Y, Niikawa N. (1999) Paroxysmal

kinesigenic choreoathetosis locus maps to chromosome 16p11.2-q12.1. Am J Hum Genet.;65(6):1688-97.

113. Tottene A, Conti R, Fabbro A, Vecchia D, Shapovalova M, Santello M, van den Maagdenberg AMJM, Ferrari MD, Pietrobon D. (2009) Enhanced excitatory transmission at cortical synapses as the basis for facilitated spreading depression in CaV2.1 knockin migraine mice. Neuron; 61: 762-773.
114. Trabzuni, D., Ryten, M., Walker, R., Smith, C., Imran, S., Ramasamy, A., Weale, M.E., and Hardy, J. (2011). Quality control parameters on a large dataset of regionally dissected human control brains for whole genome expression studies. J. Neurochem. 119, 275–282.
115. Tsien, R.W., Lipscombe D, Madison DV, Bley KR, Fox AP. (1988) Multiple types of neuronal calcium channels and their selective modulation. Trends Neurosci. 11, 431–438
116. Unno T, Wakamori M, Koike M, Uchiyama Y, Ishikawa K, Kubota H, Yoshida T, Sasakawa H, Peters C, Mizusawa H, Watase K (2012). Development of Purkinje cell degeneration in a knocking mouse model reveals lysosomal involvement in the pathogenesis of SCA6. Proc Natl Acad Sci USA.Oct 23; 109(43): 17693-8.
117. Valente P, Castroflorio E, Rossi P, Fadda M, Sterlini B, Cervigni RI, Prestigio C, Giovedì S, Onofri F, Mura E, Guarnieri FC, Marte A, Orlando M, Zara F, Fassio A, Valtorta F, Baldelli P, Corradi A, Benfenati F (2016a). PRRT2 Is a Key Component of the Ca2+- Dependent Neurotransmitter Release Machinery. Cell Rep. Apr 5; 15(1): 117-31.
118. Valtorta F., Benfenati F., Zara F., Meldolesi J. (2016) PRRT2: from Paroxysmal Disorders to Regulation of Synaptic Function Trends in Neurosciences, Vol. 39, No. 10
119. Van Petegem, F., Clark KA, Chatelain FC, Minor DL Jr. (2004) Structure of a complex between a voltage-gated calcium channel b-subunit and an a-subunit domain. Nature 429, 671–675

120. Verderio, C., Pozzi D, Pravettoni E, Inverardi F, Schenk U, Coco S, Proux-Gillardeaux V, Galli T, Rossetto O, Frassoni C, Matteoli M. (2004) SNAP-25 modulation of calcium dynamics underlies differences in GABAergic and glutamatergic responsiveness to depolarization. Neuron 41, 599–610
121. Wang X, Sun W, Zhu X, Li L, Du T, Mao W, Wu X, Wei H, Zhu S, Sun Y, Liu Y, Niu N, Wang Y, Liu Y. (2010) Paroxysmal kinesigenic choreoathetosis: evidence of linkage to the pericentromeric region of chromosome 16 in four Chinese families. Eur J Neurol; 17: 800–7.
122. Wang, J.L., Cao L, Li XH, Hu ZM, Li JD, Zhang JG, Liang Y, San-A, Li N, Chen SQ, Guo JF, Jiang H, Shen L, Zheng L, Mao X, Yan WQ, Zhou Y, Shi YT, Ai SX, Dai MZ, Zhang P, Xia K, Chen SD, Tang BS. (2011) Identification of PRRT2 as the causative gene of paroxysmal kinesigenic dyskinesias. Brain 134, 3493–3501
123. Weiss, L.A. Shen Y, Korn JM, Arking DE, Miller DT, Fossdal R, Saemundsen E, Stefansson H, Ferreira MA, Green T, Platt OS, Ruderfer DM, Walsh CA, Altshuler D, Chakravarti A, Tanzi RE, Stefansson K, Santangelo SL, Gusella JF, Sklar P, Wu BL, Daly MJ; Autism Consortium. (2008) Association between microdeletion and microduplication at 16p11.2 and autism. N. Engl. J. Med. 358, 667–675
124. Westenbroek RE, Hell JW, Warner C, Dubel SJ, Snutch TP,Catterall TP (1992) Biochemical properties and subcellulardistribution of an N-type calcium channel alpha 1 subunit.Neuron,9:1099-1115.
125. Westenbroek RE, Hoskins L, Catterall WA (1998) Localization of Ca2þchannel subtypes on rat spinal motor neurons, interneurons,and nerve terminals.J Neurosci,18:6319-6330.
126. Wheeler DB, Randall A, Tsien RW (1994) Roles of N-type and Q-typeCa2þchannels in supporting hippocampal synaptictransmission.Science,264:107-111

127. Wheeler, D.B., Randall A, Tsien RW. (1996) Changes in action potential duration alter reliance of excitatory synaptic transmission on multiple types of Ca2þ channels in rat hippocampus. J. Neurosci. 16, 2226–2237
128. Wood, H. (2012) Genetics: expanding the spectrum of neurologi-cal disorders associated with PRRT2 mutations. Nat. Rev. Neurol. 8, 657
129. Wu, L., Tang, H.D., Huang, X.J., Zheng, L., Liu, X.L., Wang, T., Wang, J.Y., Cao, L., and Chen, S.D. (2014). PRRT2 truncated mutations lead to nonsense-mediated mRNA decay in Paroxysmal Kinesigenic Dyskinesia. Parkinsonism Relat Disord. 20, 1399–1404.
130. Wu, L.G. and Saggau, P. (1994) Pharmacological identification of two types of presynaptic voltage-dependent calcium channels at CA3–CA1 synapses of the hippocampus. J. Neurosci. 14, 5613–5622
131. Wu, L.G., Westenbroek RE, Borst JG, Catterall WA, Sakmann B. (1999) Calcium channel types with distinct presynaptic localization couple differentially to transmitter release in single calyxtype synapses. J. Neurosci. 19, 726–736
132. Zamponi, G.W. (2001) Determinants of G protein inhibition of presynaptic calcium channels. Cell Biochem. Biophys. 34, 79 94
133. Zhong H, Yokoyama C, Scheuer T, Catterall WA (1999) Reciprocal regulation of P/Q type Ca^{2+} channels by SNAP-25 syntaxin and synaptotagmin. Nat Neurosci, 2:939-941.

12 . Acknowledgements

Undertaking this doctorate was an experience that changed me as a person but that made me grow professionally and this growth would not have been possible without the support I received from many people.

First of all, I would like to thank my supervisor Prof. Pietro Baldelli for the continuous support during my PhD course, for his teachings and for helping me during these years in the preparation of the reports and this thesis. He will always be one of my most important mentors.

I would also like to thank Prof. Fabio Benfenati for giving me the opportunity to work at the Italian Institute of Technology (IIT) and in the NSYN laboratories.

Many thanks also to Dr. Pierluigi Valente, who, thanks to his support, has helped me in understanding many methods and terminologies concerning my thesis.

My warmest thanks also goes to my colleagues Cosimo, Bruno, Antonella, Davide, Giorgia, Barbara, Sara, Antonio, Silvia C, Chiara, for making the long days in the lab more fun, for their support, help and for being my second family in these years: thanks you my friends!

I can't forget to thank my second family, friends. They are the real people who have supported and encouraged me in all these academic years. Thanks to my sisters Cristina, Stefania, Silvia, Michela, to my brother Marco and to all the others with whom I shared many of my evenings, Federica, Beatrice, Dario, Alessandro, Gabriele, Elena.

Finally, I would like to thank my family: my only standing point during all these years. Especially I would like to thank my parents who have always been close to me, they helped me even in the darkest moments thanks to their love and their strength to live that encouraged me to go on. I dedicate this thesis to them.

Finally, I would also like to thank myself, for continuing to believe in myself in all these years, despite the bad news, the trials of life, the difficult moments and also all the changes that have allowed me to become a man and become a best person.

13. Appendix

Articles published by Daniele Ferrante during the PhD course.

- **Spike-Related Electrophysiological Identification of Cultured Hippocampal Excitatory and Inhibitory Neurons. Mol Neurobiol. (2019) 56(9):6276-6292.**

  Cosimo Prestigio, **Daniele Ferrante**., Pierluigi Valente, Silvia Casagrande, Ennio Albanesi, Yuchio Yanagawa, Fabio Benfenati, Pietro Baldelli.

  Abstract: Cultured hippocampal neurons represent the most widely used experimental substrate for in vitro electrophysiological studies. Nevertheless, in most cases, the nature of neuron under study is not identified as excitatory or inhibitory, or even worse, recorded neurons are considered as excitatory because of the paucity of GABAergic interneurons. Thus, the definition of reliable criteria able to guarantee an unequivocal identification of excitatory and inhibitory cultured hippocampal neurons is an unmet need. To reach this goal, we compared the electrophysiological properties and the localization and size of the axon initial segment (AIS) of cultured hippocampal neurons, taking advantage from GAD67- GFP knock-in mice, which expressing green fluorescent protein (GFP) in gamma- aminobutyric acid (GABA)-containing cells, allowed to unambiguously determine the precise nature of the neuron under study. Our results demonstrate that the passive electrophysiological properties, the localization and size of the AIS, and the shape and frequency of the action potential (AP) are not reliable to unequivocally identify neurons as excitatory or inhibitory. The only parameter, related to the shape of the single AP, showing minimal overlap between the sample-point distributions of the two neuronal subpopulations, was the AP half-width. However, the estimation of the AP failure ratio evoked by a short train of high-current steps applied at increasing frequency (40-140 Hz) resulted to be indisputably the safer and faster way to identify the excitatory or inhibitory nature of an unknown neuron. Our findings provide a precise framework for further electrophysiological investigations of in vitro hippocampal neurons.

- **TBC1D24 regulates axonal outgrowth and membrane trafficking at the growth cone in rodent and human neurons. Cell Death & Differentiation (2019) 26, pages2464–2478**

Davide Aprile, Floriana Fruscione, Simona Baldassari, Manuela Fadda, **Daniele Ferrante**, Antonio Falace, Emmanuelle Buhler, Jacopo Sartorelli, Alfonso Represa, Pietro Baldelli, Fabio Benfenati, Federico Zara, Anna Fassio

Abstract: Mutations in TBC1D24 are described in patients with a spectrum of neurological diseases, including mild and severe epilepsies and complex syndromic phenotypes such as Deafness, Onycodystrophy, Osteodystrophy, Mental Retardation and Seizure (DOORS) syndrome. The product of TBC1D24 is a multifunctional protein involved in neuronal development, regulation of synaptic vesicle trafficking, and protection from oxidative stress. Although pathogenic mutations in TBC1D24 span the entire coding sequence, no clear genotype/phenotype correlations have emerged. However most patients bearing predicted loss of function mutations exhibit a severe neurodevelopmental disorder. Aim of the study is to investigate the impact of TBC1D24 knockdown during the first stages of neuronal differentiation when axonal specification and outgrowth take place. In rat cortical primary neurons silenced for TBC1D24, we found defects in axonal specification, the maturation of axonal initial segment and action potential firing. The axonal phenotype was accompanied by an impairment of endocytosis at the growth cone and an altered activation of the TBC1D24 molecular partner ADP ribosylation factor 6. Accordingly, acute knockdown of TBC1D24 in cerebrocortical neurons in vivo analogously impairs callosal projections. The axonal defect was also investigated in human induced pluripotent stem cell-derived neurons from patients carrying TBC1D24 mutations. Reprogrammed neurons from a patient with severe developmental encephalopathy show significant axon formation defect that were absent from reprogrammed neurons of a patient with mild early onset epilepsy. Our data reveal that alterations of membrane trafficking at the growth cone induced by TBC1D24 loss of function cause axonal and excitability defects. The axonal phenotype correlates with the disease severity and highlight an important role for TBC1D24 in connectivity during brain development.

Papers in preparation

- **Daniele Ferrante**, Antonella Marte, Agnes Thalhammer, Cosimo Prestigio, Bruno Sterlini, Pierluigi Valente, Lorenzo Cingolani, Franco Onofri, Anna Corradi, Fabio Benfenati, Pietro Baldelli

"Impaired presynaptic Ca2+ influx in PRRT2- deficient neurons"

- Cosimo Prestigio, **Daniele Ferrante**, Alessandra Romei, Antonella Marte, Franco Onofri, Anna Rocchi, Pierluigi Valente, Fabio Benfenati, Pietro Baldelli

  “A REST/NRSF-dependent transcriptional remodeling governs GABAergic synaptic upscaling induced by chronic hyperactivity”